Investigation into on-line optimization of Cutting Tool Geometry.

By

Christiaan Wilhelm Bosch

Thesis presented in fulfilment of the academic requirements for the degree of Doctor of Philosophy in the Department of Mechanical Engineering, at the University of Natal, Durban.

Supervisor: Prof Zvi Katz.

December 1996

ABSTRACT

Metal cutting is an important process used to manufacture components with machined surfaces or holes. Due to the wide usage of this manufacturing process, research with the aim to optimize the cutting processes is important. Improving cutting techniques even mildly can result in major cost savings in high volume production. Better machining practices will result in products of better precision and of greater useful life. Benefits can also be had from increasing the rate of production and producing a bigger variety of products with the tools available. The area of metal cutting has been researched widely by people like Tourrett, Taylor, Cohen, Davis and many others to find improved techniques and methods. This project was conducted to improve cutting conditions by ensuring that the tool geometry is always optimal. The effect of tool geometry on cutting performance has been discussed in detail by many researchers, but the practical application of these theories is an area that needs further attention. For this project a device was developed to vary the tool geometry with stepper motors on command from the controller. This device was used for research into the viability of varying tool geometry during machining to obtain different cutting conditions. Stepper motors ensure high accuracy in the control of tool geometries. The ease of controlling stepper motors, also simplified the controlling program and communication devices a lot. Rotating the stepper motors results in rotation of the tool holder around the tool tip. Tool angles are varied without affecting the other cutting parameters like the depth of cut,

metal removal rate and cutting speed. With these cutting parameters staying the same, the change in tool geometry should result in a change in the power consumed during cutting and the force required for cutting. Other measurements for cutting performance like temperature of the tool and workpiece and the acoustic print of the tool will also change. Results prove that cutting force measurement can be used effectively to measure the optimal cutting conditions. The back rake angles and side rake angles have the biggest influence of all the tool angles on metal cutting. This is demonstrated by a number of researchers[28] as discussed in section 2.2. This thesis proves how the on-line changing of tool geometry, ensures the optimal cutting conditions.

DECLARATION

I the undersigned, hereby states that this entire thesis, unless specifically indicated to the contrary in the text, is his own original work, and has not been submitted at any other university in part or as a whole, for the reason of obtaining a degree.

Research was conducted at the University of Natal under the supervision of Prof. Zvi Katz.

Work in the field of metal cutting was conducted with the purpose of optimizing cutting conditions by changing tool geometry on-line. The effect of tool geometry on cutting conditions is well known, but the on-line adjusting of geometry is relatively unknown.

ACKNOWLEDGEMENTS

The following people needs to be thanked for their assistance:

The workshop staff at the Department of Mechanical Engineering for their help in the manufacturing of the mechanism for experimental work.

The other staff members who helped in different ways.

The author's parents who encouraged and motivated him at all times.

A special mention of Prof. Zvi Katz who supervised the project.

TABLE OF CONTENTS

LIST OF TABLES

LIST OF FIGURES

LIST OF SYMBOLS

GENERAL:

x_1 = processed material type and characteristics
x_2 = Tool type
x_3 = Tool material characteristics
x_4 = Tool geometry
x_5 = Cutting speed
x_6 = Feed rate
x_7 = Depth of cut
d_1 = Tool temperature
d_2 = Cutting force
d_3 = Specific energy consumption
d_4 = Acoustic noise print
A = Cross sectional area of chip removed
V_c = Shear Velocity.
V_w = Approach Velocity.
b = width of cut dependant on feed rate.
t = depth of cut or chip thickness.
A = side length of uncut area.

FORCES:

$F_p = F_v = F_t$ = Power force in direction of motion.
$F_q = F_f = F_l$ = Force perpendicular to the work velocity.
$F_r = F_p$ = Radial Feed Force
F_s = Shear force
F_v = Cutting force related to area
F = Friction force
F_N = Force Normal to the shear plane
$F_{oblique}$ = Cutting force due to oblique cutting edge influenced by back rake angle variations.
$F_{orthogonal}$ = Cutting force due to orthogonal cutting edge influenced by side rake angle variations.

F_{actual} = Measured Force

$F_{SR\text{-}F\text{-}dev}$ = Feed Force deviation due to SR variation

$F_{BR\text{-}F\text{-}dev}$ = Feed Force deviation due to SR variation

$F_{SR\text{-}F\text{-}dev}$ = Cutting Force deviation due to SR variation

$F_{BR\text{-}F\text{-}dev}$ = Cutting Force deviation due to SR variation

R = Resultant force

ANGLES:

i = Angle of Obliguity or inclination angle or Back Rake Angle.

α = Tool rake angle.

α_v = Velocity Rake = True Rake = Side Rake Angle.

α_n = Normal Rake = Oblique Rake Angle.

α_e = Effective Rake.

β = Angle between resultant force and the normal to the rake face.

β_n = Normal Friction Angle.

η_c = Chip flow angle.

$\acute{\eta}_c$ = Friction Force direction.''

$\acute{\eta}_s$ = Shear Flow Angle.

Φ_n = Shear Angle.

Γ = shear stress of workpiece material

LIST OF ABBREVIATIONS:

d.o.c = Depth of cut

CHAPTER 1

1 INTRODUCTION

Machining processes is used widely in industry for facing and drilling operations. A small gain in the efficiency of metal cutting can result in big cost savings in high volume manufacturing. Improved machining processes will result in components machined to tighter tolerances which results in a better quality product that can perform more efficiently.[1]

The problem of increasing productivity and decreasing the cost of machining has been analysed widely. Tools have been developed with inserts with at least three cutting edges that can quickly be changed when the tool is worn. Tool materials have also been developed with varying capabilities to suit different cutting conditions.[2] It was shown that varying the tool geometry[3], cutting speed, depth of cut and feed rate all influence the cutting conditions greatly. The value of each is related and dependent on the type of metal being cut and the cutting tool material. Cutting tools available today are made of material with impressive cutting capabilities and good endurance if they are used in the right conditions.[3]

The purpose of the research conducted as described in this thesis, is to ensure that the cutting tools can always be used optimally by optimizing the tool angles, without the need to change the insert. The tool angles are optimized to ensure that the cutting process stays within the parameters set for the cutting tool being used. The tool geometry required for an optimal machining process is dependent on the type of metal to

be machined, the cutter material and the other machining conditions like d.o.c, feed rate, type of coolant used etc.

During this project the tool geometry was changed on-line to increase cutting efficiency. The cutting force was measured with the use of strain gauges to evaluate cutting conditions. These strain gauges measure the bending of the cutting tool during machining. A controlling program written in Turbo Pascal evaluates the data received from the strain gauges and sends commands to the stepper motor either to increase or decrease the rake angle for more optimal cutting conditions. A mechanism was designed to simplify changing of angles during cutting without disturbing the cutting process. The design of the tool orientator ensures that the tool tip will stay in the same position no matter to which value the rake angles are changed. A stepper motor is connected to the tool orientator to ease changing of the rake angles.

The project shows that the varying of tool geometry on-line has big advantages. Optimal tool geometry for specific cutting conditions can be attained without stopping the cutting process. The cutting conditions can be evaluated during machining and the required change in tool geometry can be selected and then carried out without stopping the machining process at any moment.[4] Depending on the material to be cut, the force values can be varied to an optimal value by changing the tool geometry for a specific feed rate, depth of cut and cutting speed. Usually, small rake angles are used for cutting hard material and larger angles for soft ductile materials. Brass is an exception, as small negative angles are used to stop

the tool from digging in.

The chip flow can also be varied by varying the tool geometry.[2] A continuous chip, although beneficial to the cutting process, adversely affects the appearance of the surface, is a hazard to the operator and is time consuming to remove. This system can be used to reduce chatter by changing the tool geometry till the forces decrease and the chatter stops. The problem can be solved without stopping the cutting process, or changing the metal removal rate. Tool life can be improved and predicted since worn tools will generate higher than normal forces during machining.[1,5,6] Tool changes can be initiated before force values become unacceptable. The tool will also last longer since the tool geometry will be changing to compensate for wear ensuring that the tool cut at an optimal angle most of the time. Insert breakage will be reduced since this problem occurs when the tool geometry is incorrect for the type of insert used. Increased productivity will result since more metal is removed per unit time due to heavier cuts and feed rates being possible when cutting at optimal tool angles.[7,8,9] The tool will also last longer when cutting at an optimal angle. When a change in tool angles is required, it can be effected without changing the way the tool is mounted.

CHAPTER 2

2 LITERATURE REVIEW

2.1 Introduction:

Turning is a machining process where the action of a cutting tool is used to generate external cylindrical surfaces on the workpiece. The action of the tool on the work-piece, results in a tangential force in value as determined by the relationship between the specific work metal, tool shape, tool material, feed rate, cutting speed and depth of cut. The power required to remove the metal from the work-piece, is related to the force and the cutting speed.[10] Traditionally these variables determining the cutting force, where selected by the machine operator. An economical selection of cutting conditions involves technical and cost data not readily available to the operator suggesting that an true optimum can only be achieved by somebody with access to all the relevant information. [11,12] With the development of programmable lathes, the relevant cutting conditions for a specific operation could be determined and then permanently programmed. The variables optimized in this manner are the cutting speed, feed rate, depth of cut, tool material, machine tool capacity and the coolant requirement. Limiting factors in the optimization process is the machine-tool maximum feed rate, the machine-tool maximum speed, the machine-tool maximum power, maximum allowable cutting or thrust force, and the feed or speed limits for the desired surface finish.[13,14]

The development of better cutter materials received much attention and optimum cutters were developed for different machining operations.[15,16] These cutters were developed with fixed tool-shape determined for optimal

cutting conditions. The improved cutters resulted in an increase in the metal removal rate and therefore an increase in productivity.[17] The tool geometry required for optimal cutting performance varies with the cutting material, cutting conditions, coolant used, wear-rate of the tool and many other variables. This is why much time was spend on the analysis of the tool geometry by many researchers in the past.[14,18,19,20,21,22]
The different tool angles describing the tool geometry, effects the cutting forces, power consumption, chip conditions and temperature distribution. Research findings on the effect of tool angles on cutting conditions show that optimization of the cutting conditions is possible by control of the tool geometry.[14,18,19,20,21,22]

The Rake angles have the biggest influence on machining conditions. The effect of the rake angle on cutting conditions, is:

- Controlling the direction of chip flow by changing the effective shear angle.[21,23]
- Controlling the cutting forces needed for chip removal.[21,23,10] See figures 2.1[a],[b],[c] and [d].

  (Kenneth [24] found the cutting forces to decrease with increasing side rake angles and to increase with increasing back rake angles. See figure 2.1[b] and 2.1[d]. Forces displayed in these graphs, are aligned relative to each other as demonstrated in figure 3.2[a]. Tourrett [18] found the normal force to decrease with an increase in side rake angle, and the normal force to decrease with an increase in back rake angle. See figure 2.1[a] and 2.1[c]. The normal force is aligned

perpendicular to the shear plane, as indicated in figure 3.2[d]. The angles describing the tool geometry is discussed in section 2.2. The American lathe tool specification was chosen as the standard specification for the purposes of this project. See figure 2.2[a])

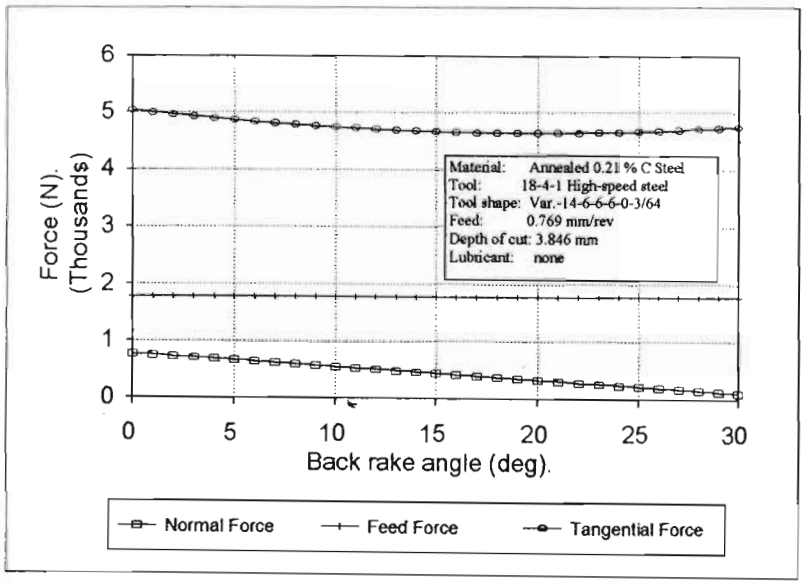

Figure 2.1[a] Effect of Back Rake angle on Tool Forces when turning steel.[18]

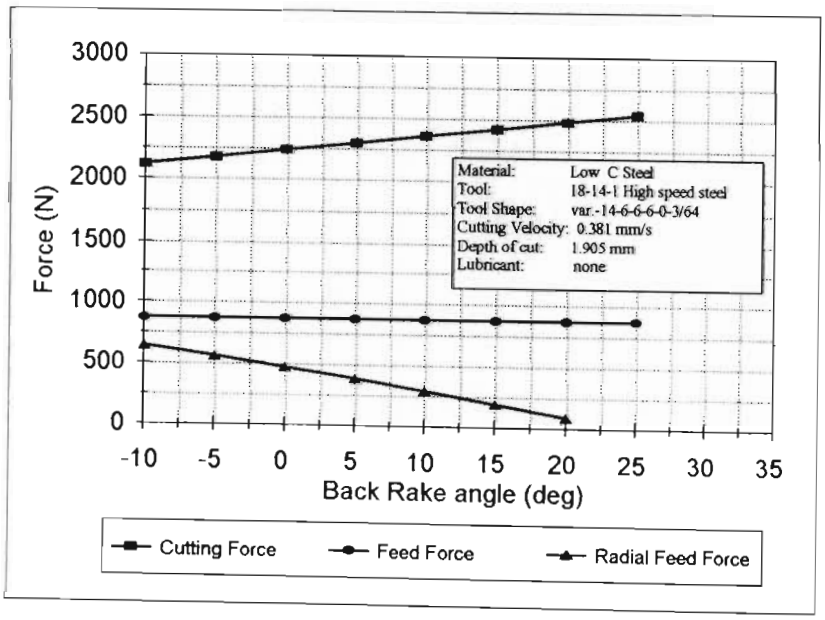

Figure 2.1[b] Effect of Back Rake angle on Tool Forces when turning steel.[28]

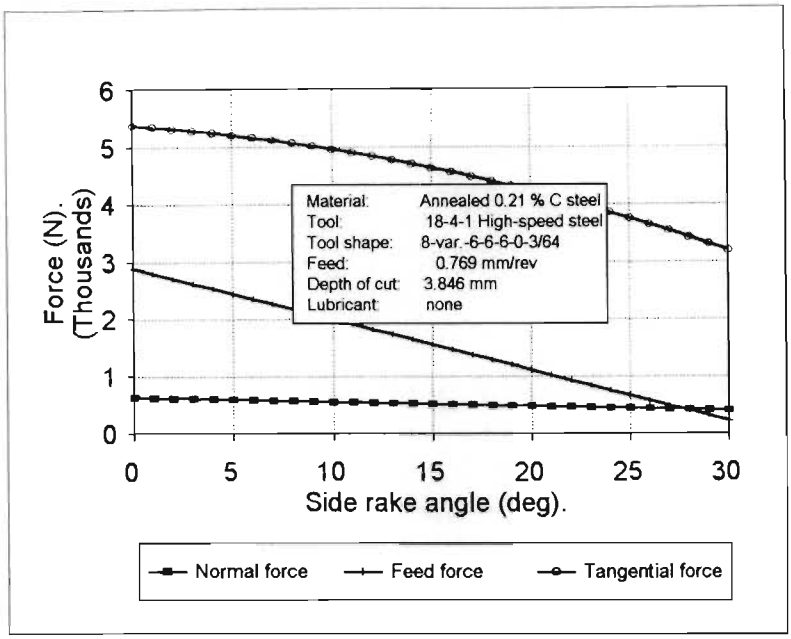

Figure 2.1[c] Effect of Side Rake angle on Tool Forces when turning steel.[18]

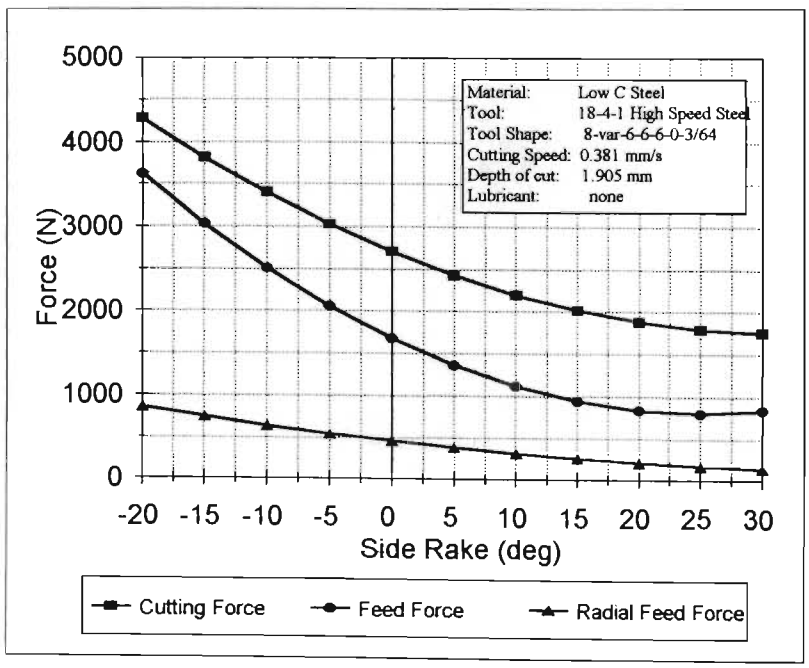

Figure 2.1[d] Effect of Side Rake angle on Tool Forces when turning steel.[24]

- Controlling the power consumption for the cutting process.[20] See figure 2.1[e].

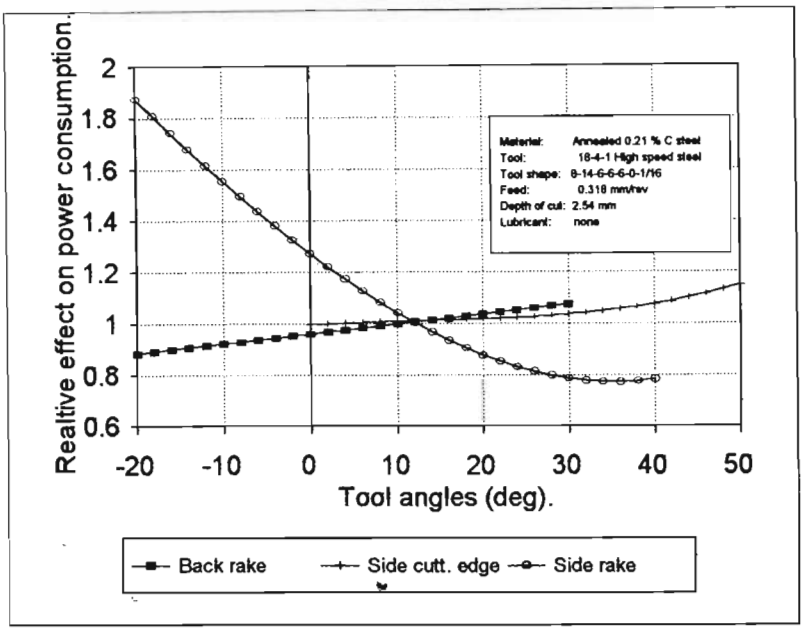

Figure 2.1[e] Effect of tool angles on Power Consumption during turning.[20]

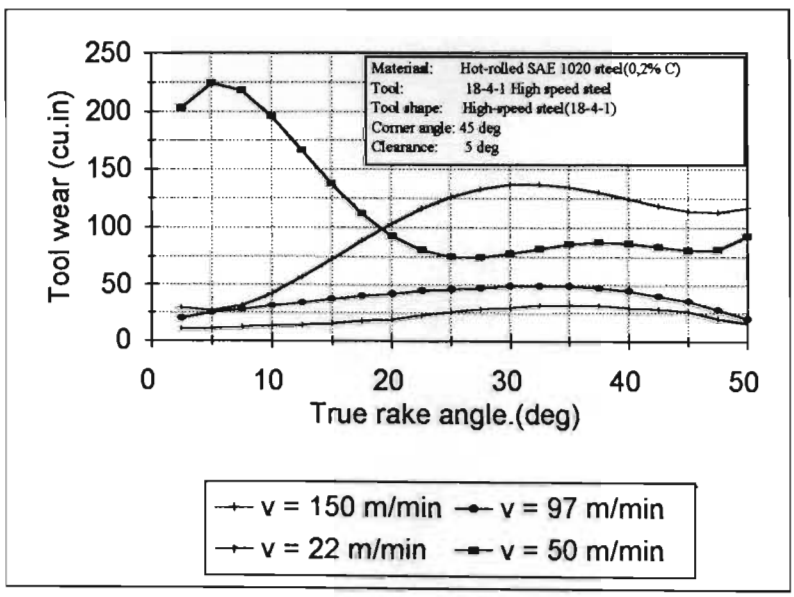

Figure 2.1[f] Effect of Rake angle on Tool life for different cutting speeds.[18]

- Controlling the tool life.[13,25] See figure 2.1[f]. The true rake angle is equal to the side rake angle in the American Lathe tool specification. See figure 3.2[a]. Figure 2.1[g] demonstrates how the attainable cutting speed will change for different back rake angles when a tool life of ninety minutes is required.

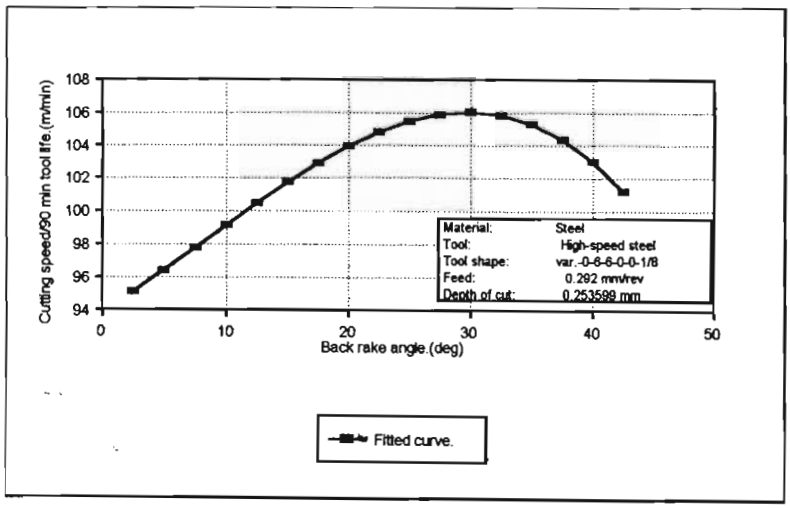

Figure 2.1[g] Effect of Rake angle on Cutting Speed when turning steel. [18]

- Controlling the quality of the surface finish. See figure 2.1[h].[18,26] The rake angle evaluated is similar to the Side Rake angle in turning. The surface finish depends on the size of the build up edge and hence is

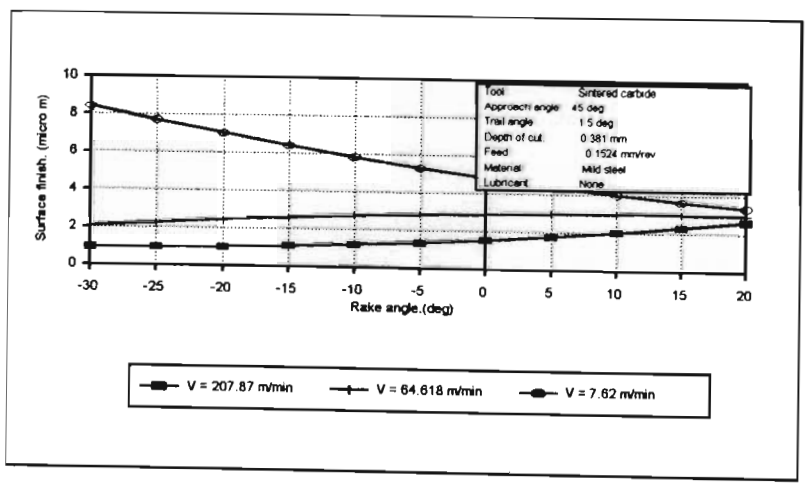

Figure 2.1 [h] Effect of Rake Angle on Surface finish when turning steel. [18]

a measure of the friction and cutting efficiency. Figure 2.1[h] shows that the best results are obtained for a high cutting speed and a high negative rake angle. With a Sintered carbide tool, low cutting speeds and negative rake angles, the surface finish is particularly bad .

- Controlling the cutting temperature.[27,10] See figure 2.1[i] and [j]. The rake angle evaluated in figure 2.1[j], is similar to the side rake in turning.

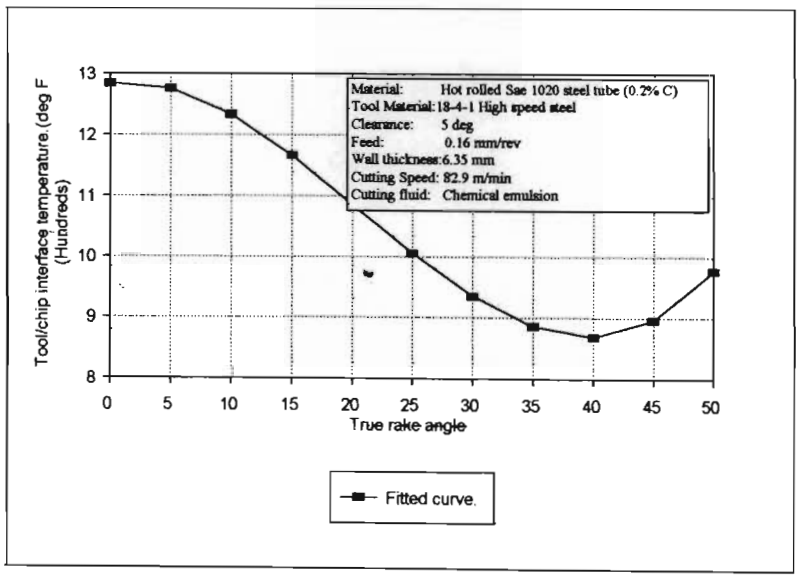

Figure 2.1[i] Effect of Rake Angle on tool/chip interface temperature in turning.[18]

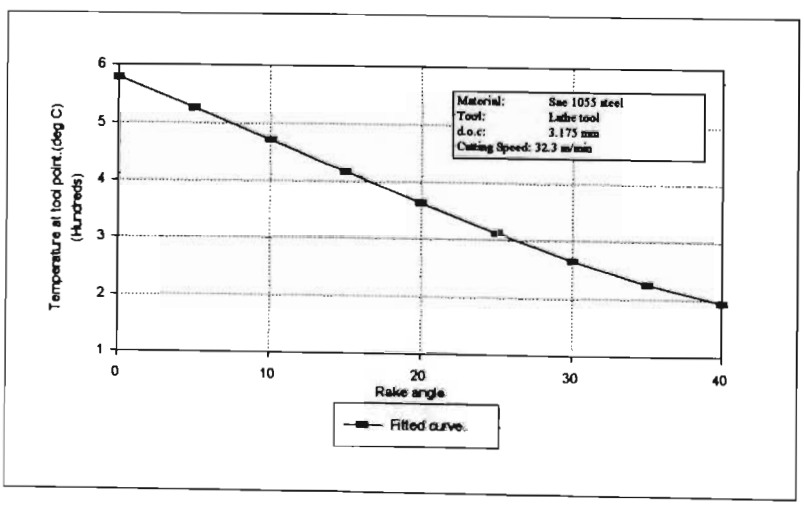

Figure 2.1[j] Effect of rake angle on temperature at tool tip.[18]

- Limiting Chatter and Vibrations.

2.2 Design of Single-Point Tools:

A typical cutter consists of many angles inter-related to form a cutter with the required geometry. See figure 2.2 [a] for a description of the tool angles as specified by the American lathe tool specification. This is the standard specification for the purposes of describing this project. Each of these angles will now be discussed in detail.

The Back rake angle is the angle between the cutting face of the tool and the tool holder, measured parallel to the side of the tool holder. The angle is positive if it slopes downwards from the cutting point to the holder. The back rake angle gives the tool a slicing action, and turn the chip away from the finished work. The usable range of back rake angles, is from minus twenty to plus thirty degrees with five to twenty degrees recommended for most applications. [13]

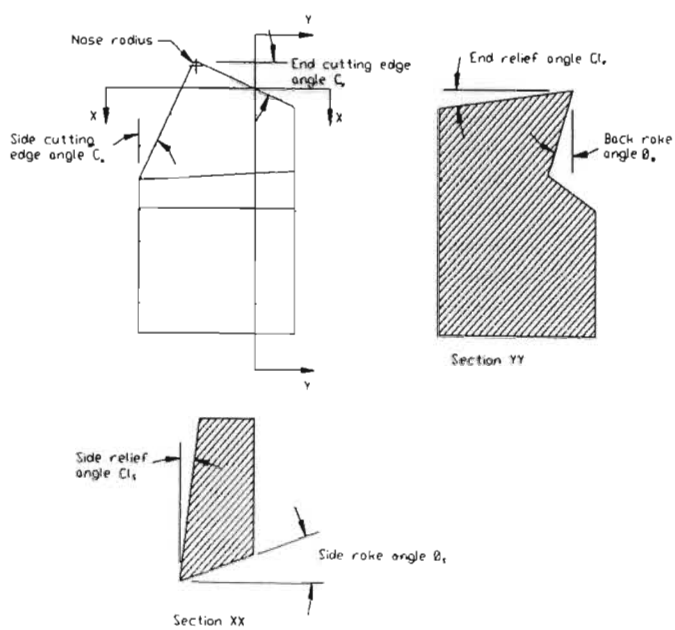

Figure 2.2[a] The American specification for angles describing the Tool Geometry. [4]

The Side rake angle is the angle between the cutting face of the tool and the tool-holder measured perpendicular to the side of the tool holder. The angle is positive if it slopes downwards from the cutting edge to the other side of the holder. Side rake angles determine the thickness of the tool behind the cutting edge. A smaller rake angle and thus a thicker tool results in a stronger cutting tool but also results in higher cutting forces needed for machining operations. This angle is also contained in the minus twenty to thirty degree range. [13]

The End relief angle is the angle between the end face of the tool and a line drawn perpendicular to the base of the tool holder. This angle provides clearance between the tool and the finished surface on the work-piece. The effect of clearance angles on forces is very low between one to sixteen degrees. When the angle drops below one degree, statistical examination show that an increase in clearance angles gives a 6.6 percent decrease in cutting forces.[14] The End Relief angle provides clearance between the tool and the finished surface. Wear reduces this angle. When the angle is too small, the tool rubs on the machined surface and destroys the finish. With the angle too large, the tool digs into the work producing chatter or show weakness failing through chipping. A Tool set above the centre of the work-piece will also reduce the relief-angle.

The side relief angle is the angle between the side flank below the side cutting edge and a line drawn through the side cutting edge perpendicular to the base of the tool. The side relief angle provides clearance between the cut surface of the work and the flank of the tool. With this angle to large, the cutting edge is to weak and the tool may dig in. If this angle is to

small, the tool rubs on the workpiece and then heats up. This angle mostly falls between six to fifteen degrees with eight to twelfth degrees recommended most often. [13] If clearance angles are big enough to avoid rubbing, they do not effect forces, power or surface finish very much. Large clearance angles weaken the tool though, making it advisable to keep the angles smaller than twelfth degrees. [18]

The side cutting edge angle, is the angle between the side cutting edge and the projected side of the tool holder. This angle turns the chip away from the finished surface. When this angle increase in size, the width of the chip increase and the chip thickness diminish. This angle is normally forty-five, sixty or ninety degrees. [13] The Side cutting edge angle determines the length of the cutting edge in action for a certain depth of cut. The bigger the angle, the more of the cutting edge in action and the cutting edge will last longer. The component of the force separating the workpiece and the tool, is bigger for greater angles. The angles are mostly fifteen degrees, but for very heavy cuts, it is an advantage to have angles as large as thirty to forty-five degrees. [19] When the cutting edge angle is changed to between thirty and ninety degrees by grinding, the effect of varying this angle on the cutting forces is small. The angle can also be changed by rotating the tool in the tool holder however, and this will result in a simultaneous increase in Rake angle and undeformed chip thickness. The increase of both will result in a decrease in cutting forces. The changing of this angle is therefore unimportant, except for the cutting of metals like cast iron or forged metal. When cutting these metals, only a small section of tool edge must be exposed to the destructive action of the hard skin, to save the rest

of the tool.

The End Cutting edge angle is the clearance between the cutter and the finished work. When this angle is close to zero, chatter will develop with heavy feeds. Small angles are needed for a smooth finish however. When the angle is too large, the material supporting the tool tip is reduced, and less heat can conduct the heat away. Typical values for this angle are between eight and fifteen degrees. [19]

The influence of a change in rake angles on the cutting process is far more important than the influence of any other tool angle. This was proven by many researchers. [28]

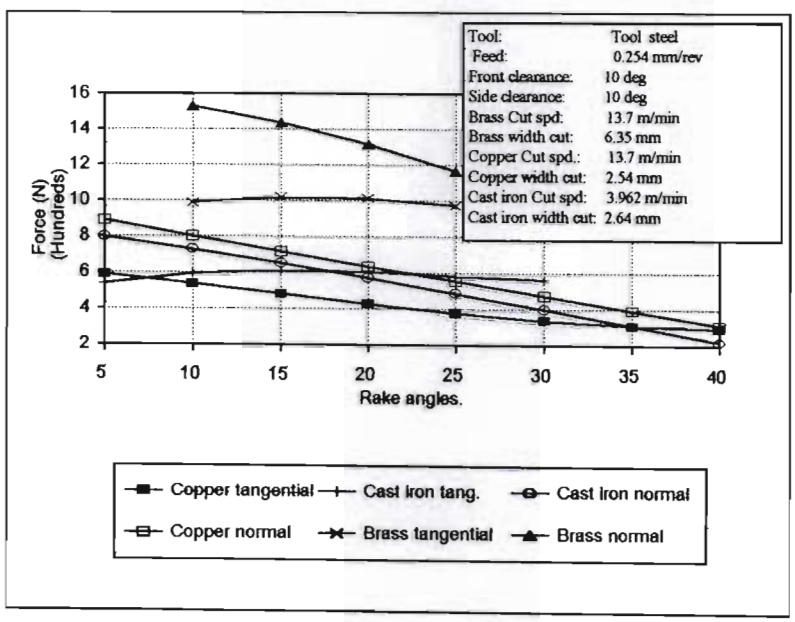

Figure 2.2[b] Effect of rake angle on tangential and normal forces in orthogonal cutting. [18]

The influence of rake angles is important when

machining softer ductile material.[29] Rake angle variations within the limits of three degrees from optimum value, results in cutting resistance changes of about 4 percent. With increased rake angles, the amount of plastic deformation is reduced. The external friction on the tool face is also reduced, resulting in changes of the cutting forces. See figure 2.2[b] and [c].

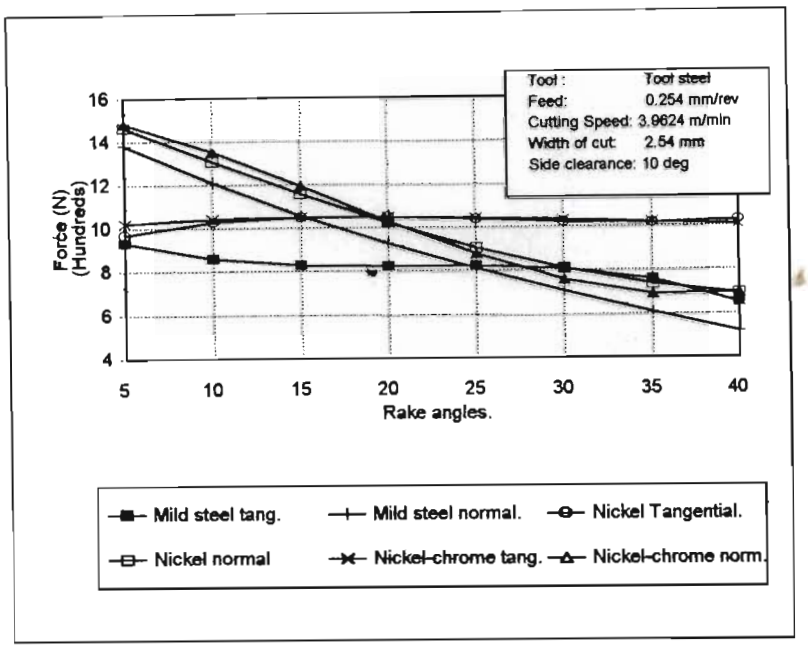

Figure 2.2[c] Effect of rake angle on tangential and normal forces in orthogonal cutting.[18]

In the Metals Handbook [20] three angles are compared namely back rake, side rake and side cutting edge angles. The side rake angle has the biggest influence on the power requirements for machining. Figure 2.1[c] shows the effect of changing these angles. These angles were varied throughout the scope of angles normally used for machining. It was also found in research that an optimal side rake angle is one of the most important factors influencing the cutting process. [30] This study

shows that the lowest cutting forces were obtained by using side rake angles in the region of fifteen to thirty degrees when cutting carbon steel. For the end cutting edge angle it was found that the optimal angle is between twenty and thirty degrees.

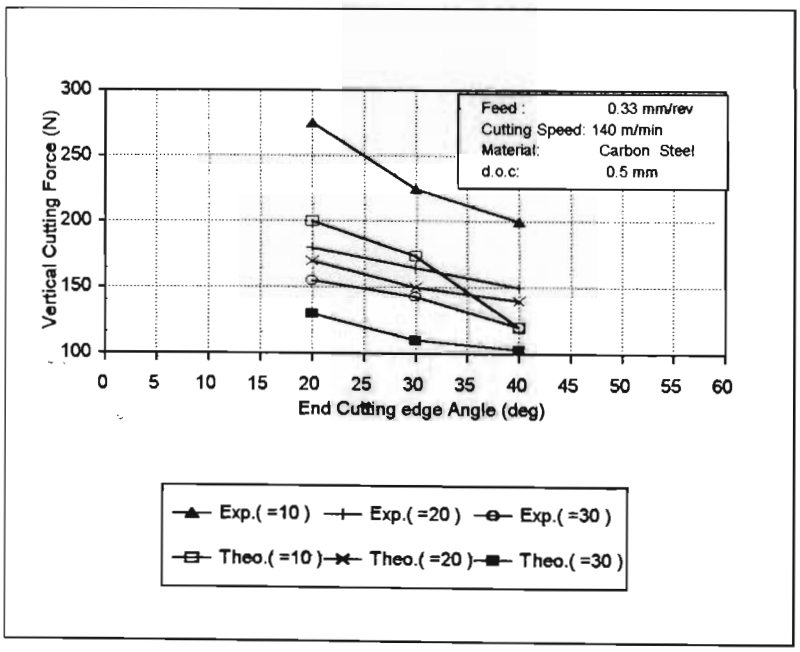

Figure 2.2[d] Cutting forces vs End Cutting edge Angle for different side rake angles. [30]

In the region of thirty to forty degrees the cutting forces increased again due to chatter developing, resulting in unstable cutting forces. Work here was done based on the work by Fue and Chang [30]. See figure 2.2 [d].

An increase in the end cutting edge angle up to sixty degrees, cause a reduction in cutting forces. [28] See figure 2.2 [e].

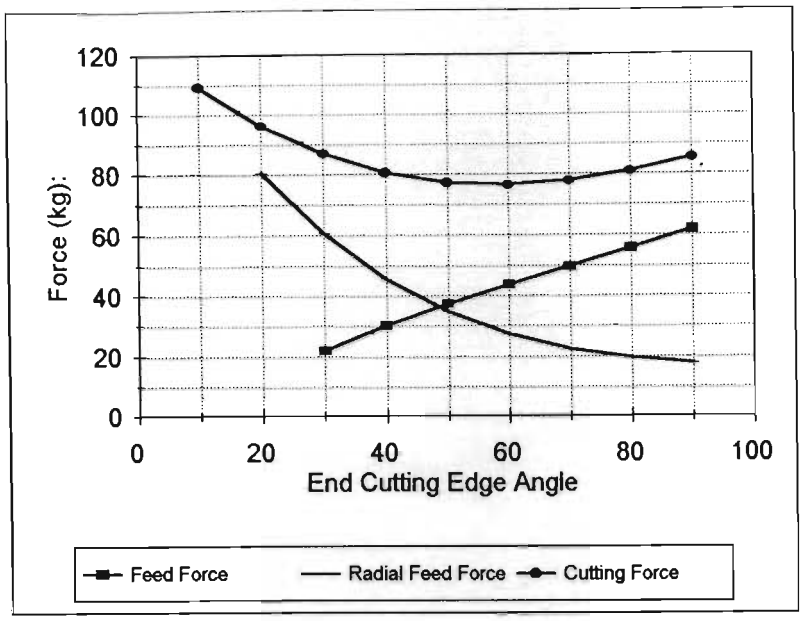

Figure 2.2[e] Influence of end cutting edge angle on variation of Cutting force.[13]

The reason for this is given as the reduction in cutting forces with the increase in rake angle and undeformed chip thickness resulting from the increase in end cutting edge angle. When the end cutting edge angle is increased more than sixty degrees, the increase in friction due to undeformed chip and trailing edge angle increases the cutting resistance. The clearance angles were found to have no influence unless they were reduced so much that rubbing of the tool on the workpiece started. [28] As the angle decrease, the friction forces rise and thus also the cutting resistance. The size of the friction force due to clearance angles, is small compared with the other friction forces.

Many researchers aim their work at understanding the influence of rake angles on the cutting process, as this plays a mayor role in tool geometry optimization. Generally increasing the rake angles reduce both the cutting and the feed forces. The friction in cutting

decrease at the higher rake angles due to the reduction in contact area on the rake face and the reduction in the amount of plastic deformation. This results in reducing the cutting forces and as a result the power consumed per unit volume.[19] The disadvantage of the decrease in contact area is the decrease in strength of the cutting edge and an inability to conduct heat away from the tip into the workpiece. When Rake angles are decreased below zero, the cutting edge increase in strength due to more metal supporting the cutting edge. Due to higher cutting forces during machining, negative rake angles are not suitable for slender shapes due to deflection or distortion by high stresses imposed on them. With negative rake angles, stress on the contact area of the rake face, is largely compressive in nature. Low cutting speeds, and low rake angles increase the ability to conduct heat into the workpiece.

2.3 Chip control and tool geometry

The geometry of the chip or its path can be altered by changing the cutting conditions.[31] Research in this field shows how some degree of control may be obtained by choosing suitable tool angles.[21] The chip can be produced in two forms, a continuous chip or discontinuous segments. Discontinuous chips have three main disadvantages. The appearance of the surface is affected adversely, the flow of the chip can be a hazard to the operator and continuous chips are more difficult to remove. Small rake angles will make the chip spiral tightly resulting in discontinuous chips. A more positive rake angle stretches the spiral, turning the chip away from the tool. Discontinuous chips are always produced when machining cast iron or

cast brass but may also be produced when machining ductile materials at very low speeds, high feeds or tool geometries adapted for chip control.[22] When cutting low carbon steel, choosing a tool geometry for chip control will result in the use of cutting conditions that is uneconomical or impractical according to normal rules. With the high cutting speeds possible today, this problem is more acute as the tendency for the chip to stream is greater. Often mechanised swarf conveyers are used in automated machines, and it is essential that the swarf produced is in the easiest form to handle. Many of these problems have been dealt with by designing chip breakers to help in chip control with positive rake angle tools. [23] Some degree of control by changing the tool geometry is still used however. Negative rake angles works well with simple to machine materials like cast iron where short chipping is produced [13,21], but with steel negative rake angles sometimes forms difficult to manage chips. The chip bends forward and down under pressure causing welding and chip evacuation problems. [28] Generally a negative rake angle will improve chip control but will negatively influence cutting performance. The ideal chip geometry for cutting is therefore a compromise between these two needs. [15]

2.4 Surface Finish and tool geometry

The effect of rake angles on surface finish depends on cutting speed.[32] Tourret [18,26] discussed some tests cutting mild steel with sintered tungsten carbide tools. Tests were conducted for minus thirty to plus twenty degrees rake angle that covers all the rake angles normally used for machining. The cutting speeds

for testing were 0.127 m/s, 1.077 m/s and 3.46 m/s. See figure 2.1 [f]. The best surface finish was obtained at the higher cutting speeds and high negative rake angles. When cutting at low cutting speeds, the best surface finish can be obtained by using high positive rake angles. Tests were also conducted cutting chromium tool steel with tungsten tool tips at thirty-two metres per second.[26] The best results were also obtained with negative rake angles. Positive rake angles resulted in a torn machined surface. This finding is in line with observations when cutting mild steel; high cutting speeds with negative rake angles are required for a good surface finish. With the machining of hot-rolled steel,[26] deep cuts with negative rake angles at high cutting speeds also give the smoothest finish. When cutting at higher cutting speeds, varying the angle between ten and thirty degrees has little effect. At the lower cutting speeds the larger rake angles give the smoothest results, especially when used with a small depth of cut.

Clearance angles do not effect the surface finish, until the angle is effectively zero. [18] The effective clearance angle should be in the one to six degree region.

The effective clearance angle can fall below zero when the tool is worn or when the tool height is set incorrectly. When a tool is worn, the surface finish deteriorates.[33] See figure 2.4 [a]. Changing the insert geometry can produce fine finishes when machining normal steel, cast iron and aluminium.[32] Negative rake angles deliver a good finish for normal steel and twenty degrees positive rake angles are recommended for stainless and aluminium. [28]

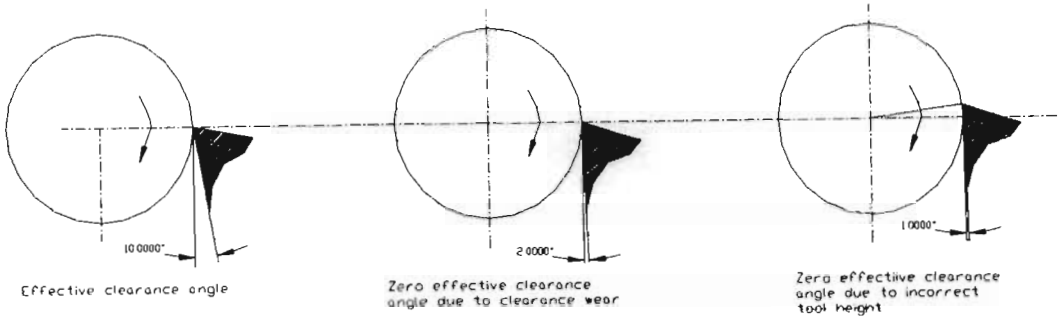

Figure 2.4[a] Clearance angle variation due to wear and incorrect tool height

2.5 Tool life and tool geometry

The effect of variation of rake angles on tool life can be related to the effect of buildup performance as discussed by Tourret [18]. A larger angle, will give less buildup edge formation and thus can afford less protection of the cutting edge of the tool. It can be seen from figure 2.1 [d] and [e] that larger rake angles achieve a better tool life at high cutting speed but is less successful at low cutting speeds. For zero to ten degrees rake, the tool life decreases regularly with increasing cutter speed in the accepted manner.[34] At these rake angles, the stronger support of the tool tip helps the cutter to withstand the chipping effect of low cutting speeds despite the built-up edge. There is an optimum angle for maximum tool life.[35,8] The optimum tool angle change with cutting speed. [8] See figure 2.1 [f] and [g].

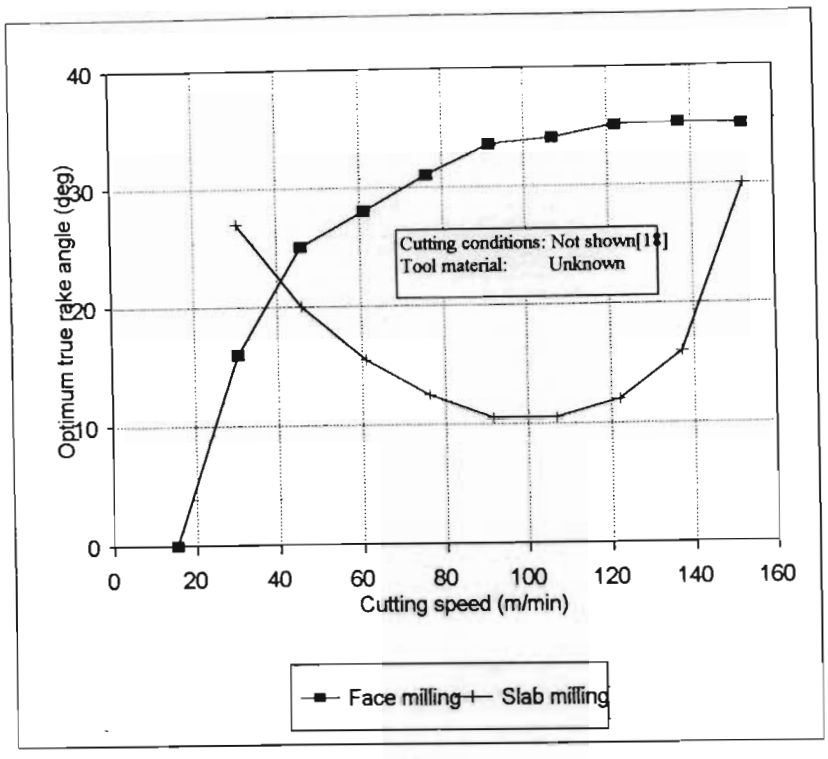

Figure 2.5[a] Effect of cutting speed on optimum Rake angle.[18]

Crawford and Merchant [18] found it possible to plot a curve of optimum true rake angles for different cutting speeds. See figure 2.5 [a] [18]. These curves were determined for face milling and slab milling. The effect of negative rake angles was not researched or discussed.

2.6 Heat generation and tool geometry

Tool/chip interface temperature decrease up to forty degrees positive rake, and increase shortly after that. See figures 2.1 [g] and [h]. This is due to the increased heat due to rubbing. The balance is to weigh the lower heat generation with positive angles, against the better ability to conduct heat away from the tool tip that generate more heat with negative angles.

Crawford and Merchant [18] and Salomon [18] came to this conclusion after experimental work with mainly positive rake angles when turning steel tube.

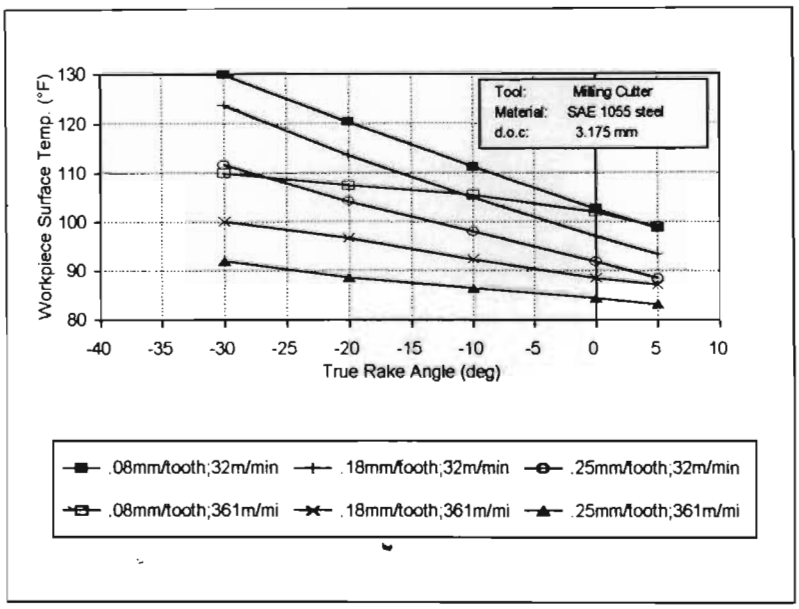

Figure 2.6[a] Effect of Rake Angle on Workpiece Surface Temperature. [18]

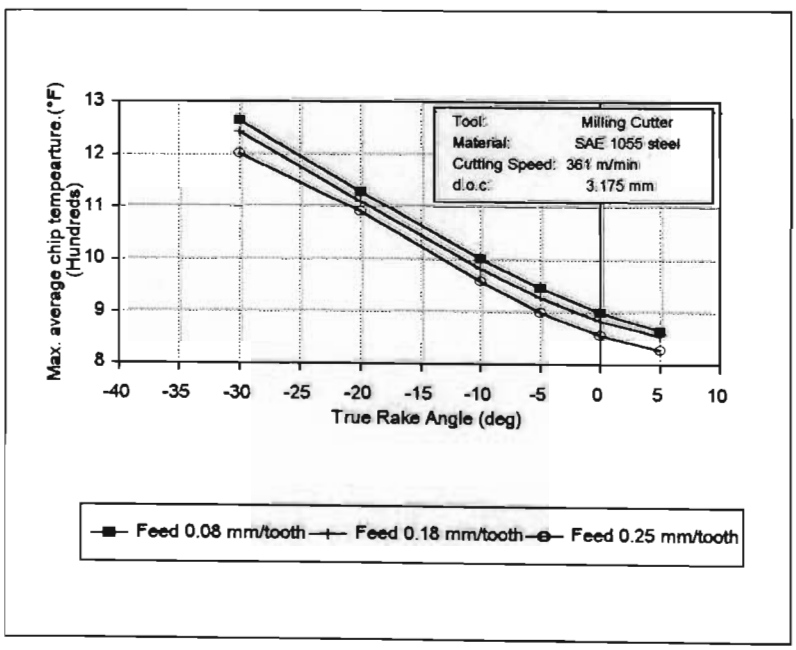

Figure 2.6[b] Effect of Rake Angle on Chip Temperature when milling. [18]

Small or negative rake tools have the added advantage of increase strength and heat dissipation. This might sometimes outweigh the benefits of positive angles and give a longer tool life. Schmidt [18] also did some research on the effect of rake angles on the workpiece surface temperature and the chip temperature. Research here was conducted for rake angles varying from minus thirty degrees to ten degrees. As expected the Workpiece temperature falls steadily as the rake angle is increasing. See figure 2.6 [a][18]. The chip temperature also falls steadily with an increase in rake angles.[36] See figure 2.6 [b][5]. These tests were conducted milling steel, but similar results will be obtainable for turning operations. All but one tooth on the slab mill were ground away to improve ease of experimental work. Chip and workpiece temperatures have a big influence on the tool life as researched in detail by Colding [27], and therefore choosing a tool geometry that will keep temperatures low, will improve efficiency of the cutting process.

2.7 Chatter and Vibration and tool geometry

The cutting tool might vibrate during machining, affecting the surface finish and increasing the cutting forces.[37,38]

Increasing the rake angle increases the stability of the cutting process. The primary chatter vibrational energy is provided by the frictional force acting on the tool flank-workpiece contact area. The flank clearance angle can therefore stabilize the cutting process by increasing the angle. Rotation of the tool increase the rake angle and can decrease the flank clearance angle. [39,40]

2.8 Tool material and tool geometry

Machining efficiency can be improved a lot by choosing the right tool geometry for the machining process. An optimal cutter geometry can eliminate traditional machining problems like chip control, power consumption, poor surface finish and reduced productivity. [10,28,41]. Machining applications can be divided into four categories of materials: aluminium and other soft materials, steels, titanium alloys and nickel-based alloys. [17] To machine these groups effectively, the cutter geometry must be adapted.[42] In practice the following choices are being made to obtain tool geometries as close as possible to the optimum.

Metal cutters made from *tool steel*, work best with large positive rake angles, which are keen but can easily be damaged. For these tools, the rake angles might be as high as thirty degrees that result in an included angle as small as fifty degrees. [18]

Carbon steel tool tips, seldom have angles greater than ten degrees. These tools are soft and wear quickly. Negative rake angles are often used for cutting harder materials. An included angle of ninety degrees can be obtained for rake angles of minus five degrees making the tool very strong. Negative angles are used specifically when cutting tools are subjected to shocks. [18]

Carbide tools often come as throwaway tips. The triangular tips, have positive rake angles, and the square tips have negative rake angles. These tools and carbon tools lack toughness. Carbide tools likes working at high speed.[43,44] With negative rake angles, it was shown experimentally that the cutting force at minus five degrees rake is 8.4 percent higher than with a zero rake angle. When machining Aluminium very high

positive rake angles can be used. [10,28]

Tungsten carbide cutting tools obtain best surface finish from high speed and high negative rake angle. [19] Turning is the most important application for coated carbides and this is the process where tool and insert geometry have the biggest effect on the cutting performance.[35] When using carbides, changing the rake form five degrees negative to five degrees positive at average speeds and feeds, cutting power will reduce by 10 percent when cutting steel and thirty five when cutting cast iron. [15] Cutting with high positive rake angles is possible due to the improved substrate strength and coating technology.

Alumina-based composites mostly cut best with a minus five degree back rake angle. [10,18]

High speed steel cut with positive rake angles, but exceeding twenty-two degrees is not advisable while cutting plain carbon steel. [10,18,45]

Indexable inserts is used to optimize cutting forces and optimize chip control conditions. The effective rake angle is positive ensuring reduced cutting force with less workpiece deflection and lower power consumption. The correct inserts must be chosen for the job, otherwise cutting forces might be to high, reducing tool life and resulting in a rougher surface finish. [18] *Polycrystalline diamond tools* have positive Rake angles for most applications especially when machining soft abrasive materials.[46] The positive rake angles produce higher shear forces but lower cutting forces. Positive rake angles of lower than twenty degrees are preferred but higher values can sometimes be used successfully. For hard materials, negative rake angles are employed. [10,16] *Cermets* (ceramic material in a metal binder) is relatively new [47], but is potentially the best cutter material yet. Cermet's high

hot hardness and oxidation resistance gives it greater stability to handle higher speeds and cutting temperatures than cemented carbides. Tool geometries are possible for optimal chip breaking and optimal machining.

2.9 Conclusion

It can be seen that Rake angles have the biggest influence on machining conditions. For optimization of the cutting process, the different advantages have to be considered to obtain a true optimum cutting condition. The effect of the rake angles on tool life, chip control and surface finish for the material machined and the type of cutter used, have to be considered when the optimal rake angle is determined. Most of these conditions can be monitored effectively by the cutting forces, but a controller should also consider the general limitations for the specific machining process when deciding on tool geometry requirements. Generally, small rake angles are being used for cutting hard materials where larger angles are used for soft ductile materials. Brass as an exception need small or negative rake angles to keep the tool from digging into the workpiece.

Industry shows that conditions occurring most are frequently those where application of rake angles between five and twenty degrees are recommended. [48] Experiments show that the influence of Rake Angle is greater for softer and more ductile work material. With material like Cast-Iron and Bronze the effect is reduced. With an increase of cutting speed the effect is also reduced. Rake angle variations of within limits of three degrees in relation to an optimal angle, cause cutting resistance changes of about 4 percent. [18]

CHAPTER 3

3 PROJECT OBJECTIVE

3.1 Introduction:

As seen in the previous chapter, a typical cutting process can be influenced by many process variables.

These process variables are independent of each-other but all effect the cutting conditions.

These process variables are typically:

x_1 = processed material type and characteristics
x_2 = Tool type
x_3 = Tool material characteristics
x_4 = Tool geometry
x_5 = Cutting speed
x_6 = Feed rate
x_7 = Depth of cut

The objective of this project was to determine the effect of one process variable, namely tool geometry on the cutting conditions, and then to show that this variable can be controlled during machining to obtain optimal cutting conditions.
The cutting conditions can be monitored measuring different output values.

These output values are typically:

d_1 = Tool temperature
d_2 = Cutting force
d_3 = Specific energy consumption
d_4 = Acoustic noise print

The output value chosen for evaluation during this project, is the cutting forces. Measuring the cutting forces give a good indication of the tool geometry and the cutting conditions as a whole, as proved theoretically in the next section.

3.2 Developing the cutting force relationship:[49,50,51]

The relationship between cutting forces and the process variables can be written as follows:

$$d_2 = f(x_1, x_2, x_3, x_4, x_5, x_6, x_9) \qquad (3.1.2)$$

To develop this relation, it was assumed that all the process variables except the tool geometry (x_4), are fixed or are known values during the machining process.

The tool orientator was designed to effect a change in the tool geometry by rotating around the x, y and z-axis aligned through the tip of the tool.

By rotating around the y-axis, a change in back rake angle can be affected. By rotating around the x-axis, a change in side rake angle can be affected. See figure 3.2[a] and figure 2,2[a]. The American specification[4] for tool angles describes the tool used for experimental work adequately but must be adapted slightly for the theoretical analysis of the relation between the cutting angles and cutting forces.[53]
The cutting process under consideration is commonly known as oblique cutting.

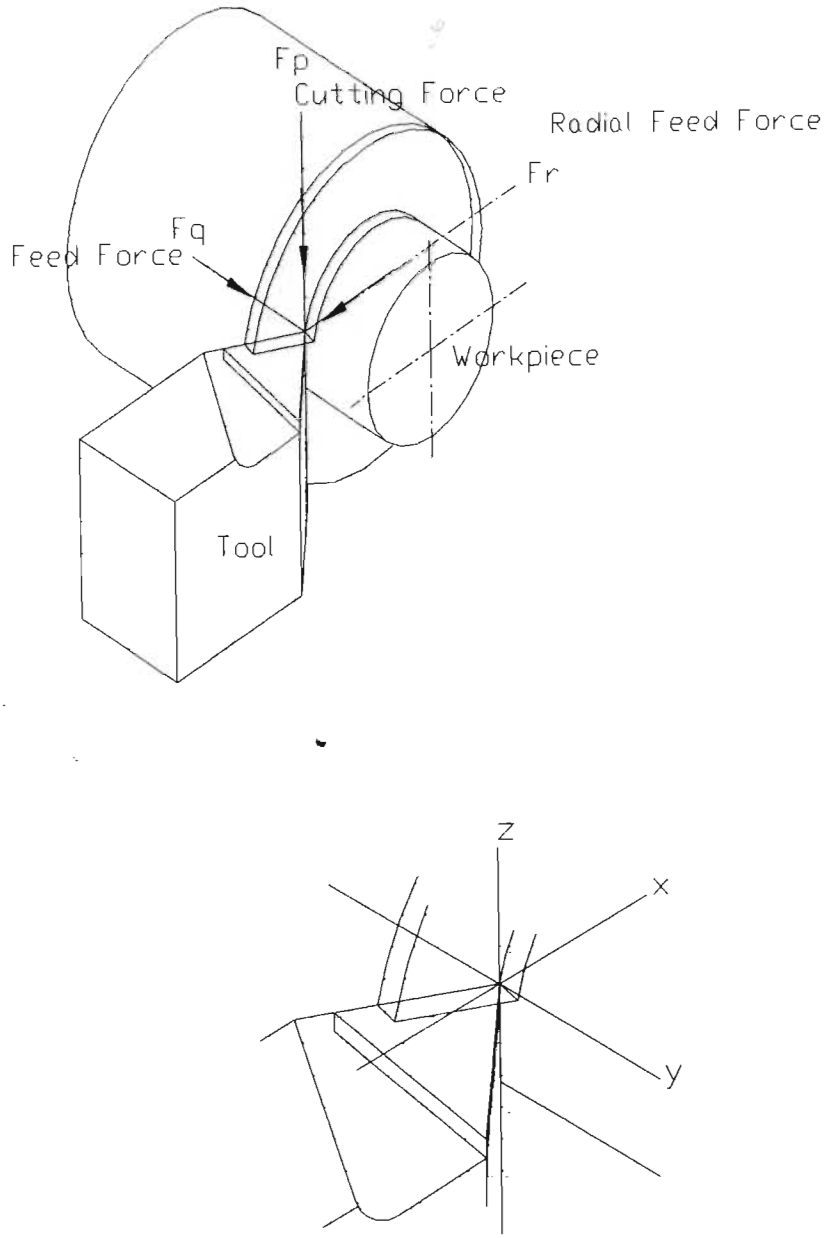

Figure 3.2[a] Forces on the tip of the tool and location of axis through the tip of the tool.

See figure 3.2[b] for the alternative geometrical definitions used for the theoretical analysis of the tool geometry.

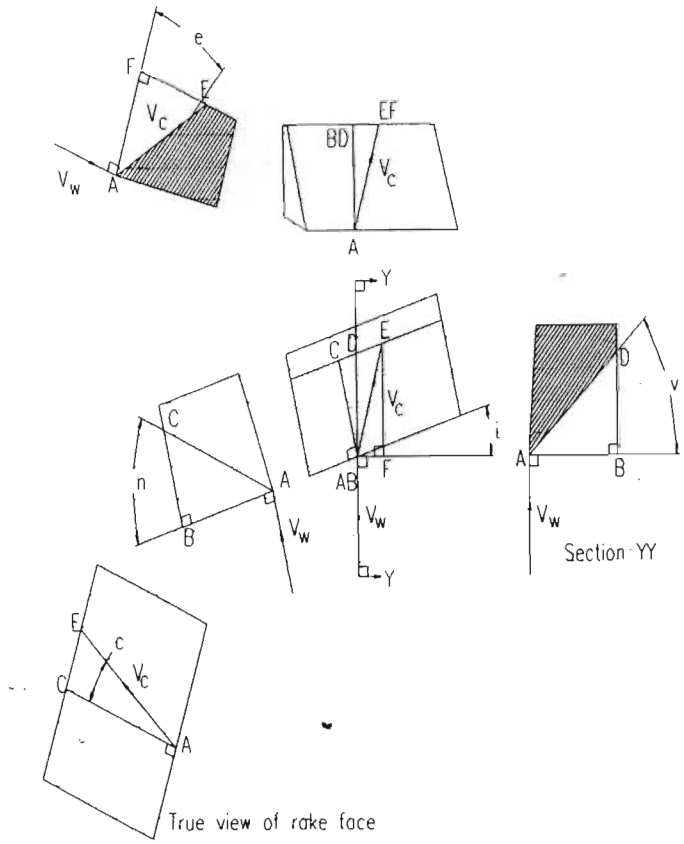

Figure 3.2[b] Alternative geometrical definition for theoretical analysis of tool geometry.[53]

$$SideRake = \alpha_v = \frac{CB}{AB}\frac{DB}{CB} = \frac{\tan\alpha_n}{\cos i}$$

where: α_v = Velocity Rake = Side Rake Angle

α_n = Normal Rake = Oblique Rake Angle

i = Angle of Obliquity or Back Rake Angle

The back Rake angle in the American specification is equal to the angle of obliquity in the alternative specification.

The insert has three cutting edges, but only one cutting edge is in operation during machining operations with low feed rates. See figure 3.2[c].

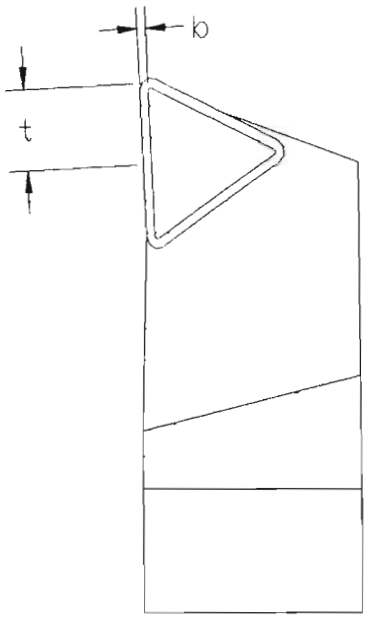

Figure 3.2[c] Only one cutting edge is in operation during machining

With low feed rates, as used during experimental work for this project, the effect of the second cutting edge can be ignored.

The main force components of interest for the analysis of cutting conditions are: (See figure 3.2[a])

1) F_p = The Cutting Force.
   This is the main contributing power force. The force is parallel with the velocity approach vector $_v$. This is also the cutting force as measured with the strain gauges during this project.
2) F_q = Feed force.
   This force is perpendicular to the finished work surface.
3) F_r = Radial feed force.
   The force is perpendicular to the other two forces.

The following assumptions are made to derive relations for these forces in terms of stress on the shear plane.[53]

1) The tool is sharp and no rubbing or ploughing forces act on the tool tip.
2) The stress distribution on the shear plane is uniform.
3) The resultant force R acting on the chip at the shear plane is equal, opposite and collinear to the force acting on the chip at the rake face.

The resultant force R, can be resolved in two components, R' in a plane perpendicular to the cutting edge, and F'_R along the cutting edge. See figure 3.2[d].

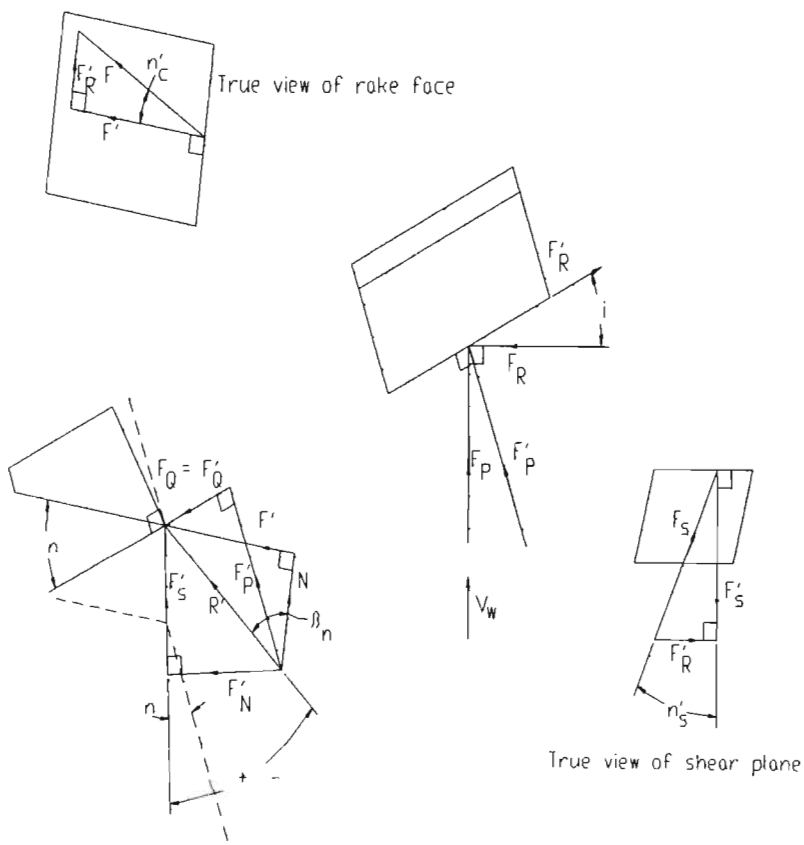

Figure 3.2[d] The force components in oblique cutting.[53]

$$R=\sqrt{(R')^2+(F'_R)^2}$$

As seen in figure 3.2[d] R′ can be resolved further.

$$R'=\sqrt{(F'_q)^2+(F'_p)^2}$$

$$\Rightarrow R=\sqrt{(F'_p)^2+(F'_q)^2+(F'_R)^2}$$

$$\Rightarrow R=\sqrt{(F_p)^2+(F_q)^2+(F_R)^2}$$

Fp can be written in terms of F'_p and F'_R .

$$F_p=F'_p\cos i+F'_R\sin i$$

Determining F'_R:

$$F'_R=F_s\sin(\eta'_s)$$

Determining F'_p:

$$\frac{F'_s}{R'}=\cos(\Phi_n+\beta_n-\alpha_n)$$

$$\Rightarrow R'=\frac{F'_s}{\cos(\Phi_n+\beta_n-\alpha_n)}$$

Also:

$$\frac{F'_p}{R'}=\cos(\beta-\alpha)$$

$$\Rightarrow F'_p=R'\cos(\beta-\alpha)$$

[3.2.4] into [3.2.5]:

$$F'_p=\frac{F'_s\cos(\beta-\alpha)}{\cos(\Phi_n+\beta_n-\alpha_n)}$$

Also:

$$F'_s = F_s \cos(\eta'_s)$$

[3.2.3], [3.2.6] and [3.2.7] into [3.2.2]:

$$F_p = F_s \left[\frac{\cos(i)\cos(\beta-\alpha)\cos(\eta'_s)}{\cos(\Phi_n+\beta_n-\alpha_n)} + \sin(\eta'_s)\sin(i) \right]$$

Also:

$$F_s = \tau A_s$$

$$F_s = \tau \left(\frac{bt}{\sin(\Phi_n)\cos(i)} \right)$$

Therefore:

$$F_p = \frac{\tau bt}{\sin(\Phi_n)} \left[\frac{\cos(\beta_n-\alpha_n)\cos(\eta'_s)}{\cos(\Phi_n+\beta_n-\alpha_n)} + \sin(\eta'_s)\tan(i) \right]$$

Also:

$$\frac{F'_R}{F'_s} = \tan(\eta' s) = \frac{F' \tan(\eta'_c)}{R' \cos(\Phi_n+\beta_n-\alpha_n)}$$

Also:

$$\frac{F'}{R} = \cos(\beta_n)$$

$$\Rightarrow \tan(\eta'_s) = \frac{\tan(\eta'_c)\cos(\beta_n)}{\cos(\Phi_n+\beta_n-\alpha_n)}$$

Substituting for $\acute{\eta}'_s$:

$$F_p = \frac{\tau bt}{\sin(\Phi_n)} \left[\frac{\cos(\beta_n - \alpha_n)\sin(\eta'_s)\cos(\Phi_n + \beta_n - \alpha_n)}{\cos(\Phi_n + \beta_n - \alpha_n)\tan(\eta'_c)\cos(\beta_n)} + \frac{\sin(\eta'_s)\cos(\eta'_s)\cos(\beta_n)\tan(i)}{\cos(\Phi_n + \beta_n - \alpha_n)} \right]$$

$$\Rightarrow F_p = \frac{\tau bt}{\sin(\Phi_n)} \left[\frac{\cos(\beta_n - \alpha_n) + \tan(i)\tan(\eta'_c)\sin(\beta_n)}{\sqrt{\cos^2(\Phi_n + \beta_n - \alpha_n) + \tan^2(\eta'_c)\sin^2(\beta_n)}} \right]$$

The theoretical relation for the feed force can be determined in the same way:

$$F_q = F'_q = R' \sin(\beta_n - \alpha_n)$$

[3.2.4] in [3.2.11]:

$$F'_q = \frac{F'_s \sin(\beta_n - \alpha_n)}{\cos(\Phi_n + \beta_n - \alpha_n)}$$

[3.2.7] in [3.2.12]:

$$F'_q = \frac{F_s \cos(\eta'_s)\sin(\beta_n - \alpha_n)}{\cos(\Phi_n + \beta_n - \alpha_n)}$$

$$F'_q = \left(\frac{\tau bt}{\sin(\Phi_n)\cos(i)} \right) \left(\frac{\cos(\eta'_s)\sin(\beta_n - \alpha_n)}{\cos(\Phi_n + \beta_n - \alpha_n)} \right)$$

Substituting for η'_s:

$$\Rightarrow F_q = F'_q = \left(\frac{\tau bt}{\sin(\Phi_n)\cos(i)} \right) \left(\frac{\sin(\beta_n - \alpha_n)}{\sqrt{\cos^2(\Phi_n + \beta_n - \alpha_n) + \tan^2(\eta'_c)\sin^2(\beta_n)}} \right)$$

The theoretical force component F_R can be determined:

$$F_R = F'_p \sin(i) - F'_R \cos(i)$$

[3.2.6] and [3.2.7] into [3.2.13]:

$$F_R = \frac{F_s \cos(\eta'_s)\sin(i)\cos(\beta-\alpha)}{\cos(\Phi_n+\beta_n-\alpha_n)} - F_s \sin(\eta'_s)\cos(i)$$

$$F_R = \left(\frac{\tau bt}{\sin(\Phi_n)}\right)\left(\frac{\cos(\eta'_s)\tan(i)\cos(\beta-\alpha)}{\cos(\Phi_n+\beta_n-\alpha_n)} - \sin(\eta'_s)\right)$$

Substituting for η'_s:

$$\Rightarrow F_R = \frac{\tau bt}{\sin(\Phi_n)}\left[\frac{\cos(\beta_n-\alpha_n)\tan(i)+\tan(\eta'_c)\sin(\beta_n)}{\sqrt{\cos^2(\Phi_n+\beta_n-\alpha_n)+\tan^2(\eta'_c)\sin^2(\beta_n)}}\right]$$

These equations can now be used to evaluate the effect of changes in the side rake angle and the back rake angle. To reduce the number of variables a shear angle relation is developed between Φ_n, β_n and η_c.

$$\tan(\Phi_n+\beta_n) = \frac{\tan(i)\cos(\alpha_n)}{\tan(\eta_c)-\sin(\alpha_n)\tan(i)}$$

$$\beta_n = \arctan\left[\frac{\tan(i)\cos(\alpha_n)}{\tan(\eta_c)-\sin(\alpha_n)\tan(i)}\right] - \Phi_n$$

Φ_n can now be determined.

$$\tan(\Phi_n) = \frac{r_t\cos(\alpha_n)}{1-r_t\sin(\alpha_n)}$$

$$\Rightarrow \Phi_n = \arctan\left[\frac{r_t\cos(\alpha_n)}{1-r_t\sin(\alpha_n)}\right]$$

And η_c can also be determined.

$$\frac{b}{\cos(i)} = \frac{b_c}{\cos(\eta_c)}$$

$$\frac{\cos(\eta_c)}{\cos(i)} = \frac{b_c}{b} = r_t$$

$$\cos(\eta_c) = \cos(i)\, r_t$$

$$\Rightarrow \eta_c = \arccos[\cos(i)\, r_t]$$

The influence of variations in the side rake angle on the cutting forces will be evaluated by setting the other variables at the following values.

b	=	feed rate	=	0.2 mm
t	=	depth of cut	=	1 mm
τ	=	Yield shear stress	=	385 N/mm
Φ_n	=	shear angle	=	calculated

(The chip-thickness ratio r_t has to be determined experimentally but a average value was taken in this case for comparative purposes.)

β_n	=	friction angle	=	calculated
η'_c	=	friction force direction	=	calculated
i	=	Back Rake angle	=	fixed
α_v	=	Side Rake angle	=	variable

The graph obtained by plotting the force values, when the side rake angle is varied from minus twenty to plus twenty degrees for back rake angle values of minus twenty, minus ten, zero, ten and twenty degrees can be seen in figure 3.2[e].

The graph obtained by plotting the force values, when the back rake angle is varied from minus twenty to plus twenty degrees for side rake angle values of minus twenty, minus ten, zero, ten and twenty degrees can be seen in figure 3.2[f].

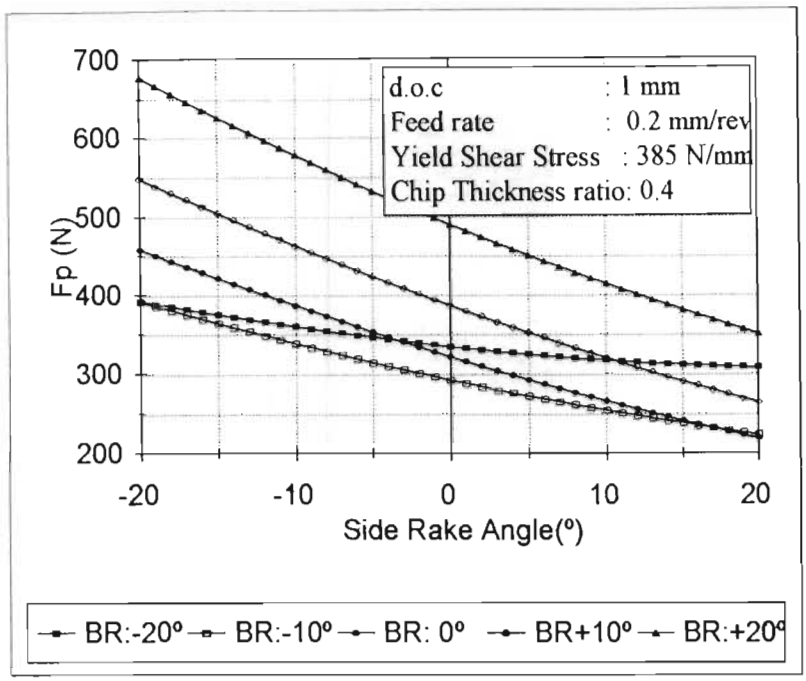

Figure 3.2[e] Theoretical representation of Cutting Force variation for a variation in Side Rake Angle.

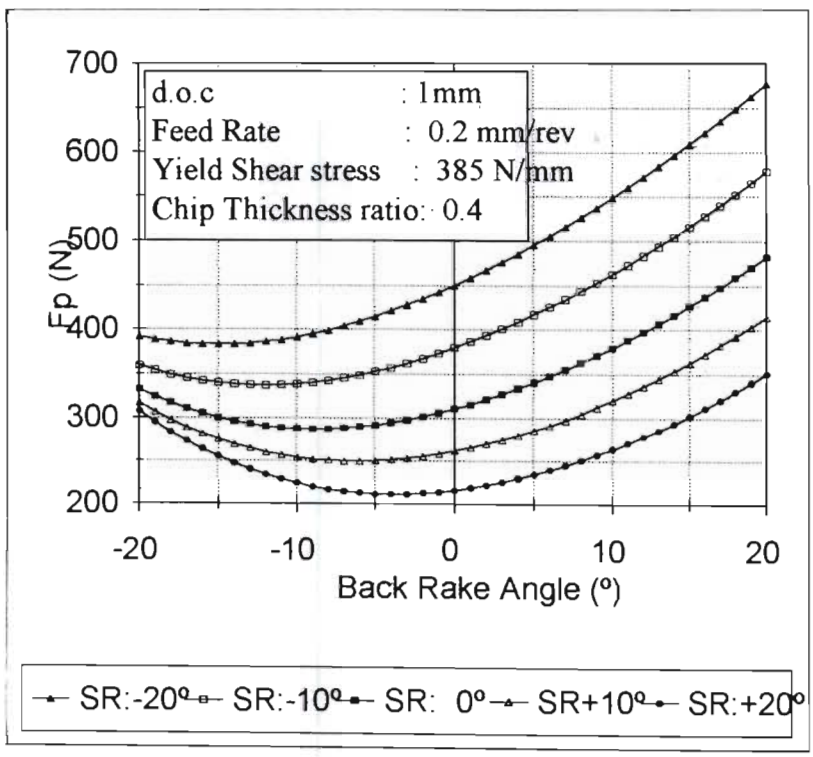

Figure 3.2[f] Theoretical representation of Cutting Force variation for a variation in Back Rake Angle.

The cutting force is the most important force for comparison with the force values obtained during experimental work for this project. As can be seen in chapter six, these theoretical values compare well with the values obtained during experimental work. For comparison with previous research work, the effect of rake angle variations on all three force components is displayed in figures 3.2[g] and 3.2[h].

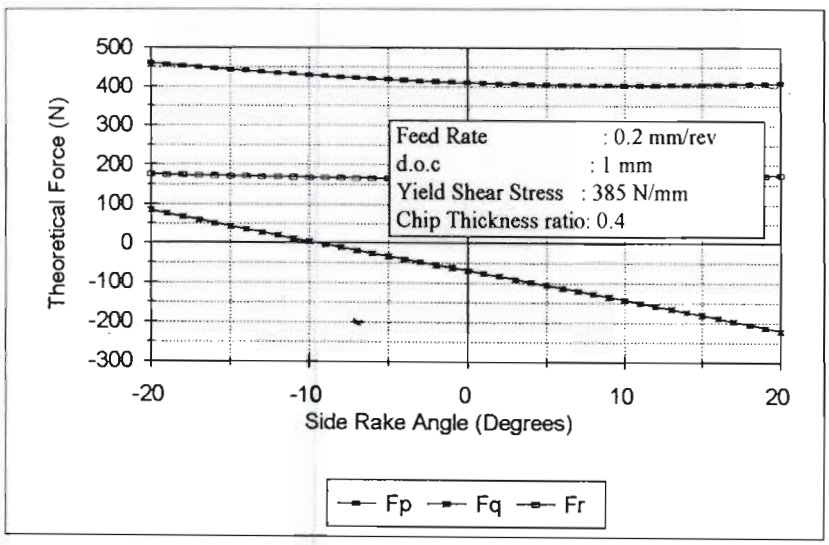

Figure 3.2[g] Effect of Side Rake angle variation on all three force components.

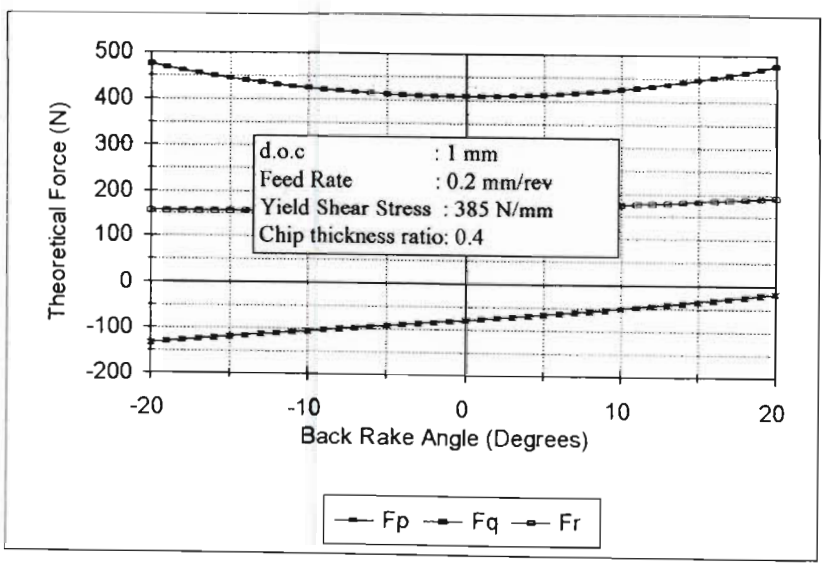

Figure 3.2[h] Effect of Back Rake angle variation on all three force components.

CHAPTER 4

4 EXPERIMENTAL SETUP

4.1 Introduction:

The evidence obtained from research as shown in the chapter two points to the important effect of tool geometry and specifically the rake angles on cutting conditions. The focus of this project is therefore on the on-line control of rake angles to improve machining efficiency. To achieve the aim of this project successfully, an instrument was required to change the geometry of the cutting tool during machining, without changing any other cutting parameters. See figure 4.1[a] for a diagram of this system.

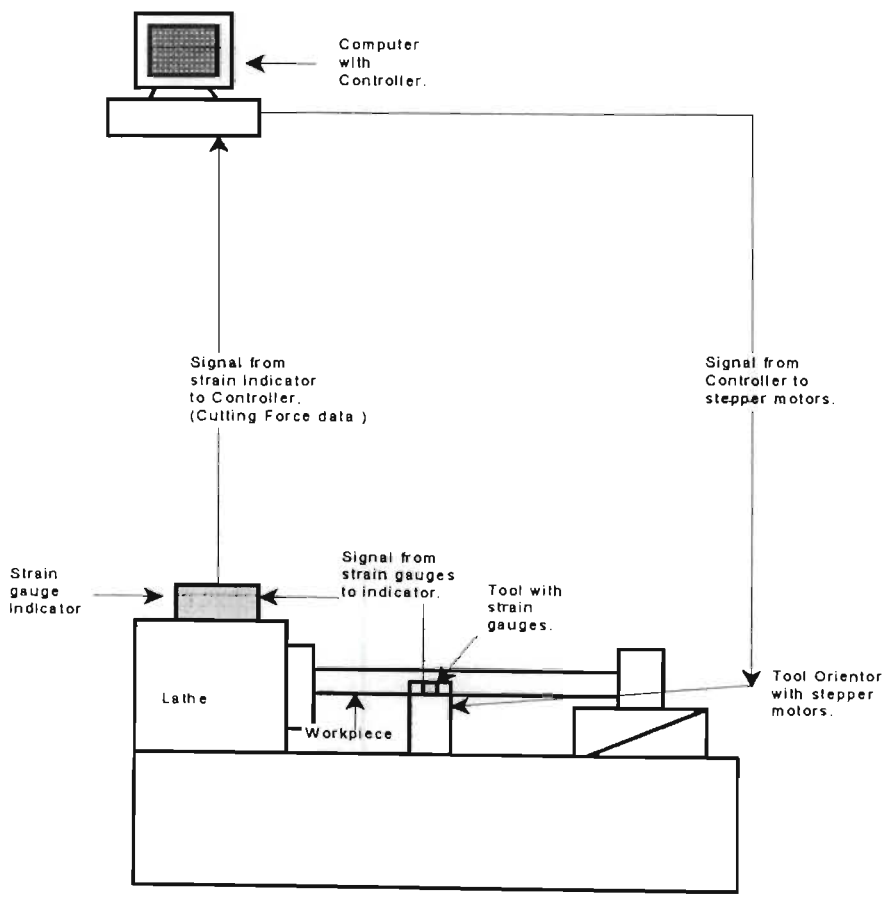

Figure 4.1[a] Experimental Setup.

Design criteria were set to ensure that the mechanism can function effectively. The design criteria are:

1) It must be possible to build the system with the funds available.
2) It must be possible to change a rake angle without influencing the other cutting parameters.
3) It must be possible to change a rake angle under computer control.
4) It must be possible to mount a conventional tool holder on the mechanism.
5) The system must be small enough to be mounted on a conventional lathe without to many modifications.

Many systems were designed to obtain geometrical variation of the cutter, but a mechanism sliding in slots which results in rotation around the tip of the tool in the different planes, met all design criteria the best.

A method was also required to monitor machining efficiency to evaluate the influence of changing tool angles. Parameters like machining forces, vibrations of the machine tool, power consumption of the lathe, acoustic emission and temperature buildup of the tool, chip and workpiece, can all be used to determine the performance of the machine tool. The measurement of cutting forces was the best measure of cutting conditions within the constraints of the budget. Strain gauges were connected to the tip of the tool holder measuring bending. Many calibration operations were needed to verify the true meaning of the voltage value obtained from the strain gauges.

A controlling program was also developed to change the tool geometry in response to information obtained from measuring the Cutting Forces. This process is called

adaptive control. [55,56] This controlling program can read the data obtained on the current cutting conditions and decide how much the tool geometry should be varied. The new rake angles determined is implemented by the program via a series of signals to the stepper motors resulting in rotation in a certain direction with the correct number of steps to achieve the desired angular adjustment.

The main aim of this project is to get this on-line controller operational and to monitor the improvement in efficiency achievable with this system. Other experiments were conducted to verify the operational characteristics of the controller, tool orientator and force measurement devices.

4.2 Tool orientator:

A tool orientator was designed to change the tool geometry on-line. This tool orientator had to be designed cheaply since limited funds were available for the project. The aim of the development of the tool orientator is to design a system that will change the tool geometry, and therefore increase cutting efficiency with every set of cutting parameters being used. It is therefore important to ensure that the mechanism does not effect the current cutting parameters like depth of cut, cutting speed, feed rate and metal removal when the geometry is being adjusted. If any of these parameters were to change as well, the cutting conditions will change due to the change in cutting parameters and not the change in tool geometry. For the best possible optimization, the tool orientator is developed for use under computer control. This ensures the best possible evaluation of the current cutting conditions at a number of times per second.

Every effort was made to design the system for ease of application to existing machine tool technology. The system is small enough to fit it on a conventional lathe. The mechanism is also designed to withstand vibrations that can develop during machining, ensuring that the cutting capability of the conventional machine tool is not influenced.

Many ideas were researched for development as a tool orientator. A pneumatic sliding mechanism, a hydraulic diaphragm, a three-dimensional rotational device and a floating tool were all evaluated as possible methods to change the tool geometry. The final system chosen has aspects of each of these conceptual models. The tool orientator eventually chosen for this project, is designed around the tip of the tool that acts as the centre of rotation in all planes of rotation. The tool orientator consists of four sections enabling rotation around every axis through the tip. See figure 4.2[a].

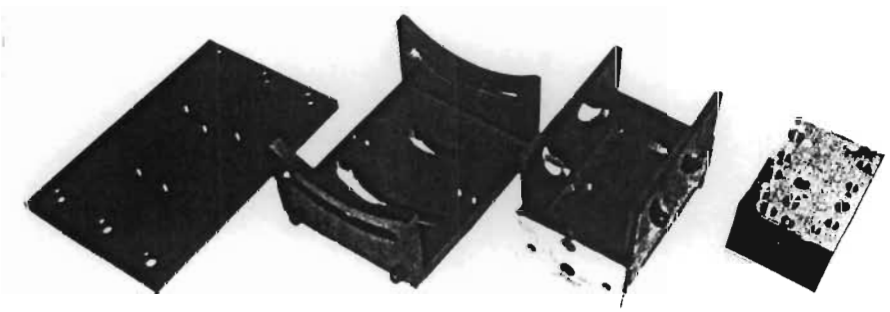

Figure 4.2[a] The four parts of the tool orientator.

Part one of the orientator slides in part two, resulting in rotation of the tool orientator around the y-axis and the tip of the tool. See figure 4.2[b]. This rotation results in a change of the Back-Rake angle and also a change in the End-Clearance angle. Dimensional accuracy of the parts is of a very high standard, and the tolerance between the different parts is tight to ensure a tight fit. This is important as the tool orientator must be able to withstand high machining forces without vibrations or unwanted movement.

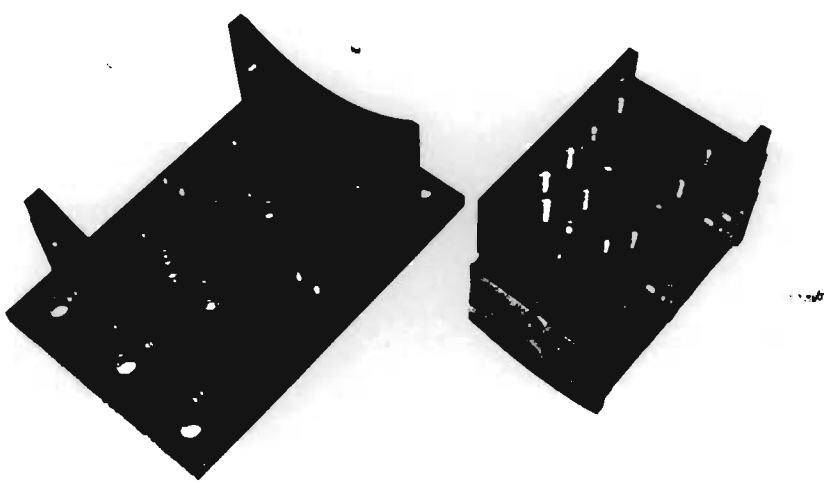

Figure 4.2[b] Assembly of the different Parts

Sliding of part two in slots provided in part three, results in rotation of the tool orientator around the x-axis. See figure 4.2[b]. Rotation around the x-axis change the Side Rake angle and also a change in the Side Clearance angle. Provision was also made for a third movement, with part three sliding in slots provided in part four. This movement results in

rotation of the tool tip around the z-axis. Rotation around the z-axis result in a change in the Side Cutting Edge Angle.

The effect of this angle on cutting conditions is less important than the effect of rake angles as seen from previous research discussed in chapter two, and for this project this adjustment capability of the tool orientator was not used.

A lead-screw is connected to the different parts to provide the sliding action between them. Rotation of the lead screw provides smooth adjustment of the angle. Rotation of the lead screw results in a change in Back Rake angle. Rotation of the lead screw can also result in a change in the Side Rake angle. The relation between rotation of the lead screw and the angular displacement is analysed in appendix 5.2[a] for back rake angle adjustment, and appendix 5.2[b] for side rake angle adjustment. See figure 4.2 [c] and [d].

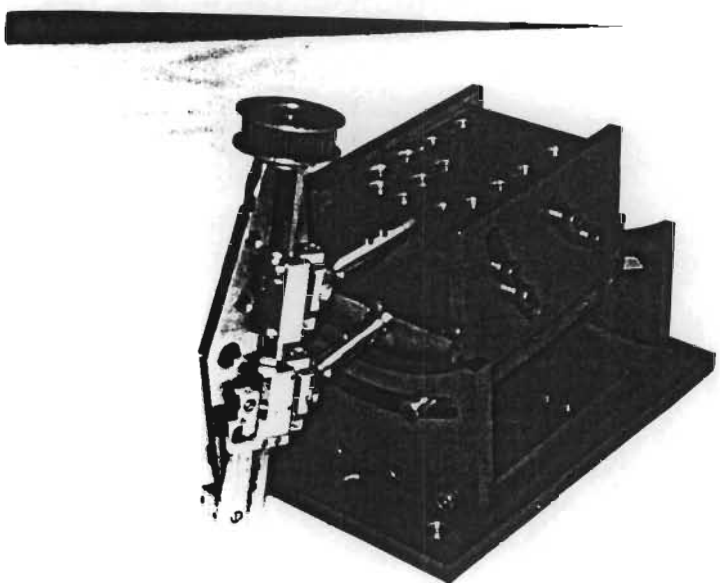

Figure 4.2[c] Tool Orientator configuration for back rake adjustment.

A stepper motor is connected to the lead screw with a

toothed belt.

Due to the rotation of the mechanism around the tool tip, no other machining parameters should be effected.

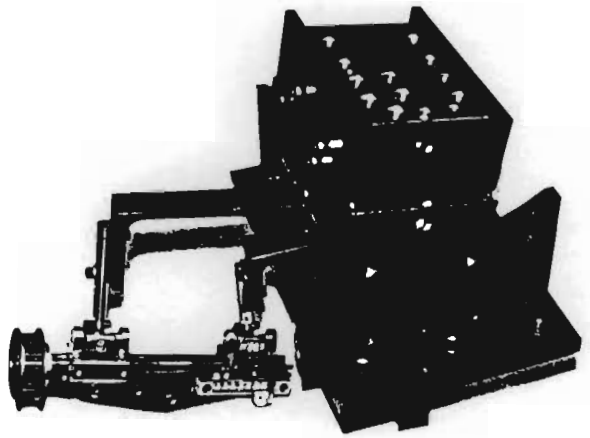

Figure 4.2[d] Tool orientator configuration for side rake adjustment.

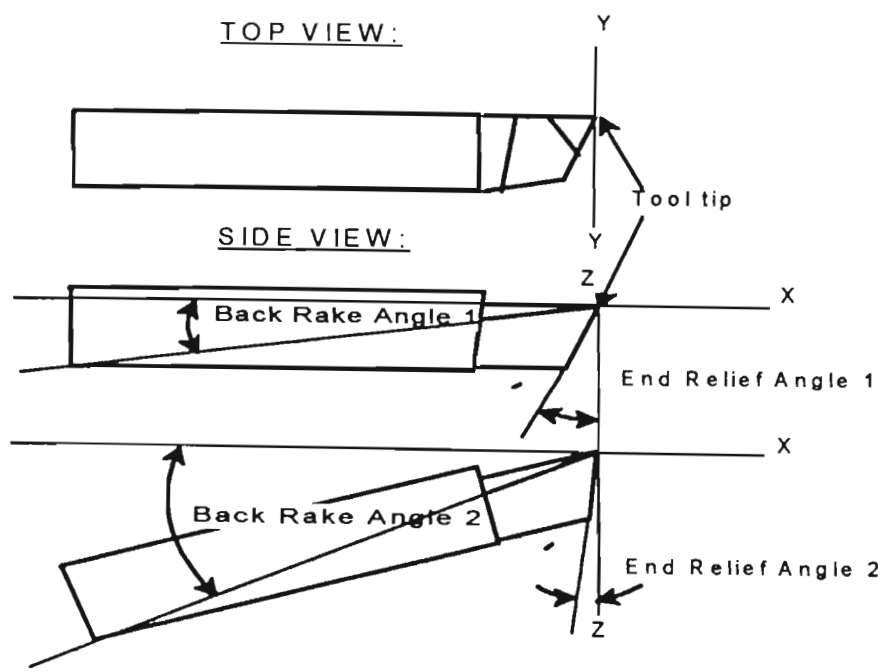

Figure 4.2[e] Effect on tool tip position when the tool is rotated around the y-axis

The effect on the tool positioning when the tool is rotated around the y-axis is shown in more detail in figure 4.2[e]. The effect on the tool positioning when the tool is rotated around the x-axis is shown in more detail in figure 4.2[f].

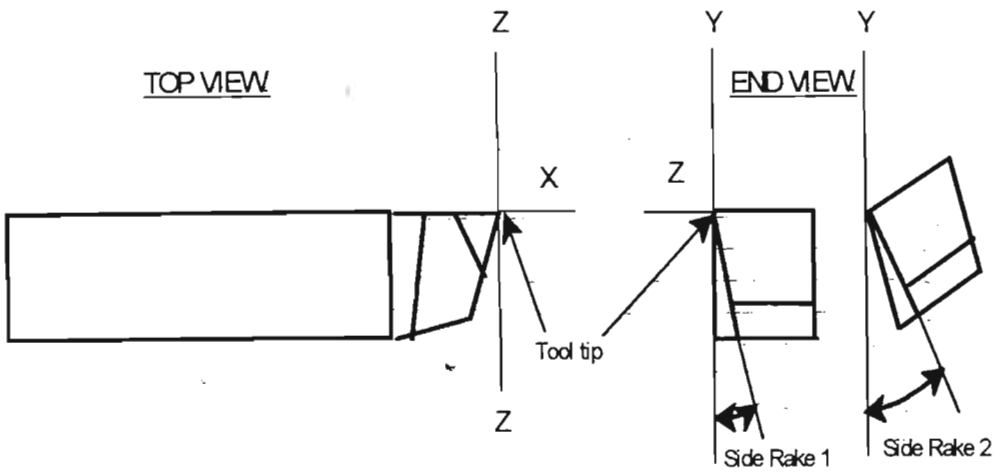

Figure 4.2[f] Effect on tool tip position when the tool is rotated around the x-axis.

4.3 Force sensing:

To measure the efficiency of the cutting process, parameters like vibrations of the machine tool [57], power consumption of the lathe, acoustic emission of the cutter [58,59], temperature buildup of the tool and machining forces can be monitored.[14,60,61,62]
The vibration of the machine tool is effected by the change of tool geometry as seen in section (2.7). The vibration of the machine tool also effects the cutting forces and also depends on the tool design. Vibration was not measured for cutting efficiency evaluation since the measurement apparatus was not readily

available for this project and is quite expensive. This measurement technique is also inaccurate since vibrations inherent to the tool design and lathe design will increase with machining speed. The vibration levels at high machining speeds is too high to be influenced by the variation in vibration due to different Back Rake angles.
Power consumption of the lathe was measured in the early stages of this project. The problem experienced here, was that the variation in the power consumption when machining at different Rake angles, was so small that it could not be read accurately. The lathe used for research work was designed for heavy machining operations, and the power consumption when the motor is running does not vary a lot for light machining operations.

Acoustic sound emission can also be used to evaluate cutting conditions if level of wear must be determined accurately.[63] The determination of the acoustic voice-print of the tool is a lengthy process that also requires some expensive apparatus.
It was decided not to measure the tool-workpiece interface temperature during machining since this parameter varies with time. The tool and workpiece act as a heat sink so that the temperature variation is not directly related to the current machining conditions, but can be influenced by previous machining operations.
Cutting forces were monitored to evaluate the efficiency of the machining operation for the purposes of this project. Varying the rake angles influence the cutting forces a lot in turning operations resulting in effective measurement of the efficiency of machining. Measuring the effect of a change in machining conditions on the cutting forces is far easier and

cheaper, than to evaluate the effect on the power consumption of the lathe, increase in temperature of the chip-workpiece or the change in acoustic emission. Forces can be sensed with pressure transducers, dynameter, dedicated computer chips and strain gauges. [64] Using strain gauges were cheap and accurate enough to prove the idea of on-line control of tool geometry in this project.

The strain gauges are arranged to measure the bending of the tool under the influence of mainly the cutting force. See figure 4.3[a]. The actual bending of the tool has to be small not to influence the cutting process itself, and therefore the strain gauges are chosen and arranged in a bridge setup to be highly sensitive. See appendix 4.3[a] for strain gauge sensitivity analysis.

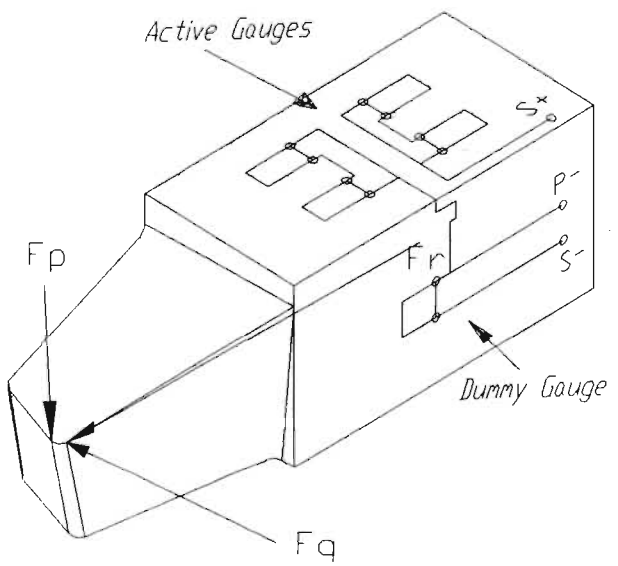

Figure 4.3[a] Strain gauge arrangement on tool holder.

Four strain gauges are placed on top of the tool

holder. These stain gauges are called the active gauges as they measure the actual values in which we are interested. The strain gauges are connected in two parallel serial pairs. See figure 4.3[a]. The reason behind this connection method is to gain maximum sensitivity without increasing the total resistance of the strain gauges. Each strain gauge has a resistance of about 350 ohms. In every leg two strain gauges are connected in series with total resistance of:

$$350ohm+350ohm=700ohm$$

two parallel legs result in a strain value of:

$$\frac{1}{R}=\frac{1}{700}+\frac{1}{700}$$

$$R=350ohm$$

This results in a sensitive 4-gauge arrangement which still acts as one gauge for input into the bridge amplifier.
The tool holder expands or contracts with a change in temperature.

This thermal expansion will influence the output value of the strain gauges resulting in inaccurate measurement of the cutting forces. The effect of this thermal expansion must therefore be calculated and subtracted from the results. Another method used to compensate for thermal expansion, is by fitting an extra strain gauge on the side of the tool holder. This ensures that this strain gauge is under the same thermal conditions but almost completely cut off from the effect of the cutting forces on the tool holder.

Every effort is made to isolate the dummy gauge from the bending effect of the tool, but to keep it at the same temperature. This gauge is not under the same bending conditions as the active gauge however. This ensures that both gauges elongate due to temperature changes, but the result is subtracted due to the way it is connected in the bridge. This results in pure strain being measured. Any strain effect measured by gauge D is also deducted from the measurement of gauge A. This method is used in the experimental setup since it is more accurate than a mathematical calculation which is always an approximation of the real conditions. The dummy strain gauge measures the real conditions and subtract that.

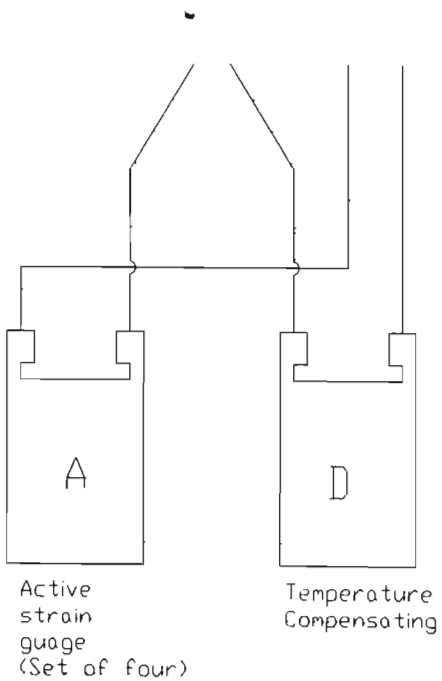

Figure 4.3[b] Attachment of dummy strain gauge for temperature compensation.

The strain gauges are connected in a Half-bridge setup as can be seen in figure 4.3[b]. The half-bridge setup

is used since we want to measure the force in only one plane but want to subtract the temperature effect as measured by the dummy gauge from the final output value. The half bridge setup subtracts the values in the two legs of the bridge from each-other. The strain gauge indicator used for initial amplification and filtering of the voltages across the strain gauges in this project, is designed to do compensation of either half bridge or full-bridge strain gauge setups.

4.4 Instrumentation:

To measure the strain, a strain gauge indicator was used. See figure 4.4[a].

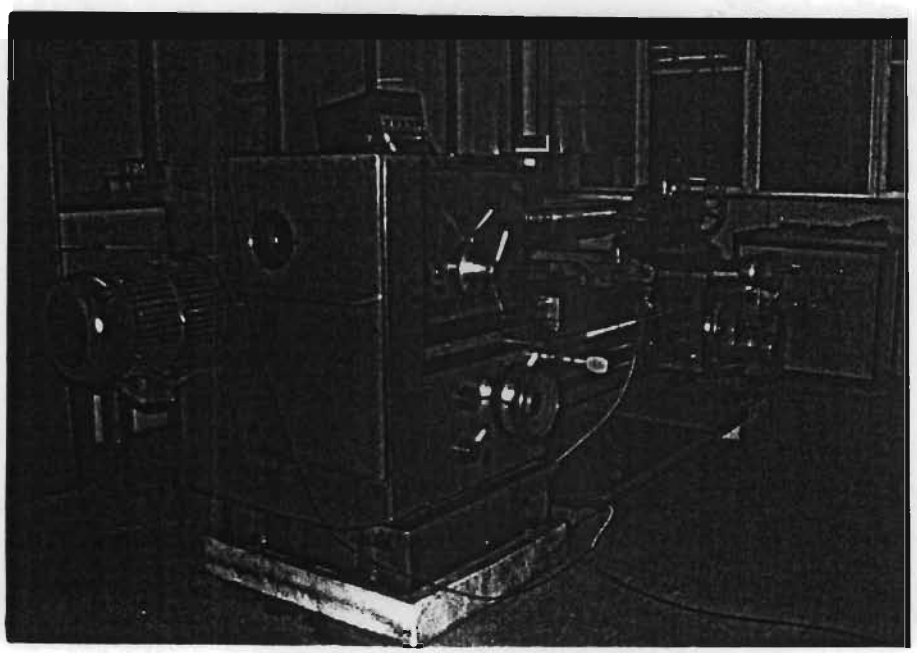

Figure 4.4[a] Experimental Lathe with Strain gauge indicator mounted on top.

See appendix 4.4[a] for a description of the strain indicator operational principles.

It was important to solve all problems related to the accuracy of the readout as the experiments conducted have to be repeatable. The strain gauge indicator comes with a balancing resistor to ensure that the two legs of the bridge have almost precisely the same resistance. The best sensitivity is obtainable when the bridge is balanced.

Another problem that can lead to inaccurate measurements is zero drift. Zero drift occurs due to some external influence like temperature on one of leg of the bridge circuit. If both legs were influenced to the same extent, the influence would balance out and will not be visible at the final output of the bridge amplifier. Besides the temperature, differences in the lengths of the lead wires, differences in the connection points of each leg of the bridge and magnetic influences on the different lead wires can also effect the zero point.

Creep can also develop as time elapses, when a constant load is applied. This is normally due to bad bonding or high temperatures.

The problem of dispersion of data obtained form strain gauges also had to be solved. This scatter of readouts results in bad repeatability occurred due to bad grounding techniques. Defective insulation of the strain gauges also plays a role.

When all these problems were researched and solved, effective force measurement was achieved.

The correct wiring techniques used for connecting the strain gauges to each other and to the bridge amplifier will be discussed in appendix 4.4[b].

4.5 Amplification circuit:

The build-in strain gauge amplifier in the strain gauge indicator amplifies the measurements to an extent, but it was found that better accuracy is required to use the data effectively.

To increase the sensitivity of the measured values, an extra amplification and filtering circuit was developed. The amplification system requires a filtering circuit. All the noise at the output of the strain gauge amplifier and in the wiring between the strain gauge amplifier and the amplification circuit will also be amplified if it is not filtered first.

A *SALLET and KEY Lowpass filter circuit* effectively filters out most of the unwanted noise.

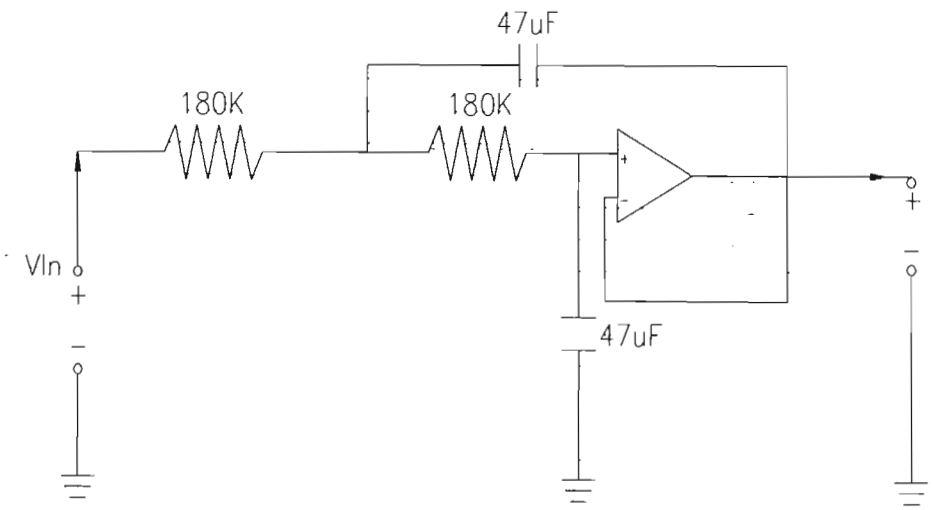

Figure 4.5[a] Filtering circuit Diagram

Different elements in the circuit were chosen to make the sensitivity to noise as low as possible.
Two of these filtering circuits are used in series. The output from this filtering circuit feeds into an amplification circuit to get maximum sensitivity of important values. See figure 4.5[a] for the circuit diagram.
The *Amplification Circuit* was also developed to suit required sensitivity without resulting in distortion of the measured values.
See figure 4.5[b].

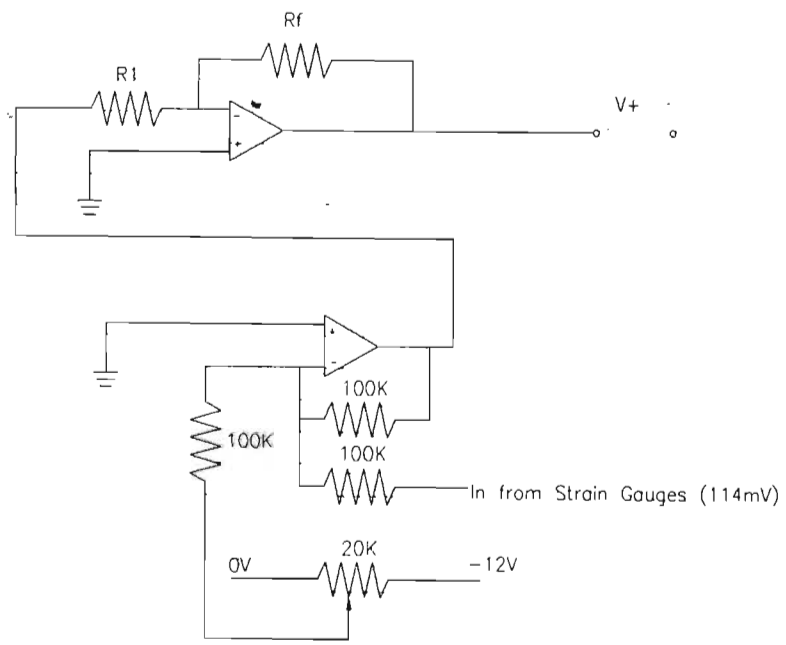

Figure 4.5[b] Amplification Circuit Diagram

4.6 Controller.

A controller was developed to do on-line control of the rake angles. This program was written in Turbo Pascal and consists of five main procedures. The flow process chart for the program can be seen in figure 4.6[a].

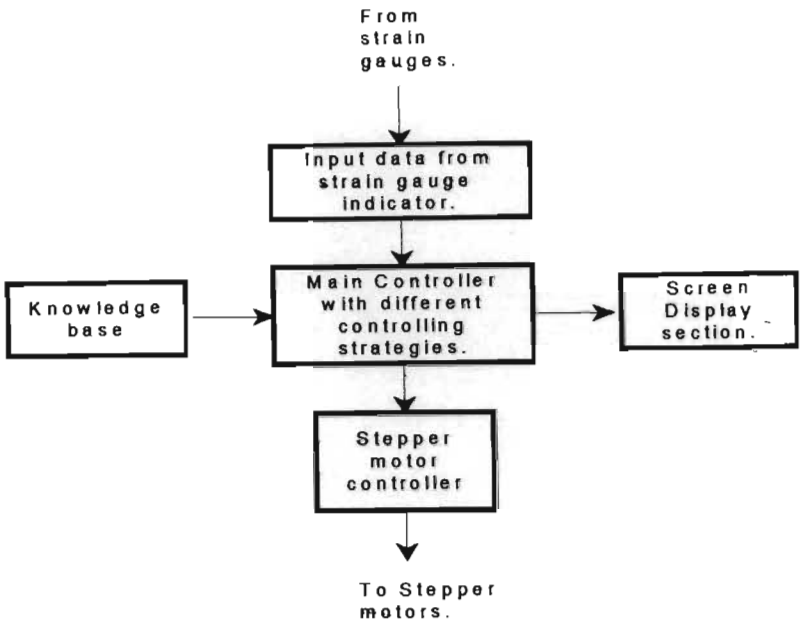

Figure 4.6[a] Main flow process chart for the controller.

The procedures act as an expert system to help the main program to evaluate the conditions for an appropriate action, to do adaptive control, to control the output of data to the screen, and to control the stepper motors. The program listing can be viewed using the stiffy supplied.(See appendix 4.6[b])

The procedure controlling the input of data obtained from the strain gauges simplifies communication between the computer and a PC30D computer card used to convert the analog signals from the bridge amplifier into digital signals used by the computer. It initializes the card and make access to the different channels easy.

An *on-line screen display section* was developed. There are two screen display options. The first screen shows the current force value and rake angle position as it

change with time. See figure 4.6 [b].

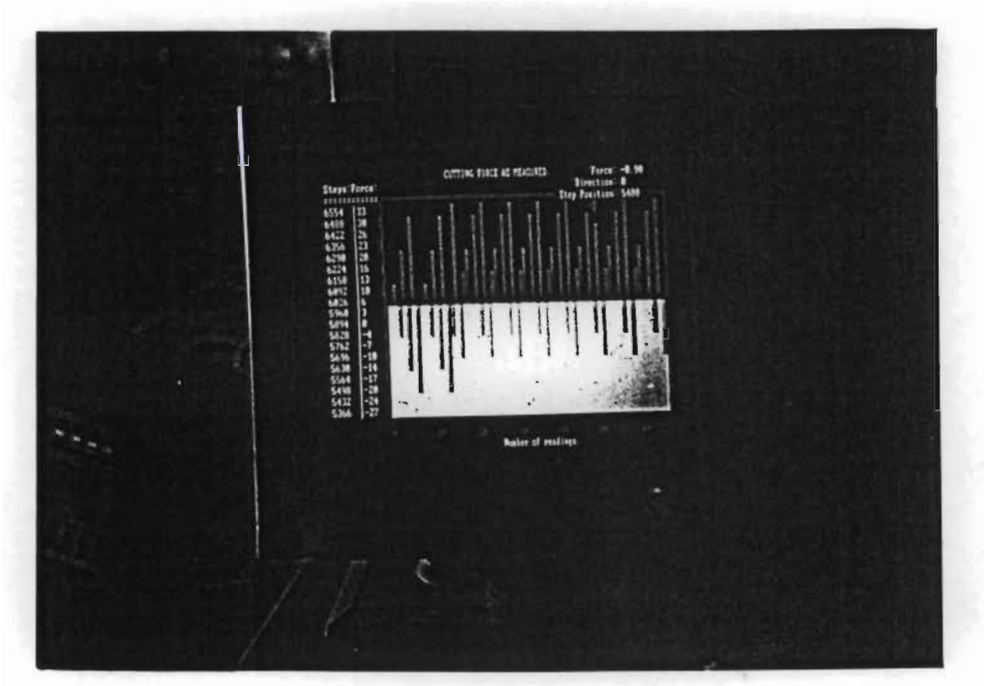

Figure 4.6[b] Controller screen display for force vs rake angle

When the screen is filled, the screen will scroll so that current data will be displayed from the start of the screen again. The actual Force values and rake angle values will also be displayed as numerical values on the screen. To make sure the resolution of the display is good, the screen only displays the relevant section of data and change the headings for the x and y-axis accordingly. The range displayed can be adjusted on request by pressing the letter C. The displayed range would then centralize around the current values. The force values are displayed as white bar-graphs. The rake angle values are displayed as grey bar graphs. When the force values are higher than the rake angle values, the force values are displayed as a dotted white bar graph.

The second screen option displays the force value vs the angular value. See figure 4.6 [c].

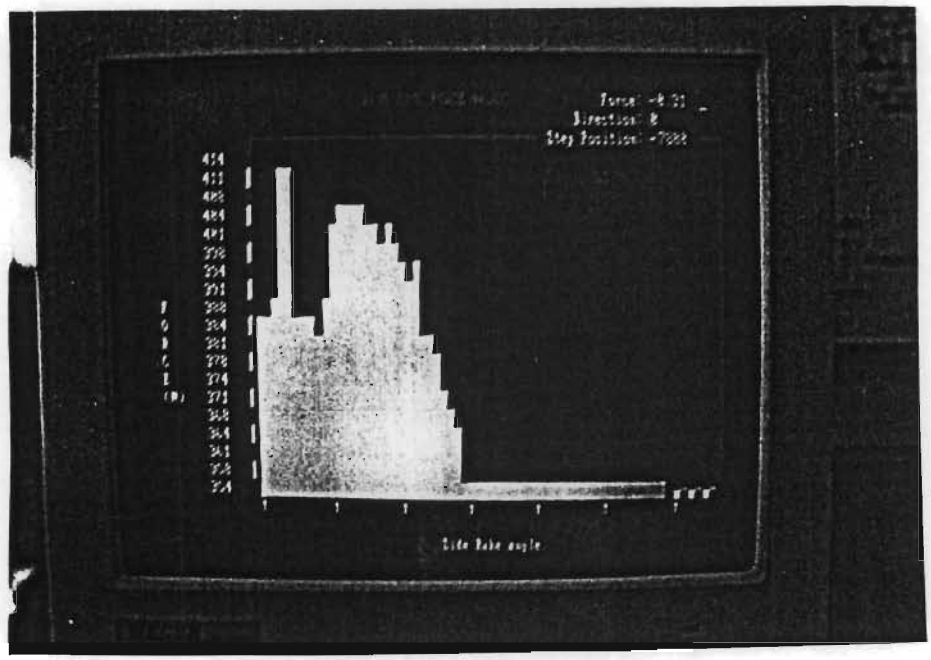

Figure 4.6[c] Controller screen display for force vs angular value.

This shows how the force value change with side rake angles or back rake angles. The x-axis of the screen will then represent the actual angle. The y-axis represent the Force value for that specific angle.
To ensure good resolution of the displayed force-values, only the current force value and the area around it is being displayed. On demand the screen can be recalibrated to show the current force value at the vertical centre of the screen. The screen will be recalibrated once it is full, since the current force will be displayed from the start again to ensure continuous updating and scrolling of the screen.

The *Main controlling procedure* handles the adaptive control of tool geometry in response to input data obtained form the strain indicator.[55] Different controlling strategies were developed to make the evaluation of the system's operation possible.[65,66]

Unidirectional optimization procedure:
This system prefers positive side rake angles and negative back rake angles. The controller will constantly aim for lower force values. See figure 4.6[d] for a flow diagram of the controller logic.

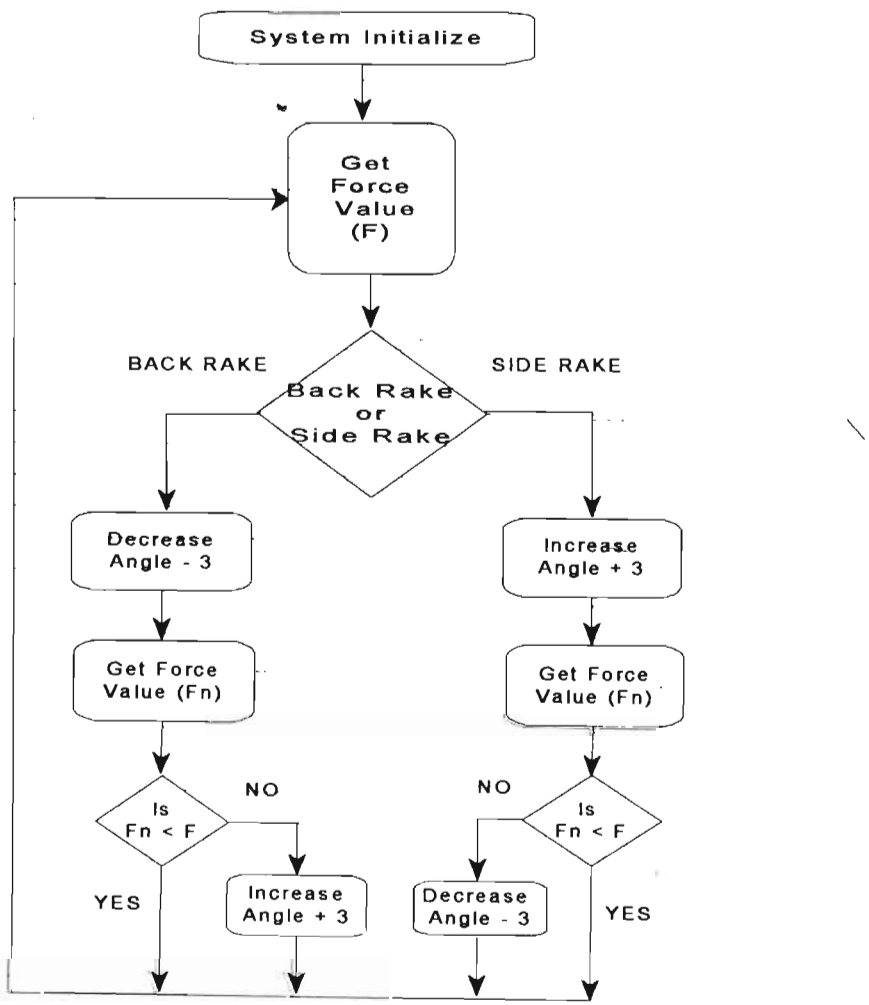

Figure 4.6[d] Unidirectional optimization procedure Controller logic.

The controller checks the force values at more positive side rake and more negative back rake angle values as for the previous optimization procedure. Adjustment in tool rake angles will only occur when it will result in a more positive side rake angle or a more negative back rake angle with lower forces. The optimization procedure can be initialized again by the operator when operating conditions change. This system was developed to evaluate the performance of the tool orientator and controller quickly under steady state operating conditions.

Continuous evaluative optimization procedure:
The controller change the angle a few degrees positive memorize the force value and then change the angle past the start position a few degrees negative. See figure 4.6[e] for the controller logic.
The force value at this point is compared with the force value stored previously and the angle is changed to the angular position corresponding to the lowest force value. At this new point, the force value at more positive and more negative angular positions to this point is evaluated and the angular adjustment needed to keep the force values low is found again, resulting in another adjustment. This evaluation system continuous indefinitely and has the added advantage that any material can be mounted for machining, and the correct rake angle settings will be found automatically. The range within which rake angles are adjusted to search for lower cutting forces will also be adjusted automatically when force values reached a minimum. No expert system is needed with this system, but the resultant force values might not be optimal. This system only observes the benefit of low forces, and will not consider the effect on surface finish, chip

control and other machining conditions as mentioned previously.

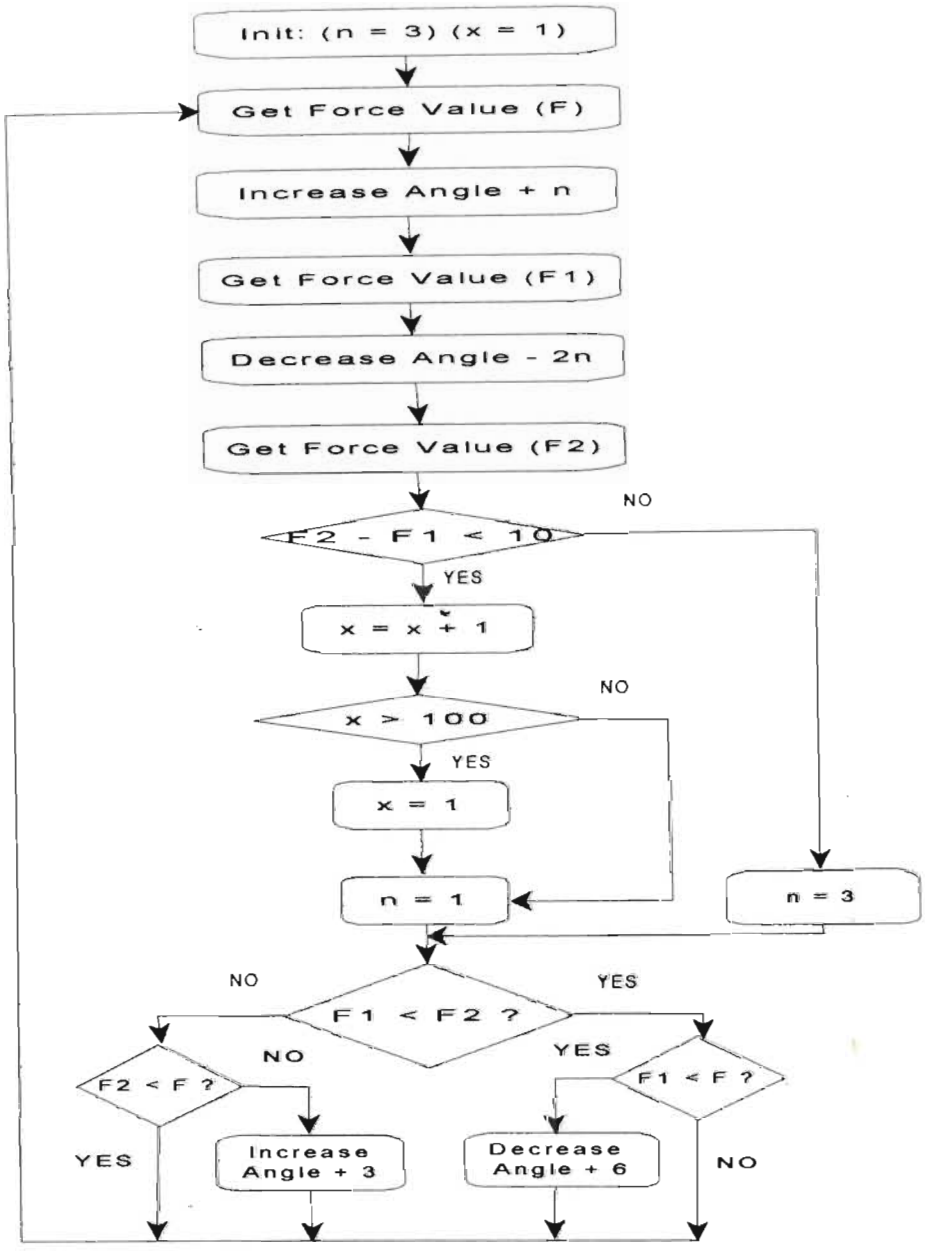

Figure 4.6[e] Continuous evaluative optimization procedure Controller logic.

Initial evaluative system with expert system:
When initiating the controller, the expert system will demand information about the material to be machined,

the type of tool to be used and the type of operation planned.[67]

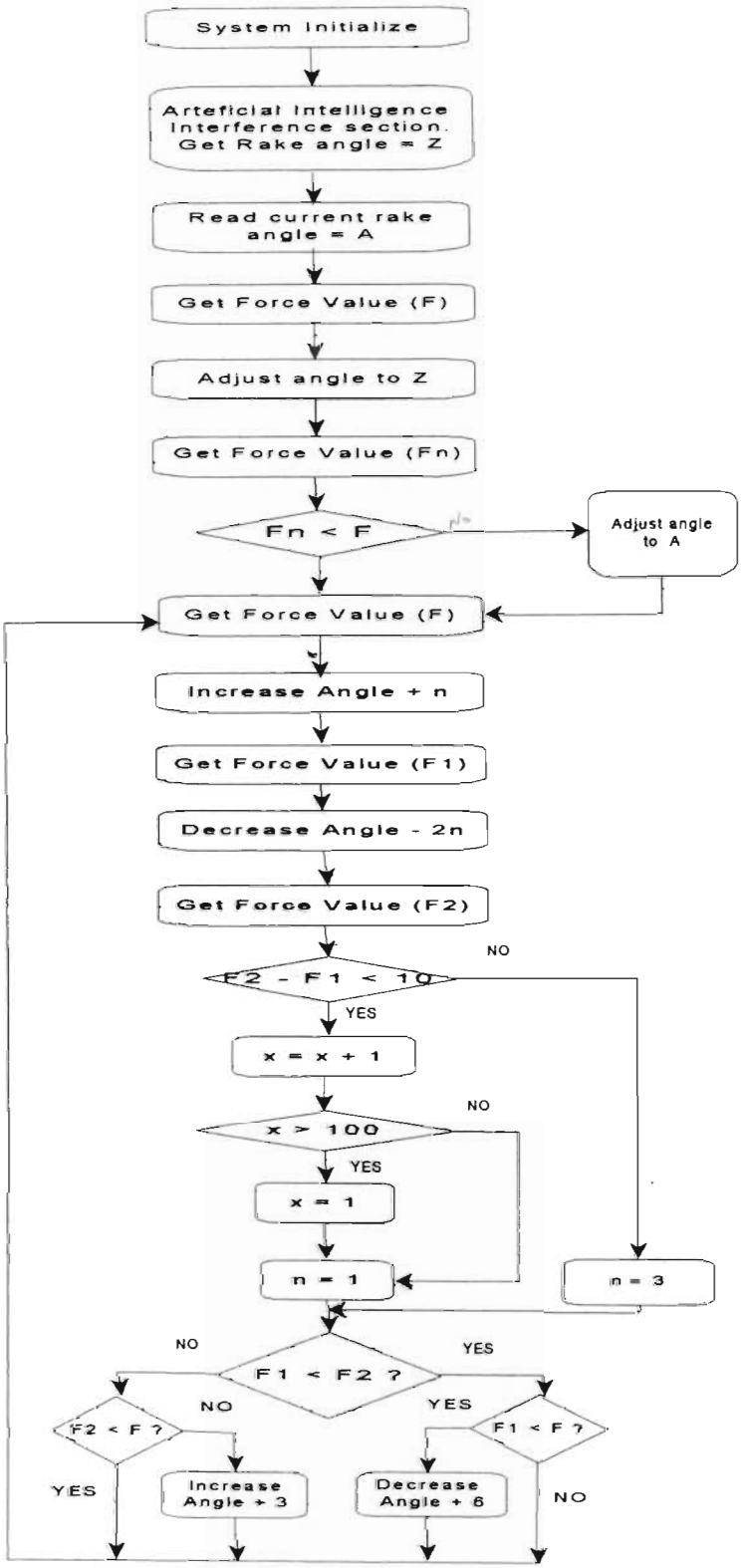

Figure 4.6[f] Initial evaluative system Controller logic.

The aim of the operation might be to machine Aluminium with a coated carbide tip while obtaining the best possible surface finish. From this information the expert system can then determine what the correct angle should be for optimum machining.[68] See figure 4.6[f] for the controller logic.
The system will bring the tool from the current angle to an angular value close to the predicted value checking the force values. If the force values increase much more than predetermined values, according to the expert system, the system will warn the operator and return the angle to a point of lower force values. This system was found to deliver the best results due to its adaptability to the required circumstances.

The *stepper motor controller* uses the basic parallel RS232 printer port. [69] See appendix 4.6 [a]. One binary output line controls the direction of turning while the other controls the number of steps.
The stepper will turn positive when analog values one and three are alternatively read to port [$3BC+000]. When converted to binary values, the analog value one, will result in a high on the first binary line and a zero on the next. The analog value three will result in a high on both the first and second binary output lines. This means the direction channel will show a high all the time while the direction channel will switch between high and low each time. For negative rotation, the direction channel will always show a low (zero). The direction channel will switch. (zero and two is read alternatively by port [$3BC+000].) The speed of binary signals switching, will determine the speed at which the stepper motor turns.

The knowledge base contains all the relevant information about cutting conditions for different types of material.[70,71] The knowledge base is part of the controlling program. See appendix 4.6[b]. A typical expert system consists of a knowledge base, an inference engine, a data acquisition module and a data processing module.[67]

The following information is typically used by the knowledge base to determine the correct tool geometry:

-The type of material to be machined.[29] As found in the literature study, the material can be classified into four sections; Aluminium and other soft metals, steel, titanium alloys and nickel-based alloys. Within these groups the rake angles have different ranges where machining is efficient.

-The cutting speed, depth of cut, feed rate and the cutting tool material influence the stress in the tool and the forces required for machining greatly. With other machining information, this influence the range of rake angles required for efficient machining greatly.

-The type of operation planned, also affects the tool geometry. As discussed previously rake angles resulting in lower efficiency has to be used at times to ensure a good surface finish or improved chip flow.

CHAPTER 5

5 EXPERIMENTAL INVESTIGATION

5.1 Introduction

The experimental work was conducted on a Boeringer research lathe situated at the mechanical engineering buildings of the University of Natal Durban. See figure 5.1[a].

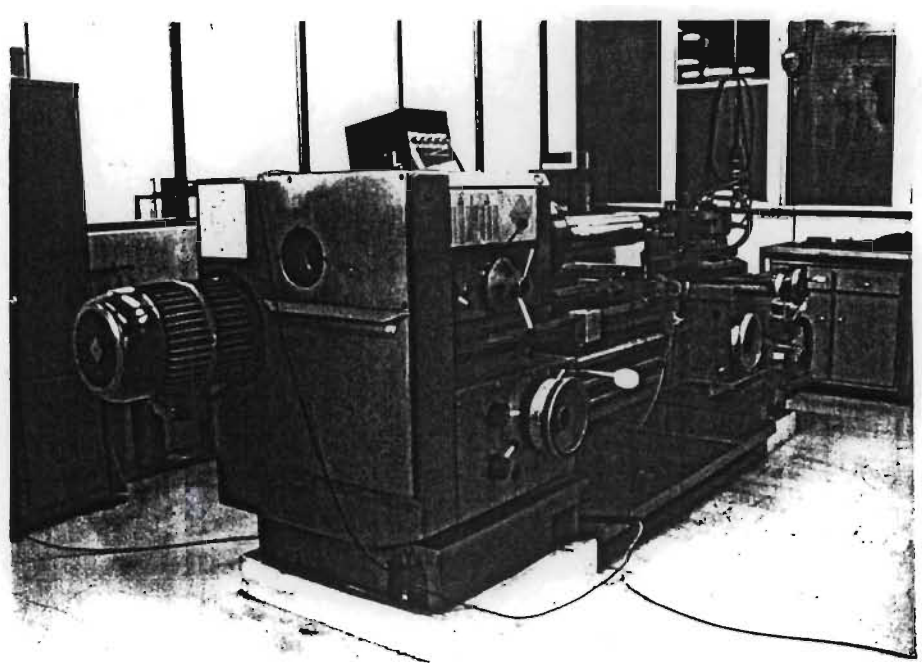

Figure 5.1[a] Boeringer Research Lathe

The lathe has a three-metre bed and a five hundred millimetres swing. The chuck through-bore diameter is ninety millimetres. Carbon tool inserts were used.
The tool orientator was designed to simplify changing of the cutter geometry during machining and mounts onto the existing tool mounting post of the lathe. Alignment of the tool orientator in respect to the workpiece is important as a change in the tool geometry must not

result in a change in other cutting conditions like depth of cut or metal removal rate. Experimental work was conducted using this setup to prove that tool geometry can be changed on-line during machining, resulting in improved machining conditions.

Calibration forms an important part of the experimental work. The purpose of calibration is to analyse the measured values in detail to decide what force values are represented. After calibration, the measured values can be used in experimental work to analyse the effect of changing rake angles on the machining conditions. Known forces were applied to the y-y and z-z planes to calibrate the strain gauges to measure force values applied in the respective planes. The force applied in the y-y plane correspond to the feed force during machining and the force applied in the z-z plane correspond to the cutting force during machining. The strain gauge readouts for both these force applications vary with a linear relationship as expected for strain gauges bonded correctly.

It was determined through experimentation, what the influence of a changing back and side rake angles respectively are on steady forces applied in the y-y and z-z planes. The relationships developed for this influence show a linear change with back rake angle and side rake angle. These calibration tests were conducted to compensate for this effect when the results are used in evaluation of cutting conditions.

A third calibration test was conducted to show what the relationship is between cutting forces and feed forces in the measured value, during actual machining.

Experimental work on the effect of changing rake angles was conducted using the calibration curves developed. These experiments were conducted over a wide range of varying cutting conditions to prove that the system

developed for experimental work proves the effect of changing rake angles effectively.
The repeatability of the results was analysed and also the effect of temperature compensation on the measured values.
Lastly the effectiveness of this system to control the rake angles during machining was evaluated. The experimental work proves that the idea of on-line control of tool geometry in a production environment is viable and has potential to improve machining efficiency.

5.2 Experimental definitions and calculations

The lead screw displacement can be calculated for a change in back rake angle. The geometrical displacement of the tool orientator is analysed in appendix 5.2[a]. The lead screw requires 4.925 rotations for one degree change in back rake angle. Every rotation of the lead screw requires 200 steps by the stepper motor.

The lead screw displacement can also be calculated for a change in side rake angle. The geometrical displacement of the tool is analysed in appendix 5.2[b]. The lead screw requires 7.6 rotations from the stepper motor for one degree change in the side rake angle.

5.3 Tool specimen and cutting conditions

Dry turning was conducted on a mild steel work piece with a diameter of about eighty millimetres and total length of about five hundred millimetres. Sections of this length was used for experimentation. A tool holder with carbon inserts was used. The aim of these tests

was to obtain evidence of the effect of different cutting angles on different cutting conditions. Only the specific angle researched was changed during the test, and all the other parameters were held constant. Operating conditions resembled real-life situations as close as possible within the limits of the tool orientator. Limitations during experimental work, are set by the tool orientator that is inherently more prone to vibrations than the conventional tool-post due to its adjustment capabilities.

5.4 Calibration

The tool orientator and the force measurement equipment had to be calibrated before experimental work could be conducted. Calibration ensures that the experimental results obtained in this project, can be compared with experimental results obtained by previous researchers.

First, the relationship between the strain gauge indicator output and the force values applied in the z-z plane had to be determined. The force value in the z-z plane is generally called the cutting force in turning operations. The effect of changes in both the back and side rake angles on this relationship was also evaluated.

Secondly the relationship between the strain gauge indicator output and the force values applied in the y-y plane had to be determined. The force value in the y-y plane is generally called the feed force in turning operations. As for cutting forces, the effect of changes in both the back and side rake angles on this relationship was also evaluated.

Thirdly the relative influence of the cutting force and the feed force on the strain gauge indicator output during machining had to be determined. The calibration experiments shows that the output value represents the cutting force, with the percentage feed force so small that it can be ignored.

5.4.1 Calibration of strain gauge output for Cutting force excitation.

This is the process where strain gauges are calibrated for pure Cutting force excitation. (The cutting force is a force applied in the Z-Z plane). The calibration values were obtained by hanging different known weights on the tip of the tool in the Z-Z plane. See figure 5.4[a].

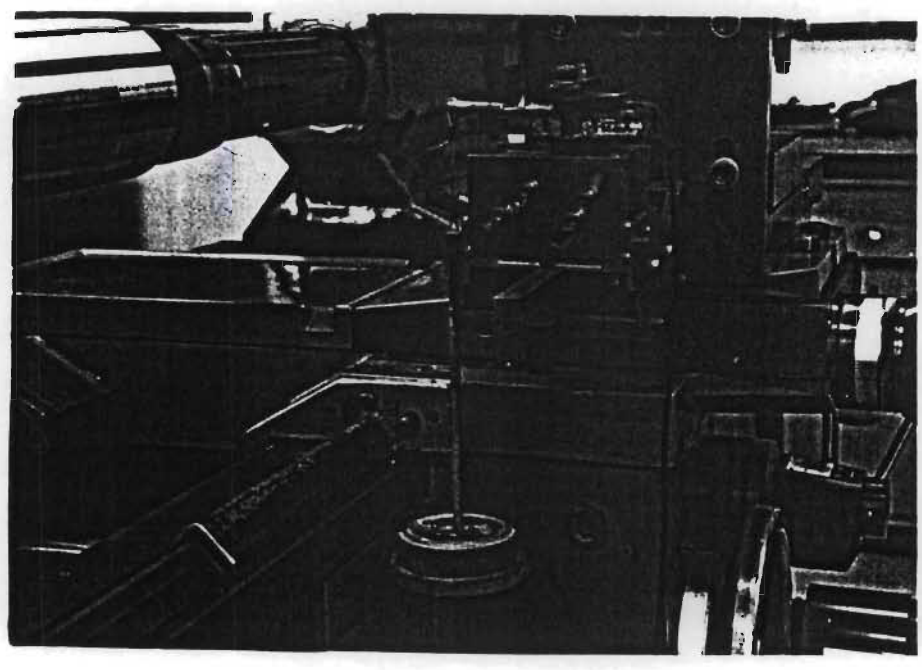

Figure 5.4[a] Calibration for force applied in the z-z plane.

The value of the weights varied from zero to seventeen kilograms in steps of one kilogram. The actual force

applied was determined by multiplying the weight in kilograms with the gravitational accelerator constant. Strain gauge indicator readouts were determined for this range of weights and the resulting graph can be seen in figure 5.4[b].

Equation 5.4.1 was developed from the calibration data and can be used to determine force values from the strain gauge indicator output.

$$F_{cut}=(F_v-0.028456)/0.017737 \qquad (5.4.1)$$

where: F_{cut} = Cutting Force (Newton)

F_v = Strain Indicator Output (Volts)

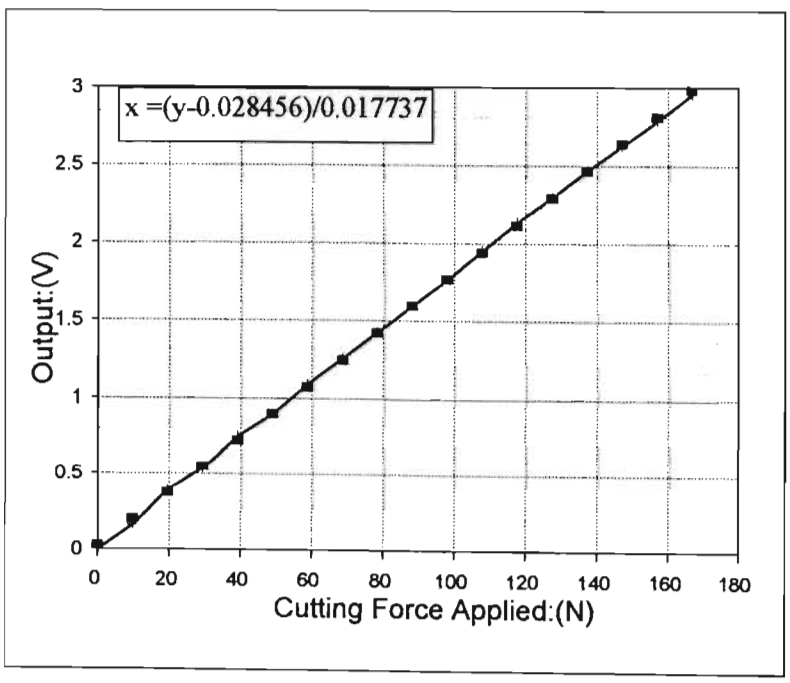

Figure 5.4[b] Bridge Amplifier Output for change in Cutting Force.

This equation is used in all experimental work to evaluate the cutting force values represented by voltage values obtained form the strain gauge indicator. This calibration relationship was developed for zero degrees back rake angle and zero degrees side rake angle. For this set of condition, the strain gauges are oriented at an angle of 90 degrees in relation to the z-z plane. Changing the side rake or back rake angle moves the strain gauges to a plane that is not oriented at an angle of 90 degrees in relation to the z-z plane. To determine the effect of changing the tool geometry on the calibration equation, force values were determined from the strain gauge indicator for a range of back and side rake angles with a known force applied in the z-z plane. The calibration values obtained for these variations can be seen in graph form in figure 5.4(c) and 5.4(d).

Equation 5.4.2 was developed to calculated the force value offset due to changes in the Back Rake Angle.

$$F_{BR\text{-}C\text{-}dev} = -0.02918(BR) + 4.5E\text{-}18 \qquad (5.4.2)$$

Where: $F_{BR\text{-}C\text{-}dev}$ = Cutting Force deviation due to change in Back Rake angle.

BR = Back Rake Angle.

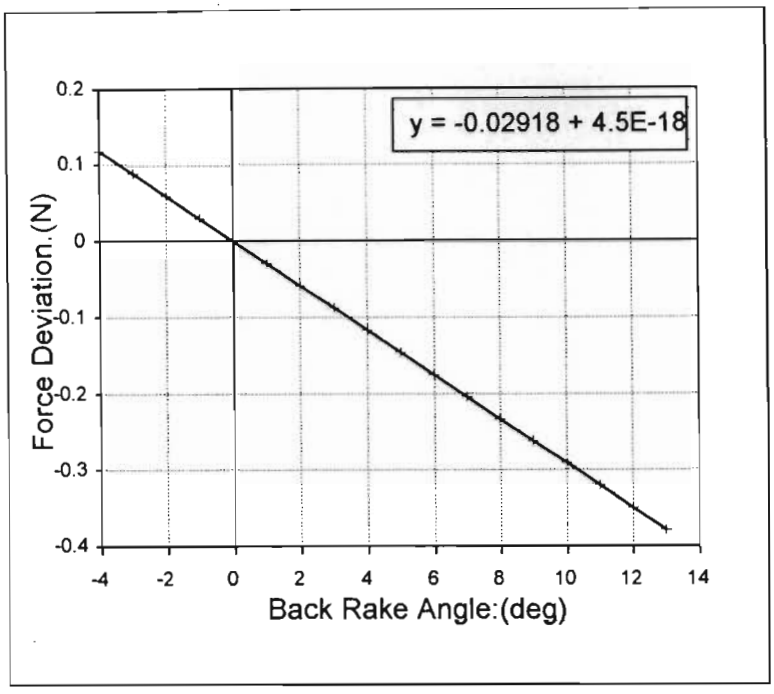

Figure 5.4[c] Deviation between measured and applied force due to a change in Back Rake Angle.

Equation 5.4.3 was developed to calculate the force value offset due to changes in the Side Rake Angle.

$$F_{SR\text{-}C\text{-}dev} = -1.59347(SR) + 3.9E\text{-}15 \qquad (5.4.3)$$

Where: $F_{SR\text{-}C\text{-}dev}$ = Cutting force deviation due to a change in Side Rake Angle.

SR = Side Rake Angle

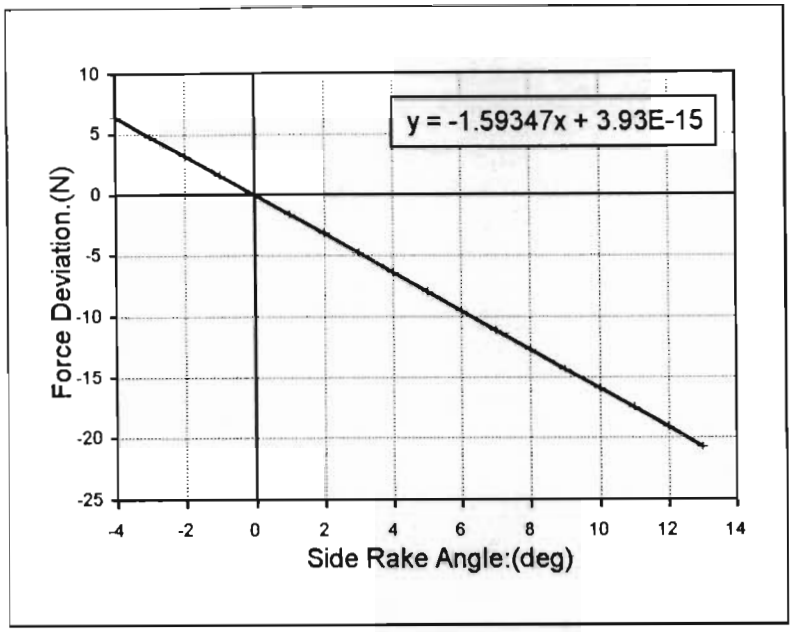

Figure 5.4[d] Deviation between measured and applied force due to a change in Side Rake Angle.

For the purposes of this project, a relation was developed incorporating equations 5.4.1, 5.4.2 and 5.4.3. This relation can be used to determine the real cutting force from the output of the strain gauge indicator for any rake angle when forces are applied onto the tool in the z-z plane

$$F_{cut}=(F_v-0.028456)/0.017737+F_{BR\text{-}C\text{-}dev}+F_{SR\text{-}C\text{-}dev} \qquad (5.4.4)$$

$$F_{cut}=56.38F_v-1.59347(SR)-0.02918(BR)-1.60433$$

This relationship will give the actual cutting force for both positive and negative rake angles.

5.4.2 Calibration of strain gauge output for Feed force excitation.

During this process the strain gauges are calibrated for pure Feed Force excitation. (Force applied in the

Y-Y plane). The calibration values are obtained by hanging different known weights on the tip of the tool in the Y-Y plane. See figure 5.4[e].

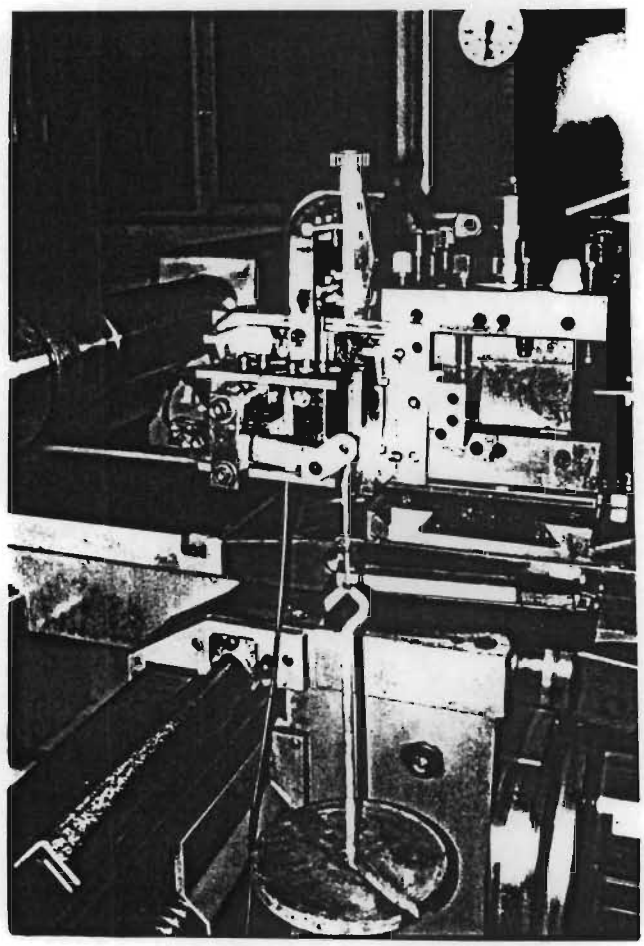

Figure 5.4[e] Calibration for force applied in the y-y plane.

Force values in steps of one kilogram where applied from zero to seventeen kilograms. The actual force applied was determined by multiplying the weight in kilograms with the gravitational accelerator constant. The strain gauge readouts for every force value applied where determined for all the force values applied and plotted. A curve fitted to this plot was used to derive a mathematical equation for the Feed force. This curve can be used to determine feed-force values from the strain gauge indicator output.

$$F_{feed} = (F_v + 0.02425)/0.010886 \qquad (5.4.5)$$

where: F_{feed} = Feed Force (Newton)

F_v = Strain Indicator Output (Volts)

The relationship between the feed forces and the strain gauge output is linear in nature like the relationship between cutting force and the strain gauge output. See figure 5.4[f].

Equation 5.4.5 is used in experimental work to evaluate the feed force values represented by the voltage values obtained from the strain gauge indicator.

This calibration relationship was developed for zero degrees back and side rake angle. For this set of conditions, the strain gauges are oriented at an angle of 90 degrees in relation to the y-y plane.

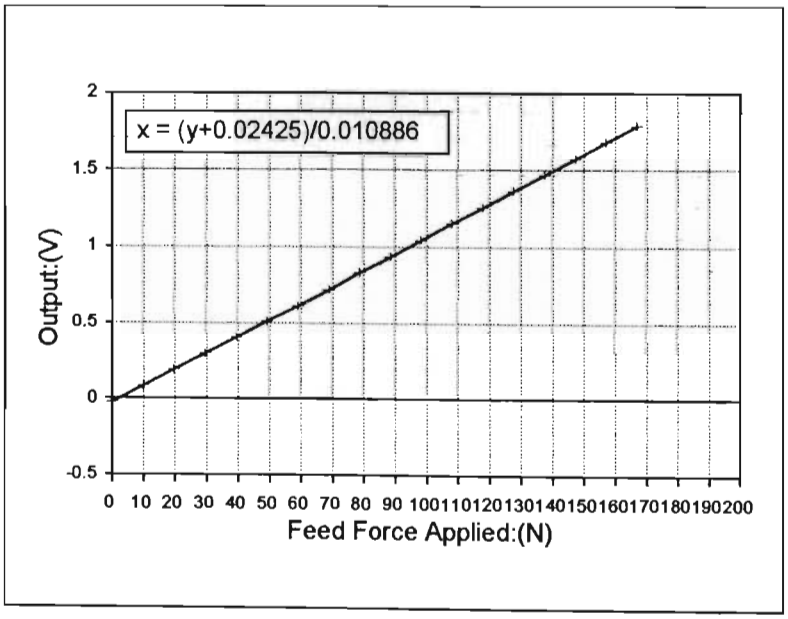

Figure 5.4[f] Bridge Amplifier Output for change in Feed Force.

Changing the rake angles moves the strain gauges to a plane that is not oriented at an angle of 90 degrees in relation to the y-y plane.

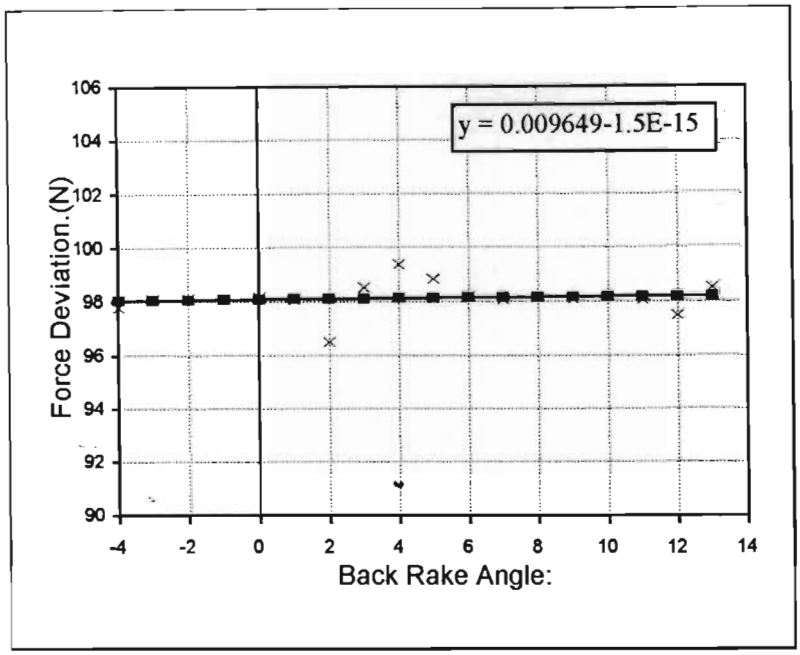

Figure 5.4[g] Deviation between measured and applied Cutting-Force due to a change in Back Rake Angle.

As for the cutting force relation, the effect of changing the rake angles on the calibration equation was determined for a range of back and side rake angles with a known force applied in the y-y plane. The calibration offsets obtained for these variations can be seen in figure 5.4[g] and 5.4[h].

Equation 5.4.5 was developed to calculate the Feed force value offset due to changes in the Back Rake Angle.

$$F_{BR\text{-}F\text{-}dev} = 0.009649(BR) - 1.5E\text{-}15 \qquad 5.4.5$$

Where: $F_{BR\text{-}F\text{-}dev}$ = Feed Force deviation due to Back Rake Angle variations.

BR = Back Rake Angle.

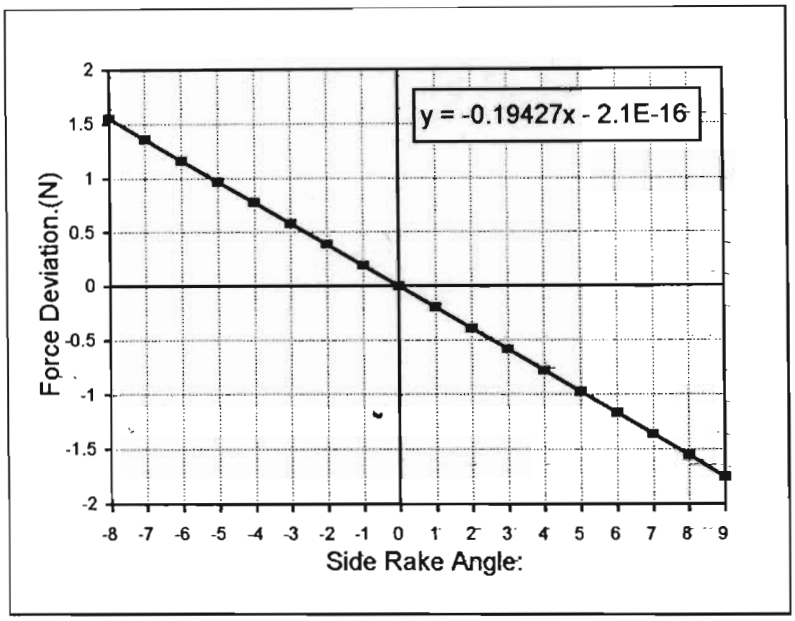

Figure 5.4[h] Deviation between measured and applied Feed-Force due to change in Side Rake Angle.

Equation 5.4.6 was developed to calculate the Feed Force value offset due to changes in the Side Rake Angle.

$$F_{SR\text{-}F\text{-}dev} = -0.19427(SR) - 2.1E\text{-}16 \qquad (5.4.6)$$

Where: $F_{SR\text{-}F\text{-}dev}$ = Feed Force deviation due to Side Rake Angle variation.

SR = Side Rake Angle.

Equation 5.4.7 was developed to determine the actual

feed force from the output of the strain gauge indicator for any rake angle when a force is applied in the x-x plane.

$$F_{feed}=(F_v+0.02425)/0.010886+F_{BR\text{-}F\text{-}dev}+F_{SR\text{-}F\text{-}dev} \qquad (5.4.7)$$

$$F_{feed}=91.86F_v-0.19427(SR)+0.009649(BR)+2.227$$

This relation holds true for both positive and negative rake angles.

5.4.3) Deriving the Cutting force vs Feed force relationship in the strain gauge indicator output.

Knowing whether the output value from the strain gauge indicator represents pure cutting forces or if feed forces are also included in this value is important for the purposes of this project. The output from the strain gauge indicator during a typical turning operation, can be converted to force values using equation 5.4.8 which is derived from equation 5.4.4 and 5.4.7.

$$F_{actual}=aF_{cut}+bF_{feed} \qquad (5.4.8)$$

Where: Factual = The force measured (Newton)

a = The fraction of strain gauge indicator output representing cutting forces.

b = The fraction of strain gauge indicator output representing feed forces.

Many experiments were conducted to determine the factors a and b.

Feed forces during turning operations develop due to the movement of the tool lateral over the surface of the workpiece. This movement with the depth of cut, determines the amount of metal removed for every revolution. When this feed rate is increased from zero while the depth of cut stays constant, the amount of metal removed, increase steadily till a specific value where the maximum tool/workpiece contact area is achieved. At this point, the maximum metal removal rate per rotation for the specific tool is achieved. When the feed rate is increased more than the value at this point, the feed rate per revolution is to fast to remove all the metal on the workpiece, and thread cutting occurs. The increase in feed force measured now, will be due to the speed of the feed motion only and not due to an increase in the metal removal rate. A number tests were conducted where the feed rate was increased steadily from zero. The feed rate was increased from zero to three-millimetre per revolution for all these tests. The force values vs the feed rate values for all these experiments are presented in graphs to display the effect described above. Tests were conducted for cutting speeds ranging from high to low to ensure that the effect of feed rate on different cutting conditions is known.

Experiment one:

See figure 5.4[i]

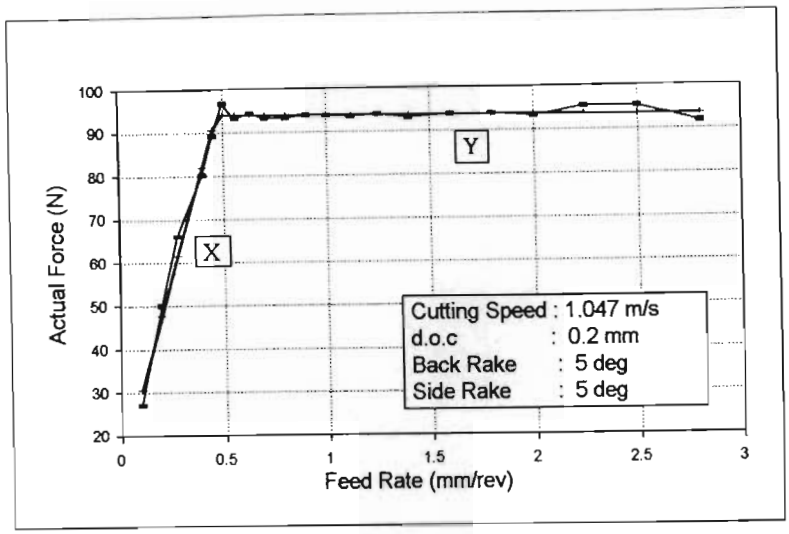

Figure 5.4[i] Actual force variation due to change in Feed rate.

Discussion:

This experiment was conducted at a relative low cutting speed of 1.047 m/s. Carbon steel tool tips were used to prevent BUE operation. The graph ,figure 5.4[i], of the experimental results can be split into two distinct sections, one linear section with the feed rate ranging from 0 to 0,5 mm/rev [X], and another linear section with the feed rate ranging from 0,5 to 3 mm/rev [Y].

The linear section [X] shows a steady increase in actual force$_{(eq.\ 5.4.8)}$ when the feed rate is increased from 0 to 0.5 mm/rev. This increase in actual force is due to the increase in the metal removal rate with an increase in the feed rate. The tool/workpiece contact area increase with this initial increase of feed rate as discussed previously.

For a feed rate of 0.5 mm/rev to 3 mm/rev, section [Y], the curve shows another linear relationship. This linear relationship represents a constant actual force measured by the strain gauges. The rate of metal removal is constant for this section since maximum

tool/workpiece contact area was already achieved with a feed rate of about 0.5 mm/rev. At this low cutting speed, the increase in feed rate can also not generate a big change in the value of the measured feed force since the strain gauges were set up to read mainly cutting forces and will therefore not pick up small variations.

Conclusion:

At this low cutting speed of 1.047 m/s, the output of the strain gauge indicator represents 100% cutting force. Therefore the cutting force is equal to the actual force. The feed force is negligible since no variation in the actual force was experienced for the feed rate ranging between 0.5 to 3 mm/rev. It can be deducted that the percentage feed force in the actual force is also negligible for the feed rate ranging between 0 and 0.5mm/rev since the feed force will be directly related to the feed rate. During turning operations, the feed rate is always less than 0.5 mm/rev unless it is a thread-cutting operation.

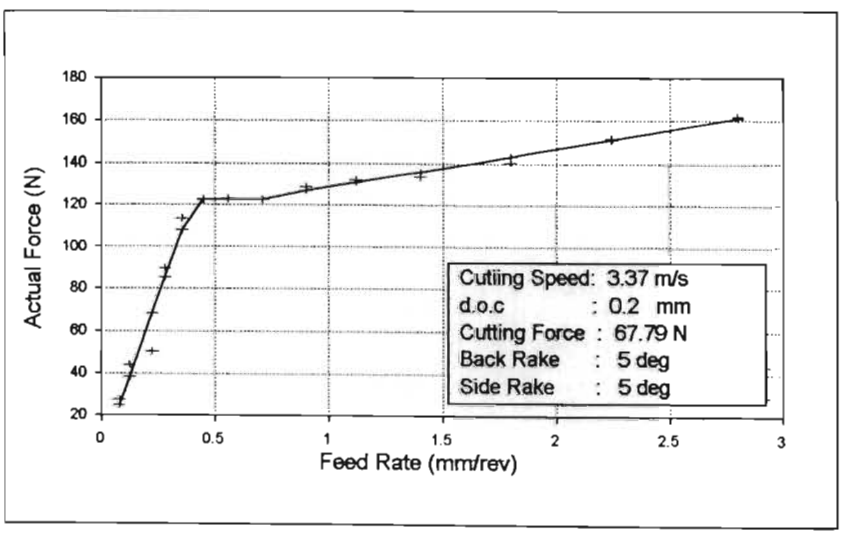

Figure 5.4[j] Actual force variation due to variation in feed rate.

Experiment two and three:

See figure 5.4[j] and 5.4[k].

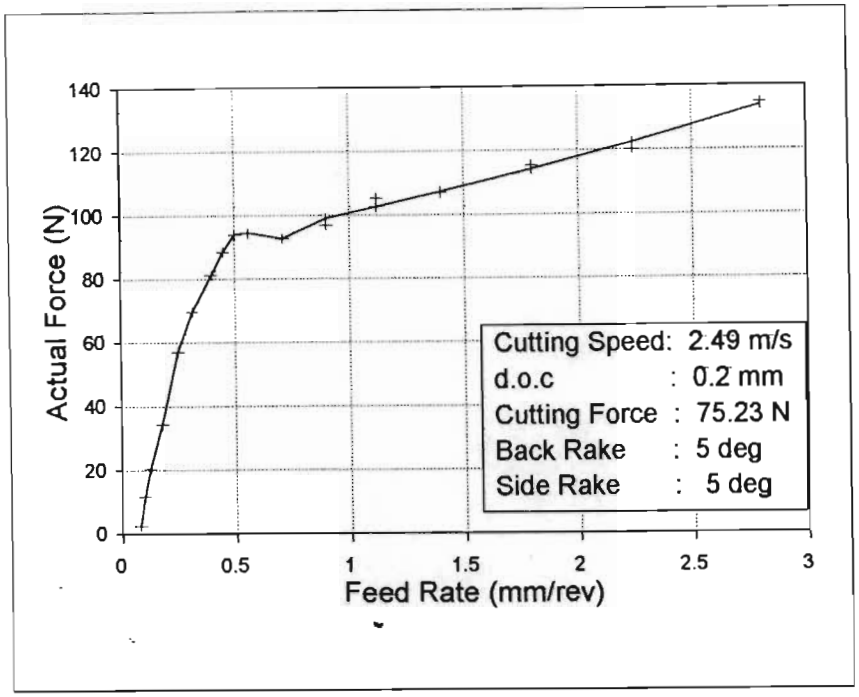

Figure 5.4[k] Actual force variation due to change in feed rate.

Discussion:

These two experiments were conducted at the higher cutting speeds of 2.49 and 3.37 m/s respectively. The graphs of the experimental results, are similar in that they can be divided into three distinct sections. The first linear section from 0 to about 5 mm/rev is similar to the first section as discussed with the first experiment.

From a feed rate of 0.4 to about 0.7 mm/rev the curve is flat which means the force values are not changing a lot. This is comparable to the second section of the plot for lower cutting speeds. The total amount of metal removed/revolution for this tool tip has been reached. Since the force stays constant in this field, it means the change in feed rate does not increase the force significantly. The cutting force should stay

almost constant in this region due to the amount of metal removed per time unit being constant. Any increase in measured force, will therefore be due to an increase in the feed force. The increase in feed force in this region is not detected by the strain gauges as in the second section of the plot for lower cutting speeds.

From a feed rate of 0.7 to 3 mm/rev the curve shows a linear increase in actual force values. The increase in feed force for this section is high enough to be detected due to the higher cutting speed and the high feed rate. Since the amount of metal removed cannot increase anymore, the cutting force should stay relatively constant.

Conclusion:

From the three graphs discussed above, it can be deducted that the strain gauges read mostly cutting forces as was intended by positioning the strain gauges on top of the tool holder. The fraction of the measured force that represents the feed force can be ignored in analysis of experimental results at the lower feed rates. If the cutting speed is low, the influence of Feed force on the strain gauges can be ignored completely as the feed force is never high enough to influence the actual force. The effect of feed forces on the actual force was ignored during experimental work conducted for this project, since the feed rate never increased more than 0.4 mm/rev.

5.5 Back Rake Angle evaluation

5.5.1 Introduction

Back Rake angles plays a mayor role in the improvement of cutting conditions. The effect of rake angles on the cutting conditions was evaluated experimentally using the apparatus developed for this project. The calibration equations as determined in the previous section, was used to determine experimental results. These experimental results are compared with the result obtained by the other researchers whose results are discussed in chapter two. The comparison will prove whether the work completed for this project is in line with common theory concerning machining operations or not. Once the experimental work is accepted as common theory, it will be shown that this theory can be implemented successfully into machining operations under computer control. To test the effect of changing back rake angles on cutting forces, a range of tests was conducted for different sets of cutting parameters. The set of cutting parameters under evaluation like cutting speed, depth of cut, feed rate and the other tool angles, was held constant during experimentation for every set of parameters while the back rake angle was varied throughout its range. Operating conditions were chosen to resemble real-life situations as close as possible.

During experimentation of the back rake angle, the tool is rotated around the y-axis going through the tip of the tool. This rotation facilitates a change in the back rake angle and a resultant change in the end clearance angle. The Back Rake angle was varied in this manner from minus four to ten degrees.

Cutting time for each test, conducted for a specific

angle, was about thirty seconds to ensure that enough time is available for the forces to stabilize. This time was short enough to ensure that the effect of tool wear can be eliminated from the tests. From these tests, a curve for cutting forces vs back rake angles was obtained. To make up the curve for minus four to ten degrees back rake, fifteen different tests had to be conducted each with a different back rake angle. In total ninety tests had to be conducted to obtain six different graphs for the variation of cutting forces with back rake angle.

5.5.2 Experimental procedure.

Experimental work to evaluate the influence of back rake angle variations on the cutting conditions is discussed in this section.

The set of cutting parameters for the different experiments were set as shown in table 5.5[a].

Table 5.5[a] shows that six different experiments were conducted. The results for a typical experiment are dependant on the set of cutting parameters chosen for that experiment. Due to the number of combinations available, only the results from the six experiments as shown in table 5.5[a] are reported.

Experiment nr.	Side Rake: (deg)	doc: (mm)	Cutting Speed: (m/s)	Feed Rate: (mm/rev)	Back Rake: (deg)
1	11	1	1	0.08	(-4 to +10)
2	11	1	1	0.2	(-4 to +10)
3	11	1	3.25	0.08	(-4 to +10)
4	11	1	3.25	0.2	(-4 to +10)
5	11	1	4.663	0.08	(-4 to +10)
6	11	1	4.663	0.2	(-4 to +10)

Table 5.5[a] Cutting parameters for Back Rake evaluation.

The *Side Rake Angle* was held constant at a positive angle of eleven degrees for all experiments. This positive side rake angle is used most often on carbon tool inserts and also on carbide inserts. This angle is generally quite efficient for the machining of steel and gives an acceptable surface finish as researched in chapter two. Although the experimental results are different for other side rake angles, it follows the same trend.

The *depth of cut* stayed constant at one millimetre for all the experiments. This depth was deep enough to create a sizeable force in metal cutting. It was also shallow enough to ensure that the tool orientator can withstand the vibrations and the cutting forces due to the worst machining conditions experienced with unsuitable rake angles.

The *Cutting Speed* was varied between ±4.663m/s, ±3.25 m/s and ±1 m/s for every back rake angle evaluated. This covers a wide range of cutting speeds used in industry.

The *Feed Rate* was varied between 0.08 mm/rev and 0.2 mm/rev for every back rake angle and cutting speed evaluated. This made sure the experimental work was conducted for high and low feed rates resembling the feed rates generally used in industry for light machining work.

Back Rake Angle was varied from minus four to ten degrees. This is the range of rake angles used most often in industry, and is also the limit of adjustment possible on the tool orientator.

For every experiment, a sequence of operations has to be followed to ensure the accuracy of the data. (See appendix 5.5[a].

5.6 Side Rake Angle evaluation

5.6.1 Introduction

The effect of the side rake angle on the cutting conditions also had to be verified on the experimental apparatus developed for this project and compared with results from other research work. The Side rake angles play a mayor role in machining efficiency. The effect of changing the side rake angle, on the cutting conditions, was tested by conducting tests for different sets of cutting parameters. The cutting parameters in the set consist of variables like the cutting speed, depth of cut, feed rate and all the different tool angles. Once all these variables have been set, a series of tests was conducted with only the side rake angle changing from test to test. The tool is rotated around the x-axis going through the tip of the tool to facilitate a change in side rake angle and also a resultant change in side clearance angle. All the other machining conditions were held constant during every test. The side rake angle was varied from minus ten to ten degrees. Cutting time for each test, conducted for a specific side rake angle, was about 30 seconds to ensure that enough time is available for the forces to stabilize. This was short enough to ensure that tool wear effects can be eliminated from the tests. From these tests, a curve for cutting forces vs rake angles was obtained. To make up the curve for minus eight to eleven degrees side rake, twenty different tests had to be conducted. Six different sets of cutting conditions were used to obtain six graphs for the variation of cutting forces with side rake angle.

5.6.2 Experimental procedure

Experiment nr.	Back Rake: (deg)	doc: (mm)	Cutting Speed: (m/s)	Feed Rate: (mm/rev)	Side Rake: (deg)
1	9	1	1.026	0.08	(-8 to +11)
2	9	1	1.026	0.2	(-8 to +11)
3	9	1	3.3	0.08	(-8 to +11)
4	9	1	3.3	0.2	(-8 to +11)
5	9	1	4.663	0.08	(-8 to +11)
6	9	1	4.663	0.2	(-8 to +11)

Table 5.6[a] Cutting parameters for Side Rake evaluation.

Table 5.6[a]shows the six different sets of parameters chosen for experimentation. As for the back rake angles, the parameters chosen for these experiments reflect typical machining conditions in industry.

The *Back Rake Angle* was held constant at a positive angle of nine degrees for all tests. This positive back rake angle is standard on most carbon tool and carbide inserts. This angle provides acceptable cutting conditions for most conditions.

The *depth of cut* stayed constant at one millimetre for all the tests. This cut was deep enough to create the forces required to measure the variation in forces with side rake angle. Vibrations due to unsuitable rake angles, start to influence the machining process at a later stage than for deeper cuts.

The *Cutting Speed* was varied between ±4.663m/s, ±3.30m/s and ±1.026m/s. The common cutting speeds used in industry, are covered within this range.

Feed Rate was varied between 0.08 mm/rev and 0.2 mm/rev. The effect of changing tool geometry on the cutting speed could effectively be measured at these

feed rates. It was noted that the effect of tool geometry on cutting conditions increased with increasing feed rate and cutting depth. The feed rates chosen for the tests, showed the effect well without putting too much strain on the tool orientator.
The *Side Rake Angle* was varied from minus eight to eleven degrees. These angles are used most often in industry for cutting steel. This is also the limit of adjustment possible on the tool orientator.

5.7 Repeatability

5.7.1 Introduction

The experimental results obtained during research, can be influenced by many factors. The *tool temperature* will be at room temperature for the first experiment of the day, but for subsequent tests, residual temperatures from the previous tests might influence the results obtained. The *tool tip* also *wears* progressively as it is being used. The *workpiece* also varies within a specified tolerance regarding hardness and ductility. These effects and others influence the repeatability of experimental results. The effect of these factors was reduced by incorporating noise filtering circuits and temperature compensation circuits into the experimental setup. The same workpiece and one type of tool tip were used throughout the experimental process.
The repeatability of experimental results must be obtained to ensure that the orientator developed for this project, can be used successfully to optimize cutting conditions. The optimization procedures evaluate the results continually to decide what is the optimal tool geometry for the current cutting conditions.

5.7.2 Experimental procedures.

Experiment 1

During experimental work in this section, a set of cutting parameters was chosen (see table 5.7[a]), and while keeping these parameters constant, fifteen separate tests with cutting time of five minutes each, were conducted. The procedure listed in appendix 5.5[a] was used to ensure similar cutting conditions. Regression analysis was used to get an average force value from the time dependant cutting data obtained for every experiment. The experiment was completed for two sets of cutting parameters, one resulting in stable cutting conditions, and the other resulting in unstable cutting conditions.
The average force values for the fifteen different tests, for each experiments, were compared to evaluate the repeatability.

Test nr.	Side Rake: (deg)	Back Rake: (deg)	doc: (mm)	Cutting Speed: (m/s)	Feed Rate: (mm/rev
1 to 15	11	0	1	3.25	0.08
1 to 15	11	0	1	1.004	0.08

Table 5.7[a] Cutting parameters for Repeatability evaluation experiment one.

Fifteen tests were conducted for both sets of parameters to consider the repeatability. The only difference between the two sets of parameters is the cutting speed. These cutting parameters were specifically chosen to evaluate repeatability for stable and unstable cutting conditions. The results

will be presented in the next chapter.

Experiment two

Further experimental work in this field, was conducted to show that the curve for force variation with side rake angle and back rake angles is repeatable. For this experiment, a set of cutting parameters was chosen and then held constant while the rake angle was adjusted. This experiment was repeated twice, once with a new tool and the second time with the same tool. See table 5.7[b] for the cutting parameters.

Test nr.	Side Rake: (deg)	Feed Rate: (mm/rev)	doc: (mm)	Cutting Speed: (m/s)	Tool condition	Back Rake: (deg)
1	11	0.08	1	3.25	new	(-4 to +10)
2	11	0.08	1	3.25	old	(-4 to +10)

Table 5.7[b] Cutting parameters for repeatability evaluation

For these experiments, the procedure listed in appendix 5.5[a] is also used to ensure the accuracy of the results. This process was repeated for new and old tools to see what the effect of wear on the repeatability of the experimental results is. The wear was not physically measured, but a tool with about twelfth hours machining time was considered to be old. The results obtained is discussed in the next chapter.

Experiment 3

The effect of temperature on the strain gauge output was also evaluated. As discussed in section 4.3, an additional strain gauge is mounted on the side of the

tool holder to provide compensation for temperature changes during machining. To evaluate the effect of this extra strain gauge on the strain gauge indicator output, two experiments were conducted, one with the temperature compensation, and one without. The use of a dummy strain gauge for temperature compensation was discussed on page fifty one. This dummy was excluded from the strain gauge circuit to do experimental analysis without temperature compensation. Table 5.7[c] lists the cutting parameters for evaluation of temperature compensation.

Test nr.	Side Rake: (deg)	Feed Rate: (mm/rev)	doc: (mm)	Cutting Speed: (m/s)	Temperature compensation:	Back Rake: (deg)
1	11	0.08	0.5	0.21	yes	8
2	11	0.08	0.5	0.21	no	8

Table 5.7[c] Cutting parameters for temperature compensation evaluation.

5.8 Evaluation of on-line control capabilities

5.8.1 Introduction

The previous sections in this chapter evaluate the functioning of the cutting condition monitoring system. Section 5.8 will evaluate the effectiveness of the controller to use the cutting condition monitoring system to improve cutting efficiency.

A controlling program described in section 4.6 was developed to evaluate the cutting conditions and to determine the appropriate tool geometry adjustment required to improve the cutting conditions. Different control algorithms were developed, and the functioning of each algorithm is evaluated in this section.

5.8.2 Experimental procedure

Experiment 1

The unidirectional optimization procedure allows the orientator to adjust the side rake angle more positive with a few degrees at a time, continually monitoring the cutting conditions, till a minimum force value is reached. The controller will look for decreasing force values with more positive side rake angles, since during stable machining of mild steel, the side rake angles should theoretically be high positive for efficient machining. (See chapter two). The same experiment is repeated for optimization of back rake angles, but then the cutting forces will increase with higher back rake angles. The algorithm is started when the stable machining conditions are reached, and the metal removal rate will not vary for some time. The aim of this algorithm is to find the most efficient positive angle for the cutting conditions. This algorithm can be used on a CNC machine where the optimization algorithm is called when stable cutting conditions is reached. The controller is set to initially searching a six-degree range for lower cutting forces, and then switch to only search a two-degree range.

The effect of this algorithm was shown by only controlling the rake angle using the following procedure:

1) Set the rake angles at the value suggested in table 5.8[a] and initiate the cutting process.
2) Allowed the cutting conditions to stabilize. Initiate the control algorithm to effect a change to more positive rake angles.

3) Run this experiment for at least 1 minute or till the cutting forces stabilize and evaluate the tool geometry and cutting conditions at the end of this period.

See table 5.8[a] for the cutting parameters. The results for this experiment are discussed in chapter six.

Experiment nr.	Side Rake: (deg) init.	Feed Rate: (mm/rev)	doc: (mm)	Cutting Speed: (m/s)	Controller option:	Back Rake: (deg)
1(a)	-6	0.08	1	1.026	one	0
1(b)	10	0.08	1	3.25	one	8
2(a)	-6	0.08	1	1.026	two	0
2(b)	10	0.08	1	3.25	two	8
3(a)	-6	0.08	1	1.026	three	0
3(b)	10	0.08	1	3.25	three	8

Table 5.8[a] Cutting parameters for performance evaluation.

Experiment two

The continuous evaluative optimization procedure option allows the orientator to search for a minimum force value by decreasing or increasing the rake angles dependent on the output from the strain gauge indicator. The objective and constraints of the optimization procedure is as discussed in chapter three. Lower force values or higher force values can be shown at the new tool geometry. The controller will continuously adjust the angles more positive and more negative evaluating the cutting conditions after every adjustment. When a lower force value is detected, the controller adjusts the orientator to the new tool geometry with better overall cutting efficiency. The evaluation procedure as discussed in detail in section

4.6 will restart at this new tool geometry, and the process to optimize the cutting conditions will start again. Separate experiments were conducted for side rake and back rake optimization, since the experimental setup cannot handle both at the same time. See table 5.8[a] for the cutting parameters at the start of each experiment. The controller was again set initially to search a six-degree range for lower cutting forces, and then switch to search a two-degree range. The effect of this algorithm was demonstrated using the following procedure:

1) Set the rake angle at the correct single as shown in table 5.8[a] and initiate the cutting process.
2) Allowed the cutting conditions to stabilize. Initiate the control algorithm to optimize cutting conditions.
3) Run this experiment for at least one minute and evaluate the tool geometry and cutting conditions at the end of this period.

The results for this experiment are discussed in chapter six.

Experiment 3

The initial evaluative controller with expert system loads information from the expert system on the material to be machined. See appendix 5.8[a] for explanation of expert system. The expert system will set a list of cutting parameters according to the cutting process requirements. These requirements might vary from the requirement to remove metal as quickly as possible to the need of obtaining a very precisely

machined surface at the highest possible cutting speed. Typical information obtained from the expert system will be the correct tool geometry for a set of cutting parameters like cutting speed, feed rate and depth of cut, for optimal cutter performance. Using this information, the controller will estimate what the optimal cutting conditions should be, and will adjust the orientator to try to obtain these values. The controller will evaluate the output from the strain gauge indicator to ensure that the cutting conditions change as anticipated. Separate experiments were conducted for side rake and back rake optimization, since the experimental setup cannot handle both at the same time.

The effect of this algorithm was demonstrated using the following procedure:

1) Enter data into the expert system. (The expert system needs to be told the cutting speed, depth of cut, feed rate and rake angle. The uncontrolled rake angle must be set here for the other one to be calculated by the expert system.)
2) Set the rake angles as suggested in table 5.8[a] and initiate the cutting process.
3) Allowed the cutting conditions to stabilize. During stable machining conditions, the controller is initiated to effect a change. The controller will automatically read the information from the expert system and change the tool geometry to the proposed value.
4) Run this experiment for at least one minute and evaluate the tool geometry and cutting conditions at the end of this period.

The results for this experiment are discussed in chapter six.

CHAPTER 6

6 DISCUSSION

It is demonstrated in chapter two that previous researchers identified tool geometry as an important factor in machining efficiency. Rake angles was identified as playing the most important role in this respect and therefore the focus of attention for this project was on the on-line optimization of rake angles for improved cutting efficiency. Chapter two also demonstrates how previous research links the changing of cutting forces to changes in the tool geometry and as a result, cutting conditions. They effectively calibrated the strain gauge set-up as described in section 5.4. The calibration ensures that the data obtained during experimental work can be compared directly with results obtained during previous research work. The strain gauge indicator output represents cutting forces that is not influenced by external effects like temperature and electrical noise. The cutting conditions for experimentation were chosen to reflect real-life cutting conditions as close as possible. The tool orientator developed for experimental work has limited capabilities. This resulted in little experimental work on high metal removal rate cutting conditions. It could still be shown effectively that the idea of optimization the tool geometry on-line is viable and can improve cutting conditions. The effective monitoring of cutting conditions and the repeatability of it, for both back and side rake angles, is shown in chapter five followed by the demonstration of on-line optimization capabilities. The on-line control capability is successfully proved during experimental work.

6.1 Back Rake Angle evaluation.

For each of the six experiments completed as discussed in section 5.5, tests were completed for fifteen back rake angles. A graph for force versus time was obtained from the strain gauge indicator for each of these fifteen rake angles. See figure 6.1 [a far two graphs obtained in this manner.

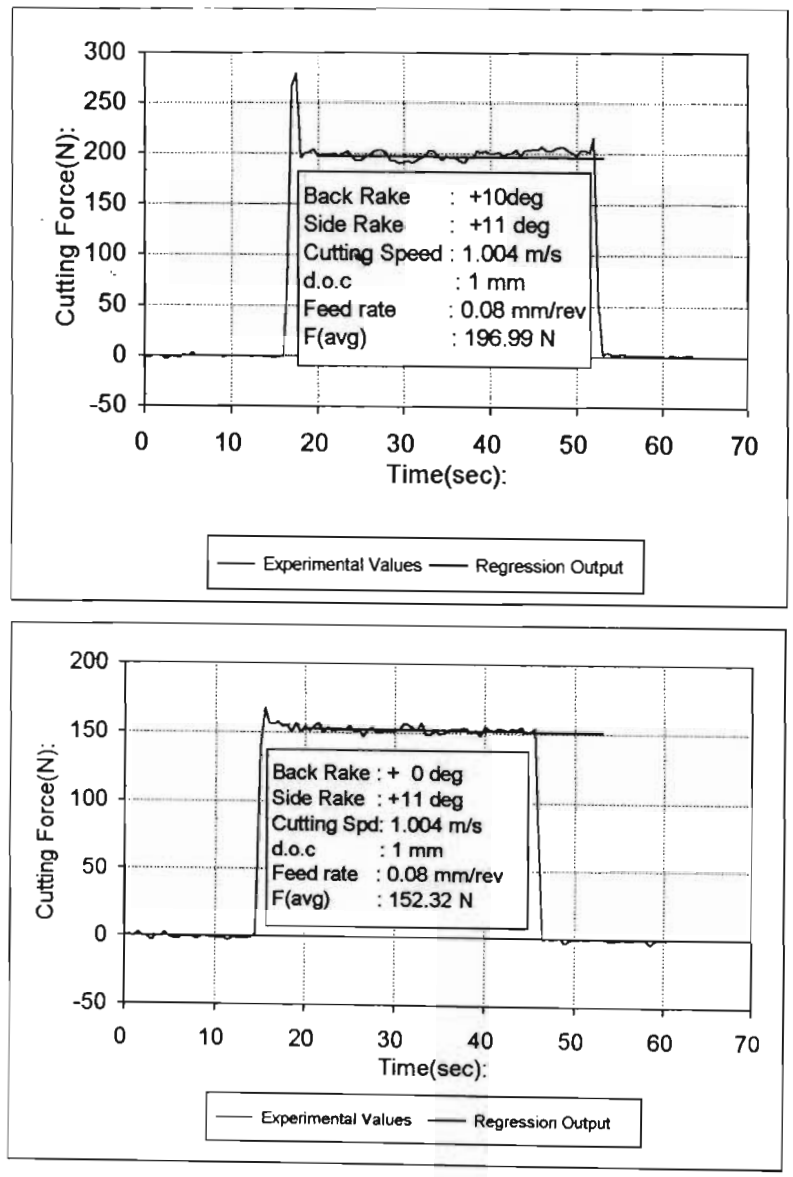

Figure 6.1[a] Cutting Force vs Time for different Back Rake angles.

The graphs show that the cutting force was monitored for seventy seconds. For the first twenty seconds and the last forty seconds of this period the tool was not in contact with the work-piece. In both these periods the force values were stable around the zero value. This demonstrates the effective elimination of noise and compensation for temperature effects. Almost no creep effects the output values of the strain gauges. Force values read during this period were actual values without any external values influencing cutting forces. When the tool contacts the workpiece, the output from the strain gauge jumps up to a peak force value, and then settles down as the cutting process stabilizes. The impact force value at the start of machining, show in both graphs as a peak in the force vs time curve. The circuit filtering the bridge output signal, produces a bigger than normal impact force value due to the amplification build into this circuit. This instability will increase for higher values of amplification. The machining process is presented as an irregular line in the graphs, after the initial peak value. The line is irregular due to irregularities in the workpiece surface, vibrations of the machine tool and other machining conditions.

The average cutting force values for the machining process as indicated on the graphs, were determined by doing a regression analysis on the strain gauge output data. The result of this analysis shows on the graph as a straight line of mean cutting force value for the cutting period.

One average force value for this cutting period is obtained by adding all regression values obtained and dividing the total with the number of regression

values. The average cutting force value obtained in this manner is also shown on the graph. This value is used as the experimentally determined force for this set of cutting parameters. Regression analysis of data obtained over a period, is also used in the controlling program to ensure accurate measuring of force values used for evaluation purposes.

To make up the graph for cutting force versus back rake angles, all the average force values as obtained for every specific Back Rake angle had to be combined in one graph. Six graphs as shown in figures 6.1 [b] to 6.1 [g] were obtained.

The first three graphs represent data for experimentation at a low feed rate of 0.08 mm/rev, and with cutting speeds of ±1.004 m/s, ±3.25 m/s and ±4.663 m/s. For each of these cutting speeds experiments were conducted for back rake angle values ranging from -4 to 10 degrees.

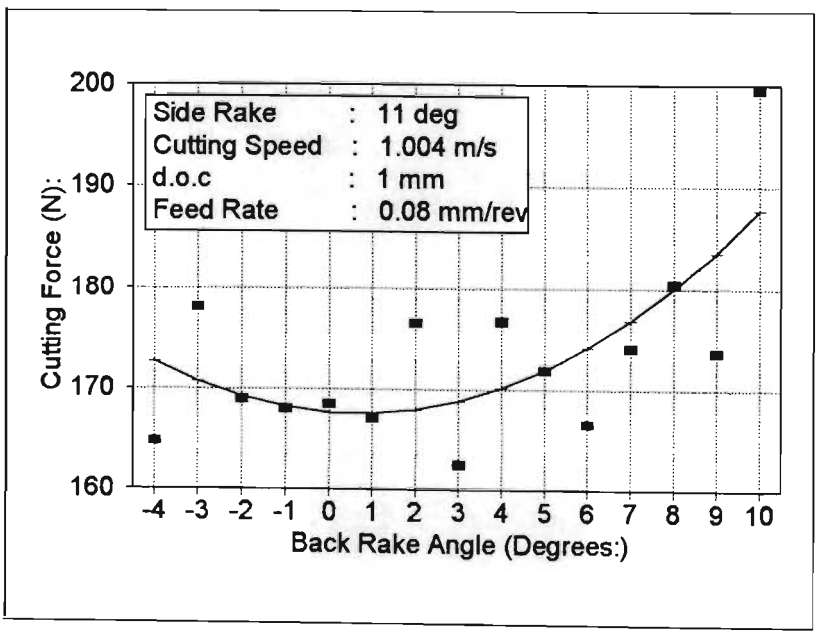

Figure 6.1[b] Cutting force vs Back Rake Angle for cutting speed of 1.004 m/s.

At the low cutting speed of 1.004 m/s, the values obtained from regression analysis on the cutting force data for each separate back rake angle, are scattered as shown in figure 6.1[b]. This curve is typical of the type of curve obtained for many experiments under the same cutting conditions. Regression analysis on the scattered data provides a curve for cutting force versus back rake angle. As shown in table 6.1[a], the maximum deviation of experimental data from the regression curve value, is 27.1% of the force range value. The data can therefore only be used to predict the correct back rake angle for efficient cutting, to the closest four degrees. This data compares well with the theoretical model as demonstrated in figure 3.2[f], and previous experimental work as discussed in chapter two. (See figure 2.1[b]). It can be derived that the data obtained at low cutting speeds must be evaluated carefully when used for optimization purposes.

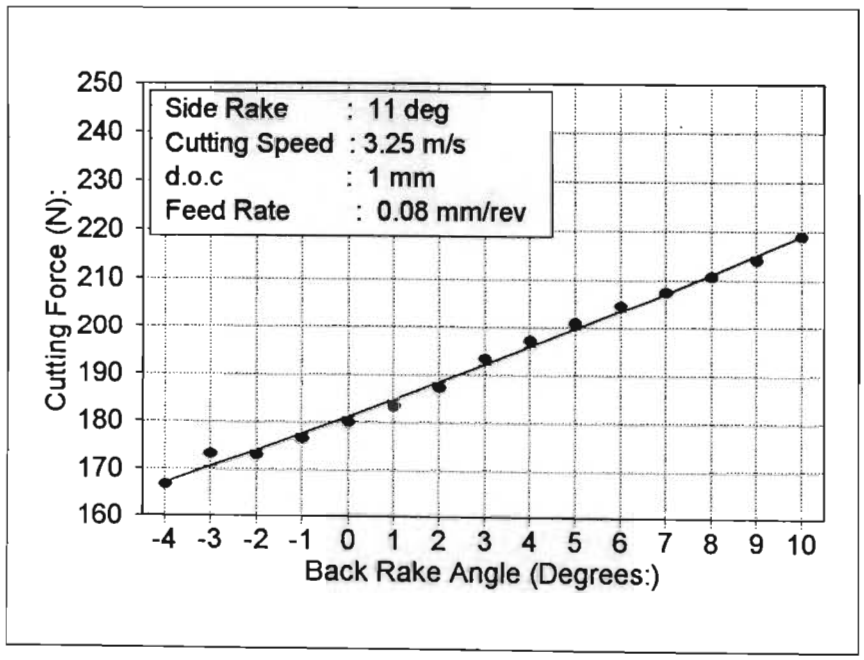

Figure 6.1[c] Cutting force vs Back Rake Angle for cutting speed of 3.25 m/s.

The force measuring technique is not able to obtain reliable data at this low cutting speed.

In figure 6.1[c] it can be seen that the experimental data is much more reliable when the cutting speed increases to 3.25 m/s. The maximum deviation here is 5.22 % of the force range. The regression curve calculated from these experimental values forms a straight line that is comparable to the results obtained for back rake angle influence on cutting conditions as shown in figure 2.1[b]. The output values from the strain gauge indicator can therefore safely be used to control the tool geometry during cutting for higher cutting speeds.

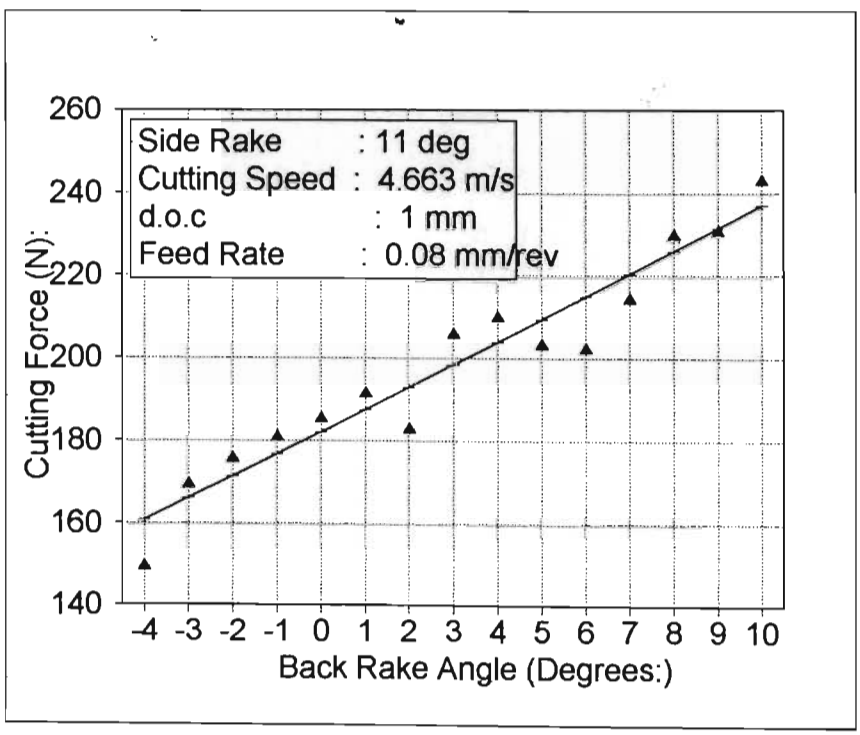

Figure 6.1[d] Cutting force vs Back Rake Angle for cutting speed of 4.663 m/s.

The high cutting speed of 4.663 m/s also results in experimental output data that can be used for optimizing tool geometry on-line. The data obtained is more unstable than that for the intermediate cutting

speed of 3.25 m/s. The regression analysis on these values produces a straight line that is again comparable to the results obtained by previous researchers as shown in figure 2.1[a] and 2.1[b]. Here the maximum deviation of experimental data to the regression values is 11.66% of the total force deviation. The controlling program developed for controlling of tool geometry optimization, analyses many different strain gauge indicator output values before selecting a new tool geometry. This procedure ensures that the data is filtered before being used in the controlling process.

Table 6.1[a] compares output data for the six experiments represented on figures 6.1[b] to 6.1[i]. The minimum and maximum scatter values were determined by finding the difference between experimental force values and the regression output value at the closest point on the regression curve. The maximum scatter expressed as a percentage of the force range covered in the graph, shows the accuracy of the values. At the low cutting speed of 1 m/s, BUE conditions are possible and this unstable condition results in a high scatter of values.

Graph nr.:	Feed Rate: (mm/rev)	Cutting speed: (m/s)	Min Force: (N)	Max Force: (N)	Force Range: (N)	Max Scatter: (N)	Min Scatter: (N)	Max Scatter vs Force Range: (%)
6.1(b)	0.08	1.00	162.51	199.47	36.96	10.02	0.46	27.10
6.1©	0.08	3.25	166.68	218.98	52.30	2.73	0.15	5.22
6.1(d)	0.08	4.66	149.92	243.23	93.31	10.88	0.81	11.66
6.1(f)	0.20	1.00	271.48	303.03	31.55	15.02	0.28	47.61
6.1(g)	0.20	3.20	290.63	475.39	184.77	14.92	0.27	8.08
6.1(h)	0.20	4.63	286.45	541.60	255.15	26.13	6.13	10.24

Table 6.1[a] Comparative data for the six back rake angle experiments.

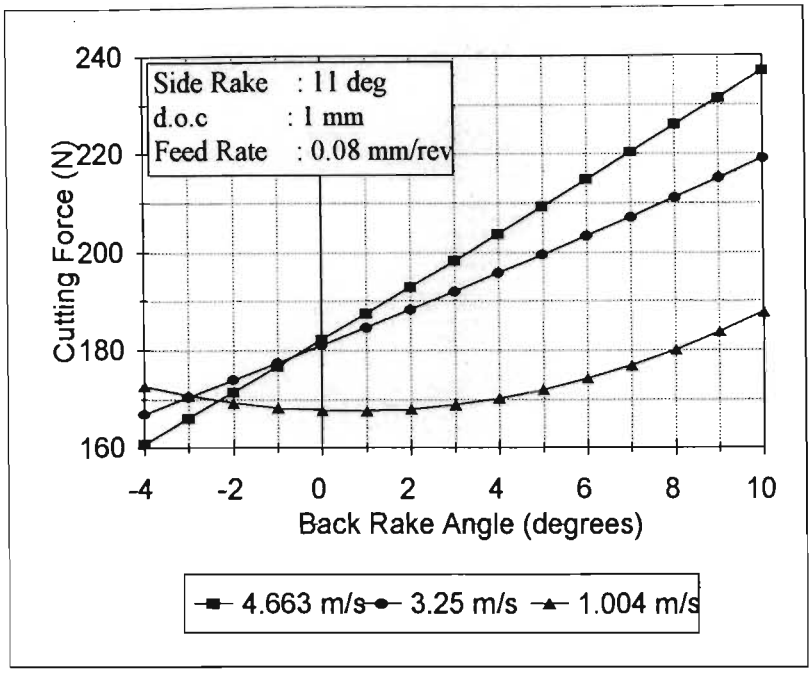

Figure 6.1[e] Effect of back Rake Angle on Cutting Force for different cutting speeds with Feed Rate set at 0.08 mm/rev.

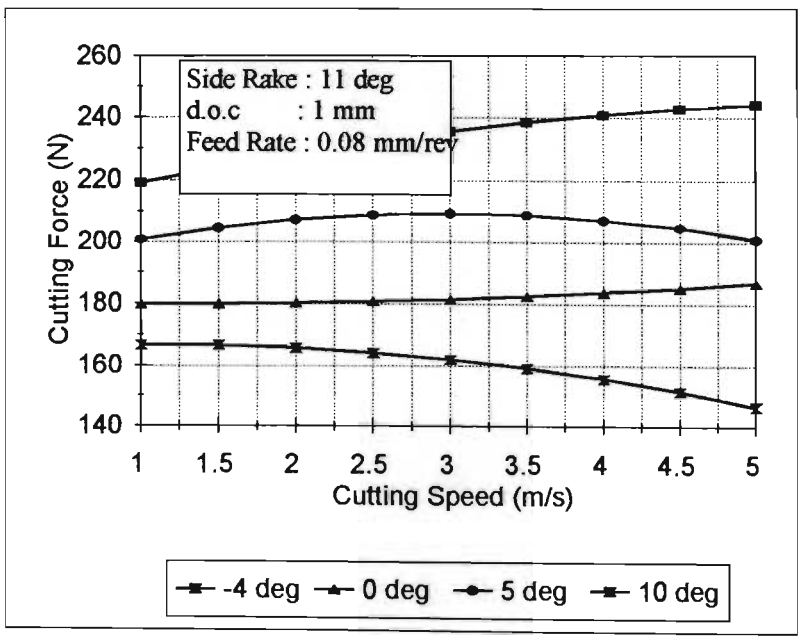

Figure 6.1[f] Effect of cutting speed on tool forces for various back rake angles.

In figure 6.1[e], the different graphs for force vs back rake angle are combined to display the effect of increasing cutting speed on the relationship between cutting forces and back rake angles. This graph compares well with relationships observed by previous researchers as discussed in chapter two. (See figure 2.1[b]). It also compares well with theoretically calculated values in chapter three. (See figure 6.1[e])

The effect of cutting speed on the tool forces for various rake angles is evaluated from the experimental data. The force difference at different cutting speeds for the different curves is tabled in table 6.1[b]. It can be seen that the cutting forces generally vary more between the different back rake angle curves at the higher cutting speeds. This is true up to a cutting speed of three m/s, but then the curves for the intermediate rake angles seem to come closer together.

Cutting Speed: (m/s)	Force change per degree for (-4 to 0 deg) (N)	Force change per degree for (0 to 5 deg) (N)	Force change per degree for (5 to 10 deg) (N)
0.00	15.53	9.72	17.67
0.50	13.92	15.98	17.62
1.00	13.21	20.93	18.15
1.50	13.42	24.59	19.26
2.00	14.53	26.95	20.96
2.50	16.56	28.01	23.24
3.00	19.50	27.77	26.11
3.50	23.35	26.24	29.56
4.00	28.11	23.40	33.59
4.50	33.78	19.27	38.21
5.00	40.36	13.85	43.41
5.50	47.85	7.12	49.20

Table 6.1[b] Force variance between Back Rake Angle curves for different cutting speeds.

The small difference between the curves makes it more difficult for the controller to decide which back rake angle is best suited to the current machining conditions. The tool geometry optimization technique is therefore better suited to the intermediate cutting speed ranges. At higher cutting speeds the optimization technique will work very well if the back rake angles are low or high.

The next three graphs represent data for experimentation at a feed rate of 0.2 mm/rev, and with cutting speeds of ±1 m/s, ±3.20 m/s and ±4.63 m/s. For each of these cutting speeds experiments were conducted for back rake angle values ranging from -4 to 10 degrees.

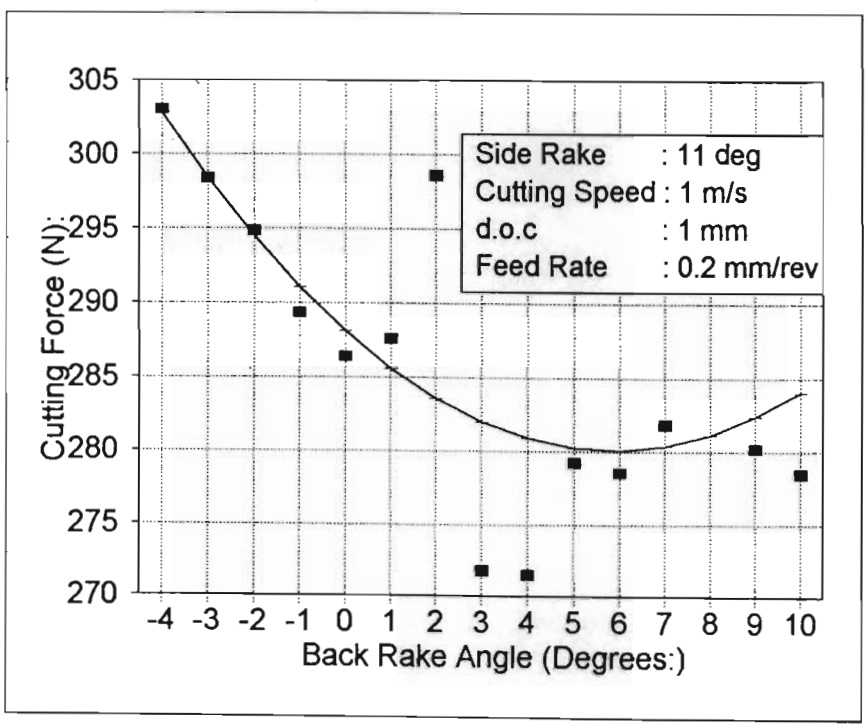

Figure 6.1[g]Cutting speed vs Back Rake Angle for cutting speed of 1 m/s.

As for figure 6.1[b] the experimental values are also scattered. The curve plotted from the regression values

deviates from the other experimental graphs in that this curve shows a reduction in cutting forces with an increase in back rake angle. The other graphs all show an increase in cutting force values with an increase in back rake angle. This change in behaviour might be due to the inaccuracy of the data, but the experimental data is scattered worst around the centre of the graph with the ends more stable. This suggests that the graph follow the correct trend, and that cutting forces do decrease at low cutting speeds with an increase of back rake angles. The experiment was also repeated and the same type of graph was obtained. Previous research work showed that it is possible to a decrease in normal forces with an increase in back rake angle but not cutting forces. (See figure 2.1[a] and 2.1[b]) As shown in table 6.1[a] the maximum deviation of experimental data from the regression curve value, is 46.71% of the total force range. It best not to us this system at low cutting speeds to optimize tool geometry.

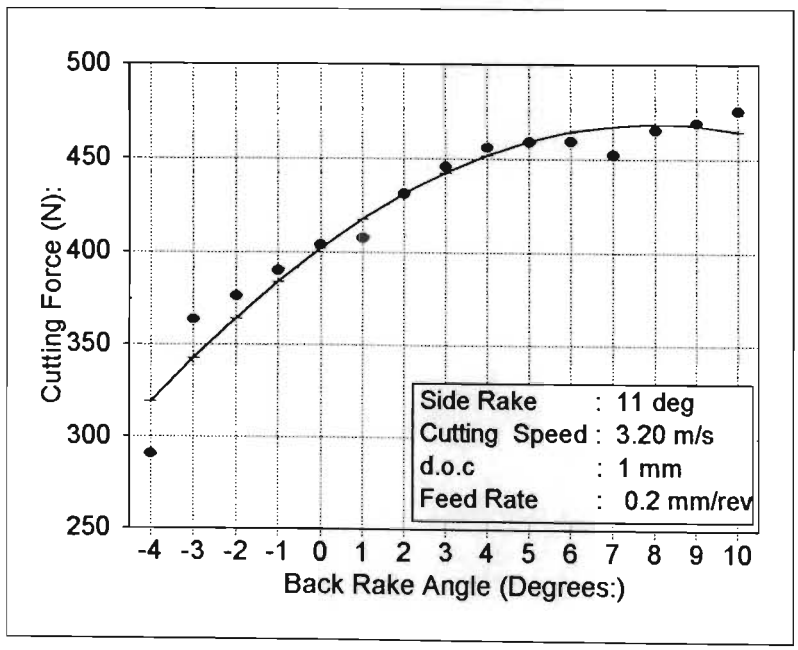

Figure 6.1[h] Cutting speed vs Back Rake Angle for cutting speed of 3.20 m/s.

Graph 6.1[h] shows increasing force values with an increase of back rake angles. The maximum deviation of experimental values from the regression values is 8.08% of the total force range. The curve is comparable to the results obtained for back rake angle influence on cutting conditions as shown in figure 2.1[b]. The output values from the strain gauge indicator can safely be used to control the tool geometry during cutting at these intermediate cutting speeds.

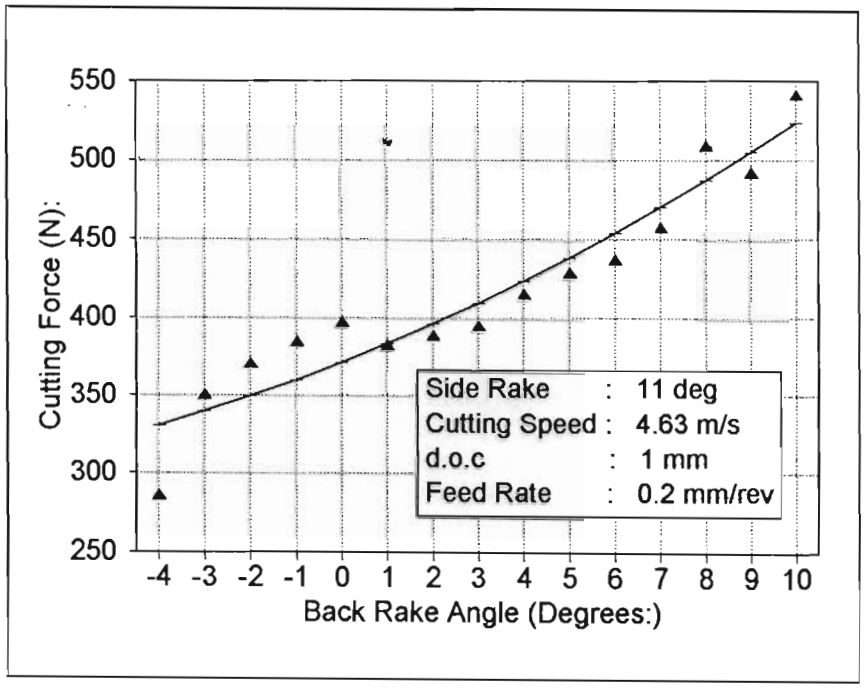

Figure 6.1[i] Cutting Force vs Back Rake Angle for cutting speed of 4.63 m/s.

The high cutting speed of 4.63 m/s again results in experimental output data that is consistent enough to be used to optimize the tool geometry on-line. The regression analysis on these values is again comparable to the results obtained by previous researchers as shown in figure 2.1[b] and the theoretical model as

demonstrated in figure 3.2[f]. Here the maximum deviation of experimental data to the regression values is 10.24% of the total force deviation.

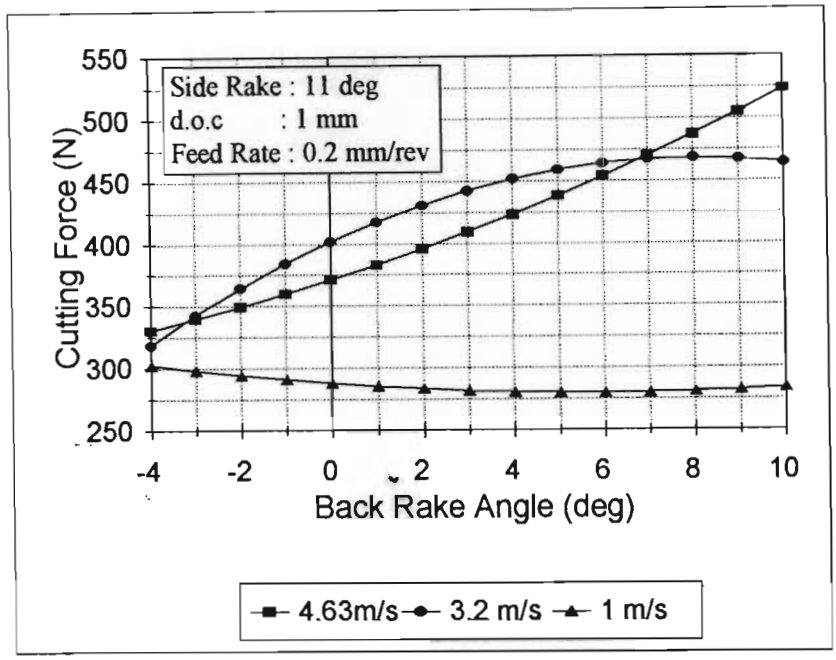

Figure 6.1[j] Effect of back Rake Angle on Cutting Force for different cutting speeds with Feed Rate set at 0.2 mm/rev.

In figure 6.1[j], the different graphs for force vs back rake angle are combined to display the effect of increasing cutting speed on the relationship between cutting forces and back rake angles. The curves for the two higher cutting speeds compare well with relationships observed by Kenneth [24] (See figure 2.1[b]). The curve for the low cutting speed of one m/s compares with research work for back rake angle values from six to ten degrees.

The effect of cutting speed on the tool forces for various rake angles are evaluated from the experimental data and is displayed in figure 6.1[k].

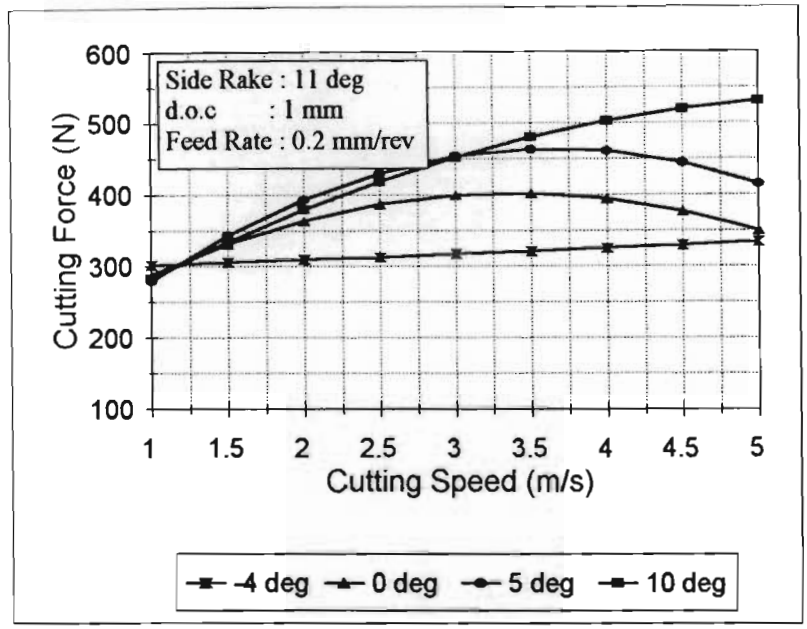

Figure 6.1[k] Effect of cutting speed on tool forces for various back rake angles.

The graph is compiled for a feed rate of 0.2 mm/rev. At the higher cutting speeds, changing the tool geometry has the biggest influence on cutting forces unless the back rake angle values are low.

Cutting Speed: (m/s)	Force change per degree for (-4 to 0 deg) (N)	Force change per degree for (0 to 5 deg) (N)	Force change per degree for (5 to 10 deg) (N)
1.00	-14.72	-7.88	3.81
1.50	24.91	12.21	-8.82
2.00	54.31	29.18	-13.83
2.50	73.48	43.03	-11.21
3.00	82.42	53.76	-0.98
3.50	81.12	61.36	16.88
4.00	69.58	65.84	42.35
4.50	47.82	67.20	75.45
5.00	15.82	65.43	116.17

Table 6.1[c] Force variances between Back Rake Angle curves for different cutting speeds at feed rate of 0.2 mm/rev.

At the lower cutting speeds the back rake angle does not affect cutting forces. The using of tool geometry optimization techniques is best suited to the medium to high cutting speeds. This graph also shows how the cutting forces increase with an increase in back rake angles. Table 6.1[c] proves that the back rake angle variation at the low cutting speeds does not influence the cutting forces much. At intermediate cutting speeds, force variations are large for different back rake angles when the back rake angles are still negative and low positive. For higher back rake angle values, the cutting force variation is small. At the higher cutting speeds, the mayor influence of back rake angle variation on the cutting forces, is at the higher back rake angle values.

6.2 Side Rake Angle Evaluation

As for Bake Rake angles a graph was obtained of cutting forces vs time for each set of cutting parameters. This graph can be compared directly with the graphs in figure 6.1[a] obtained for Back Rake Angle evaluation. The discussion about the graph for Back Rake angles can be related to this section as well.

To make up the graph for cutting force vs Side Rake Angle, all the average force values as obtained for every specific side rake angle had to be combined into one graph. In this manner six graphs are obtained which can be placed into two groups.

The first three graphs represent data for experimentation at a low feed rate of 0.08 mm/rev, and with cutting speeds of ±1.026 m/s, ±3.30 m/s and ±6.597 m/s. For each of these cutting speeds experiments were conducted for side rake angle values ranging from -8 to 11 degrees.

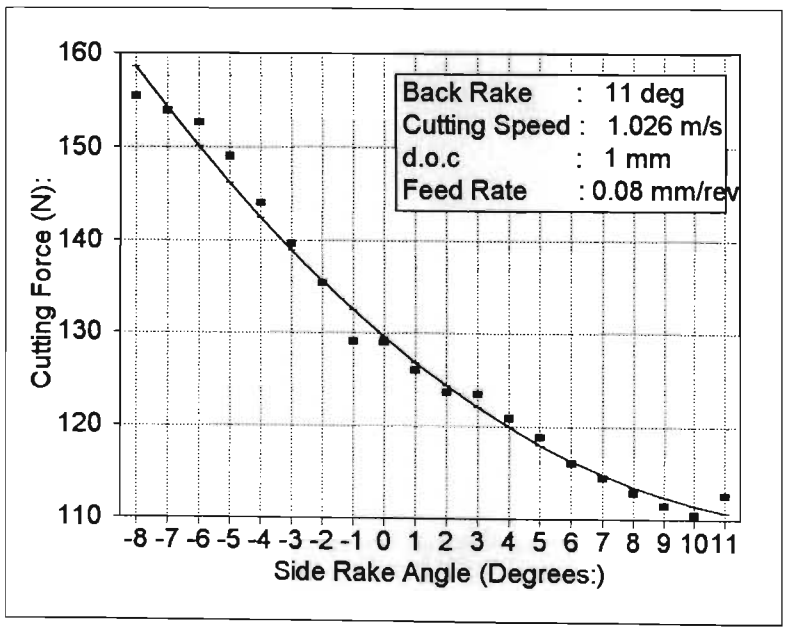

Figure 6.1[i] Cutting force vs Side Rake Angle for cutting speed of 1.026 m/s.

At the cutting speed of 1.026 m/s, the experimental data gives a stable representation of the cutting conditions as shown in figure 6.2[a]. Regression analysis on the experimental data provides a curve for cutting force vs back rake angle.

As shown in table 6.2[a], the maximum deviation of experimental data from the regression curve value, is 7.14% of the force range value. Table 6.2[a] compares output data for the six experiments represented on figures 6.2[a] to 6.2[j]. The minimum and maximum scatter values were determined by finding the difference between experimental force values and the regression output value at the closest point on the regression curve. The maximum scatter expressed as a percentage of the force range covered in the graph, gives a good indication of the accuracy of the values.

Graph nr.:	Feed Rate: (mm/rev)	Cutting speed: (m/s)	Min Force: (N)	Max Force: (N)	Force Range: (N)	Max Scatter: (N)	Min Scatter: (N)	Max Scatter vs Force Range
6.2(a)	0.08	1.03	110.53	158.61	48.07	3.43	0.28	7.14
6.2(b)	0.08	3.30	124.47	153.64	29.17	2.21	-0.02	7.56
6.2©	0.08	6.60	128.76	178.53	49.77	3.13	-0.06	6.29
6.2(f)	0.20	1.01	235.26	287.81	52.54	5.14	0.49	9.78
6.2(g)	0.20	3.25	265.07	297.61	32.54	6.31	0.25	19.39
6.2(h)	0.20	4.70	234.58	269.73	35.16	4.84	0.32	13.76

Table 6.2[a] Comparative data for the six side rake angle experiments.

This data compares well to theoretical evaluations (figure 3.2[a]), and previous experimental work (figure 2.1[c] and 2.1[d]), as discussed in chapter two. The data obtained at this cutting speed is reliable and can be used for optimization purposes.

In figure 6.2[b] it can be seen that the experimental data is also reliable when the cutting speed increases to 3.30 m/s. The maximum deviation here is 7.56% of the force range. The regression curve calculated from these experimental values is comparable to the results obtained for side rake angle influence on cutting conditions as displayed in figure 2.1[c] and 2.1[d].

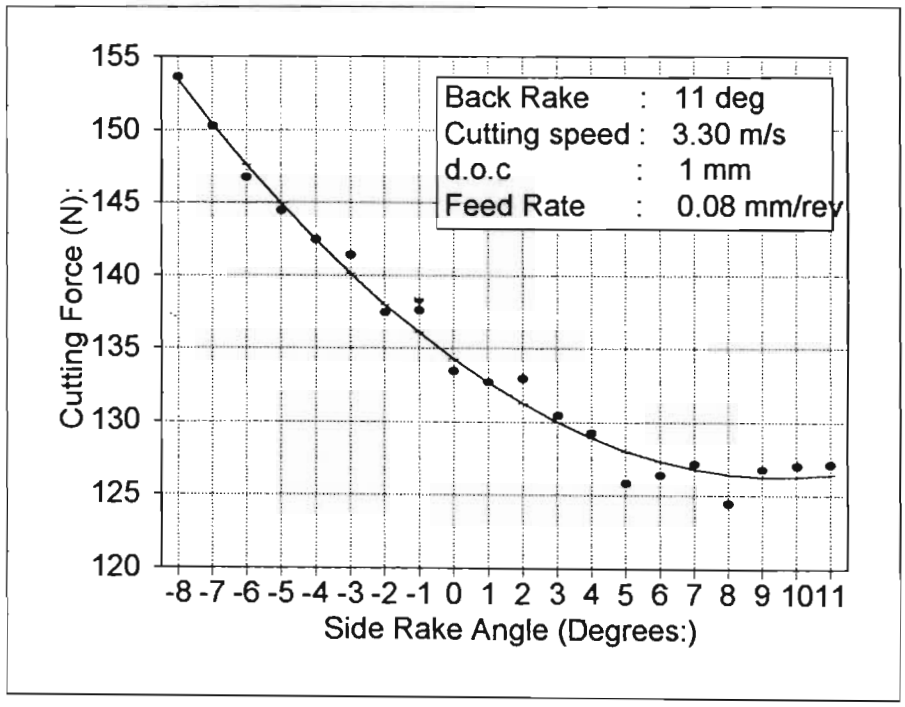

Figure 6.2[b] Cutting force vs Side Rake Angle for cutting speed of 3.30 m/s.

The output values from the strain gauge indicator can therefore safely be used to control the tool geometry at cutting speeds around 3.30 m/s.

The high cutting speed of 6.597 m/s also results in experimental output data that can be used for optimization of the cutting process. The regression analysis on these values produces a straight line that is again comparable to the results obtained by previous

researchers as displayed in figure 2.1[c] and 2.1[d].

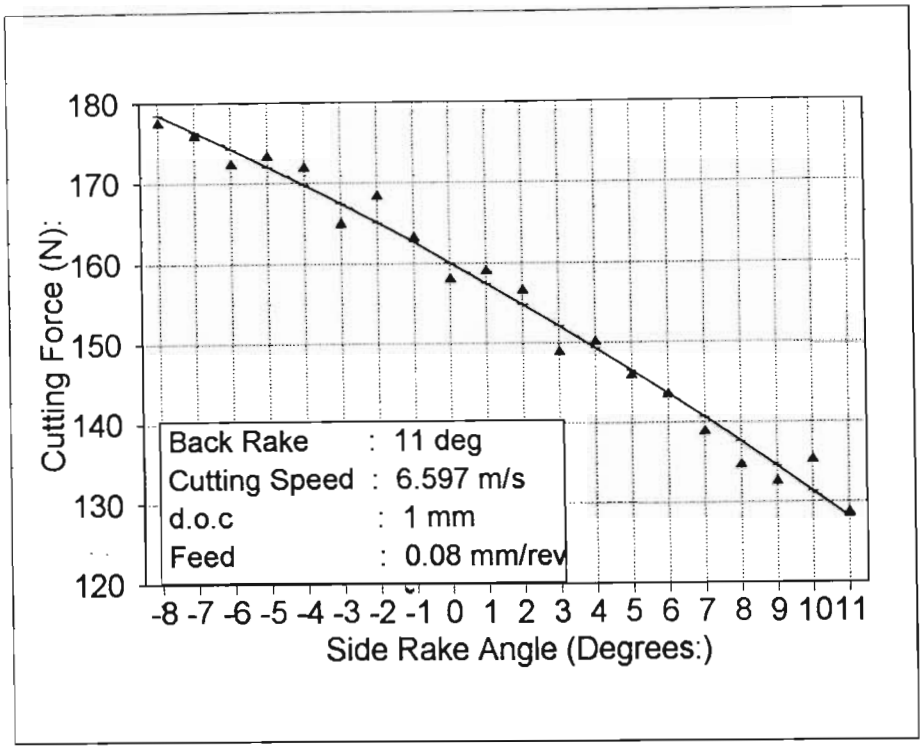

Figure 6.2[c] Cutting force vs Side Rake Angle for cutting speed of 6.597 m/s.

In this case the maximum deviation of experimental data to the regression values is 6.29% of the total force.

In figure 6.2[d], the different graphs for force vs side rake angle are combined to demonstrate the effect of increasing cutting speed on the relationship between cutting forces and side rake angles. This graph compares well with relationships observed by previous researchers as discussed in chapter two. (See figure 2.1[c] and 2.1[d])

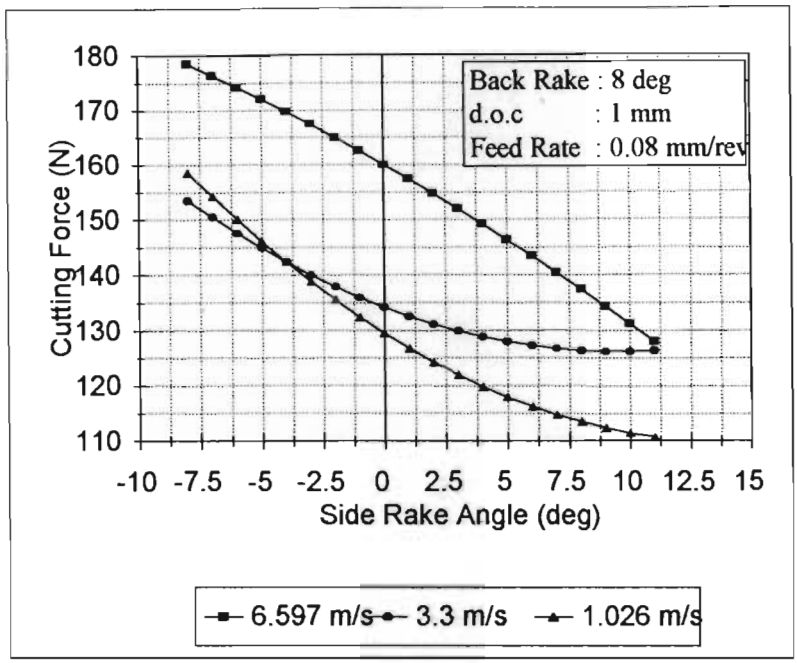

Figure 6.2[d] Effect of Side Rake Angle on Cutting Force for different cutting speeds with Feed Rate set at 0.08 mm/rev.

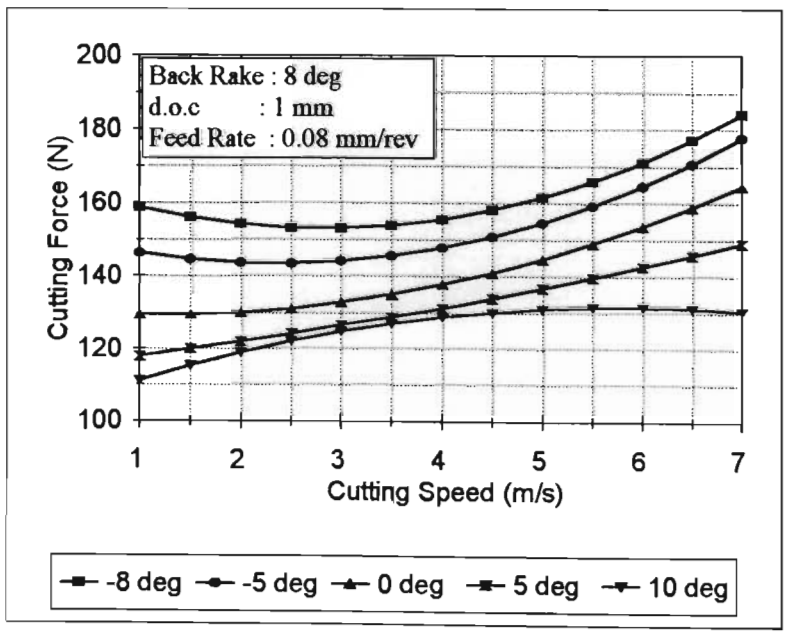

Figure 6.2[e] Effect of cutting speed on tool forces for various side rake angles.

The effect of cutting speed on the tool forces for various side rake angles are evaluated from the experimental data. The force difference at different cutting speeds for the different curves are tabled in table 6.2[b]. It can be seen that the cutting forces vary most between the different side rake angle curves at the low and high cutting speeds. The curves are closer together for cutting speeds in the region of m/s making it more difficult for the controller to decide which side rake angle is more optimal for machining conditions.

Cutting Speed: (m/s)	Force change per degree for (-8 to 0 deg) (N)	Force change per degree for (-5 to 0 deg) (N)	Force change per degree for (0 to 5 deg) (N)	Force change per degree for (5 to 10 deg) (N)
1.00	12.43	16.71	11.70	6.69
1.50	11.42	14.91	9.77	4.63
2.00	10.50	13.39	8.25	3.12
2.50	9.67	12.13	7.15	2.17
3.00	8.93	11.14	6.45	1.76
3.50	8.30	10.42	6.17	1.92
4.00	7.75	9.98	6.30	2.62
4.50	7.30	9.80	6.84	3.88
5.00	6.95	9.90	7.79	5.69
5.50	6.69	10.26	9.16	8.05
6.00	6.52	10.90	10.93	10.97
6.50	6.45	11.80	13.12	14.44
7.00	6.47	12.98	15.72	18.46

Table 6.2[b] Force variance between Side Rake Angle curves for different cutting speeds.

The tool geometry optimization technique is therefore best suited to the high and low cutting speed ranges. At higher cutting speeds the optimization technique will work best when the side rake angle is less than five degrees of side rake angle. At the lower cutting

speeds the optimization technique will work best when the side rake angle is high. At a cutting speed of about three m/s the optimization technique will work best at the intermediate side rake angles.

The next three graphs represent data for experimentation at a feed rate of 0.2 mm/rev, and with cutting speeds of ±1.012 m/s, ±3.25 m/s and ±4.70 m/s. For each of these cutting speeds experiments were conducted for side rake angle values ranging from -4 to 10 degrees.

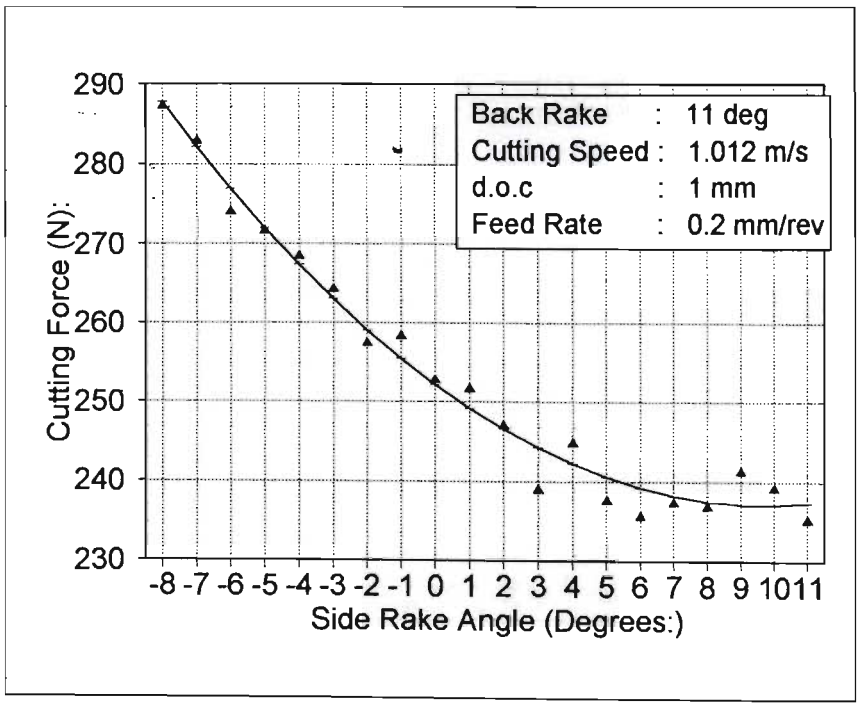

Figure 6.2[f] Cutting speed vs Side Rake Angle for cutting speed of 1.012 m/s.

As shown in table 6.2[a] the maximum deviation of experimental data from the regression curve value, is 9.78% of the total force range. This is acceptable to use the experimental data to control the optimal tool geometry. The 9.78% deviation of data is found at the higher side rake angles, with the lower side rake

values falling very close to the regression curve. The curve corresponds with curves obtained by previous researchers as discussed in chapter two. See figure 2.1[c] and 2.1[d].

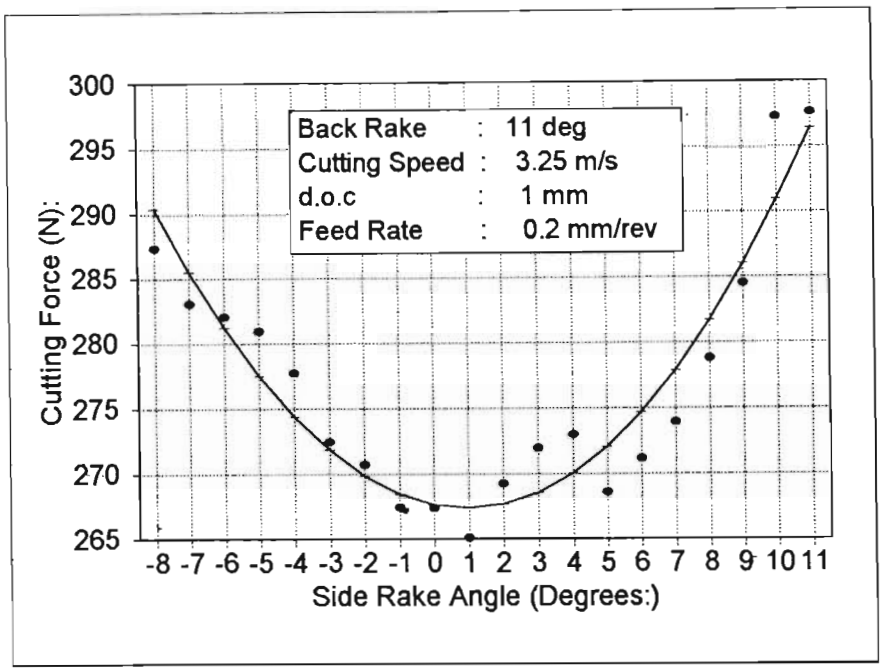

Figure 6.2[g] Cutting speed vs Side Rake Angle for cutting speed of 3.25 m/s.

Graph 6.2[g]. Shows low force values for side rake angles around zero degrees, and higher cutting forces for both negative and positive side rake angles. The maximum deviation of experimental values from the regression values is 19.39% of the total force range. The experimental data is therefore a true reflection of the cutting conditions and the output values from the strain gauge indicator can safely be used to control the tool geometry during cutting at cutting speeds around m/s.

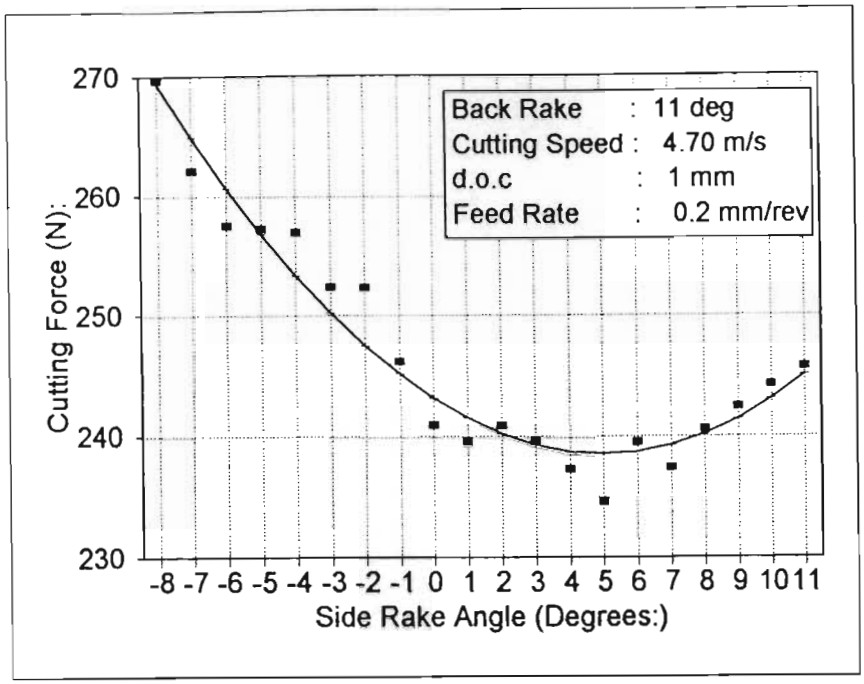

Figure 6.2[h] Cutting speed vs Side Rake Angle for cutting speed of 4.70 m/s.

The high cutting speed of 4.70 m/s again results in experimental output data that is consistent enough to be used to optimize the tool geometry on-line. The regression analysis on these values is again comparable to the results obtained by previous researchers as shown in figure 2.1[c] and 2.1[d]. Here the maximum deviation of experimental data to the regression values is 13.76% of the total force deviation.

In figure 6.2[i], the different graphs for cutting force vs side rake angle are combined to show the effect of increasing cutting speed on the relationship between cutting forces and side rake angles. The curves for the high and the low cutting speed compare well with relationships observed by Tourrett[18] and Kenneth[24]. See figure 2.1[c] and 2.1[d].

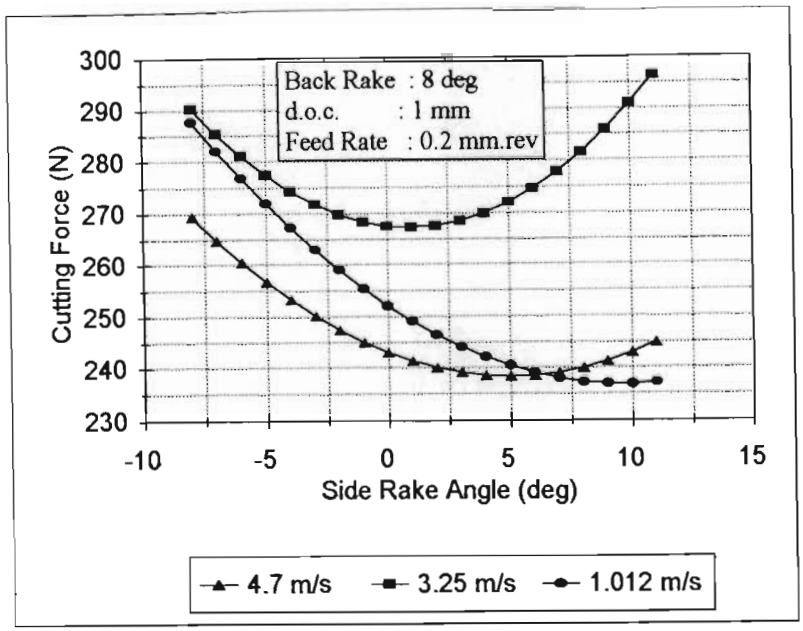

Figure 6.2[i] Effect of Side Rake Angle on Cutting Force for different cutting speeds with Feed Rate set at 0.2 mm/rev.

The curve for the intermediate cutting speed of 3.25 m/s differs from the other two in that the cutting forces increase again up to 11 degrees side rake after the initial decrease in cutting forces to 0 degrees side rake. The cutting forces are also higher than for the other two curves. At a cutting speed of 4.7 m/s the cutting force is the lowest, which is also reflected by previous research in chapter two.

The effect of cutting speed on the tool forces for various rake angles are evaluated from the experimental data. Graph 6.2[j] is compiled for a feed rate of 0.2 mm/rev. For positive side rake angles, the cutting forces show a tendency to decrease when the cutting speed increase. For negative to zero side rake angles, the cutting forces increase with an increase of cutting speed up to three m/s, and then decrease when the cutting speed increases more than three m/s. The use of

tool geometry optimization techniques is useful at all cutting speeds.

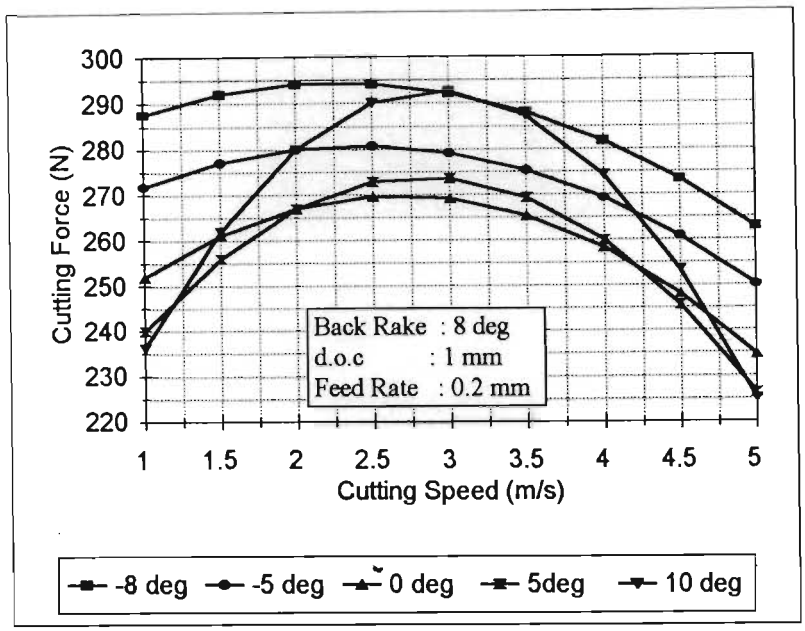

Figure 6.2[j] Effect of cutting speed on tool forces for various side rake angles.

Cutting Speed: (m/s)	Force change per degree for (-8 to 0 deg) (N)	Force change per degree for (-5 to 0 deg) (N)	Force change per degree for (0 to 5 deg) (N)	Force change per degree for (0 to 10 deg) (N)
1.00	15.82	19.91	11.83	3.76
1.50	14.89	16.02	5.02	-5.98
2.00	14.12	13.09	0.03	-13.03
2.50	13.50	11.10	-3.14	-17.38
3.00	13.03	10.08	-4.48	-19.04
3.50	12.72	10.00	-4.00	-18.00
4.00	12.56	10.88	-1.69	-14.27
4.50	12.56	12.71	2.43	-7.84
5.00	12.70	15.49	8.39	1.28

Table 6.2[c] Force variance between Side Rake Angle curves for different cutting speeds at feed rate of 0.2 mm/rev.

Table 6.2[c] demonstrates that the force difference for different side rake angles from zero to five degrees is very small. At the intermediate cutting speeds optimizing the rake angle by measuring the cutting force is especially difficult. For negative side rake angles, up to zero degrees, the force variation is big between different angles. When the side rake angle is bigger than five degrees, the cutting forces differ most when the cutting speed is around three m/s. When forces differ a lot between different rake angles, the control of side rake angles will be the most accurate.

6.3 Repeatability

For the first repeatability experiment, the same cutting parameters were used for fifteen different tests. The output curve for the test results of each test is comparable with the curves in figure 6.1[a].

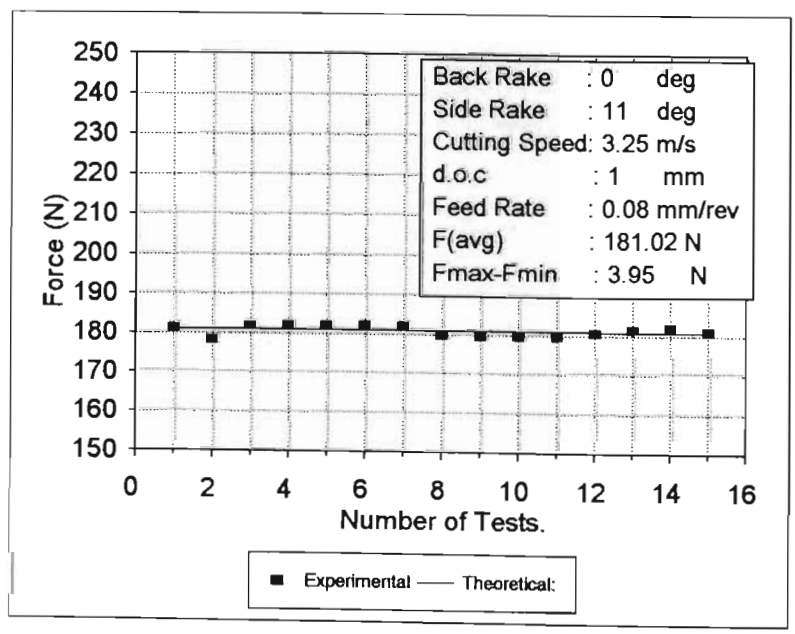

Figure 6.3[a] Repeatability analysis output results for experiment one.

The change in force value between the different tests can be observed by calculating an average force value by doing regression analysis on the data in each curve. These calculated values can then be plotted as the force value vs the number of experiments. Figure 6.3[a] shows the results obtained from experiments conducted in this manner for the stable cutting conditions when the cutting speed is 3.25 m/s and the feed rate 0.08 mm/rev.

A difference of 3.95 Newtons is measured between the maximum and minimum forces. The average force value as measured was 181.02 Newtons. The force variance is 2.18 percent of the average force value. Figure 6.3[b] shows the results obtained from experiments conducted in this manner for the more unstable cutting condition when the cutting speed is 1.004 m/s and the feed rate 0.08 mm/rev.

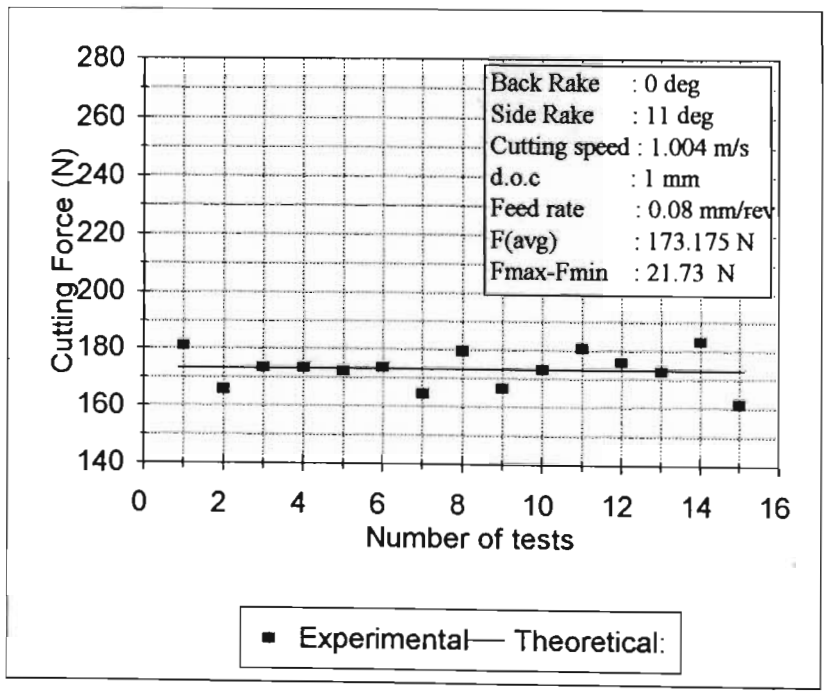

Figure 6.3[b] Repeatability analysis output results for experiment two.

Here a difference of 21.73 Newtons is measured between the maximum and minimum forces. The force variance is 12.55 percent of the average force value.

When the tool tip is not exchanged for a period, the tests drift apart even further, showing that the condition of the tool tip influence the reading greatly.

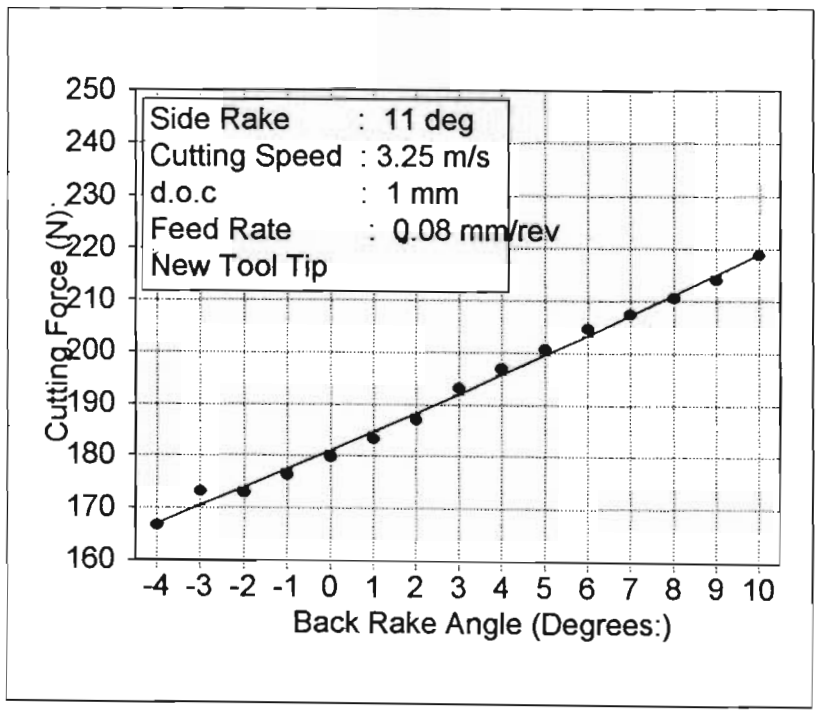

Figure 6.3[c] Cutting Force vs Back Rake angle using new tool tip.

Two graphs for back rake angle evaluation with only the back rake angle changing are shown in figure 6.3[c] and 6.3[d]. Two experiments under identical conditions were conducted and these graphs were plotted from the data obtained. In figure 6.3[c] a new tool tip was used, and in figure 6.3[d] an old tool tip.

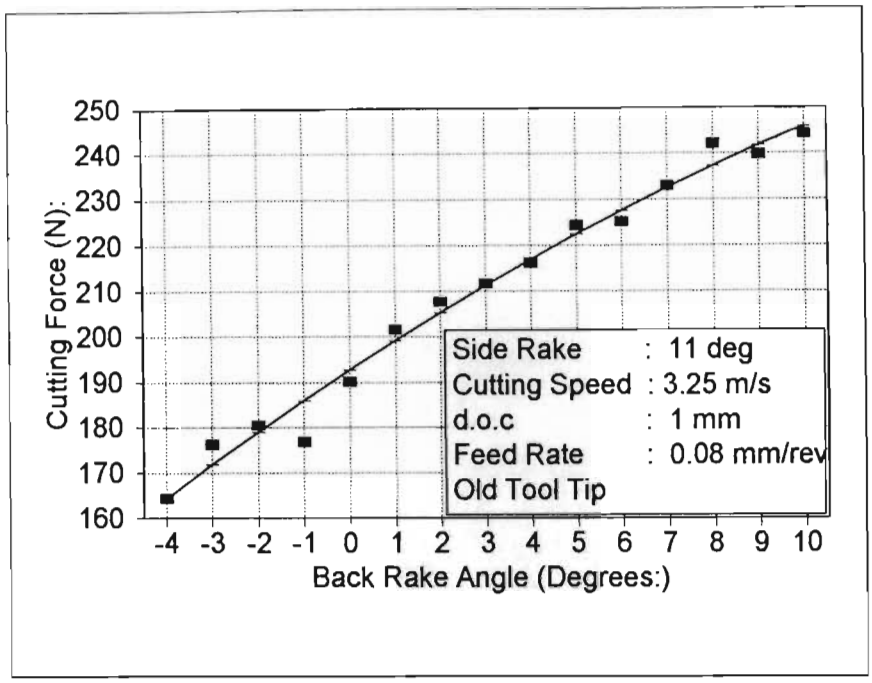

Figure 6.3[d] Cutting Force vs Back Rake angle using old tool tip.

The graphs look quite similar except for the variation in force values. As expected the worn tool needs more force at the high back rake angles to remove the same amount of metal. The system developed here will still work for optimization of tool angles, due to the trend in cutting forces with change in side rake angle or back rake angle staying the same.

Temperature can affect the output data from the strain gauge indicator. See figure 6.3[e].

The temperature influences the strain gauge indicator output excessively after only ten seconds of machining. After only twenty seconds of machining, the average force values measured with no compensation, is already 8.12 Newton higher than that obtained for the compensated experiment. It is therefore important to incorporate strain gauge compensation in the experimental setup.

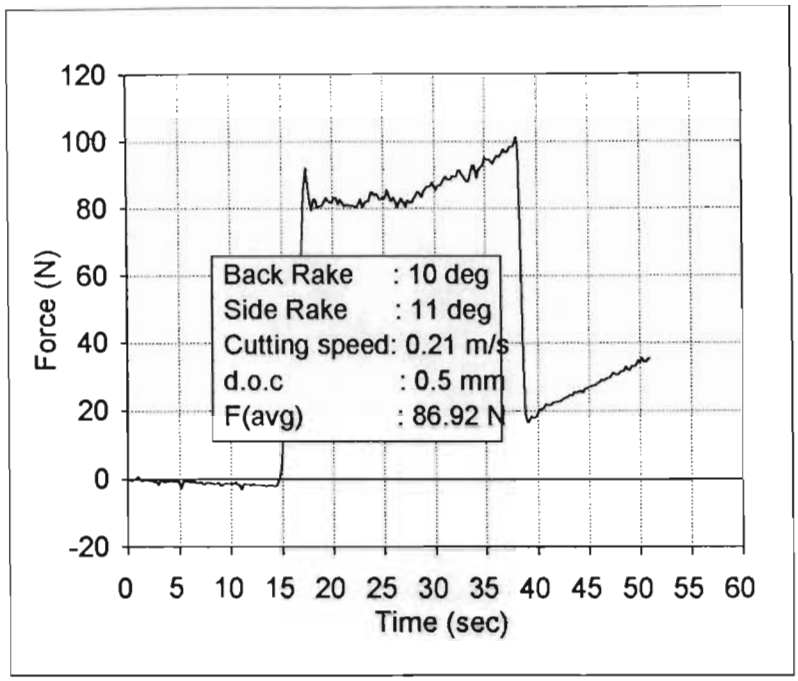

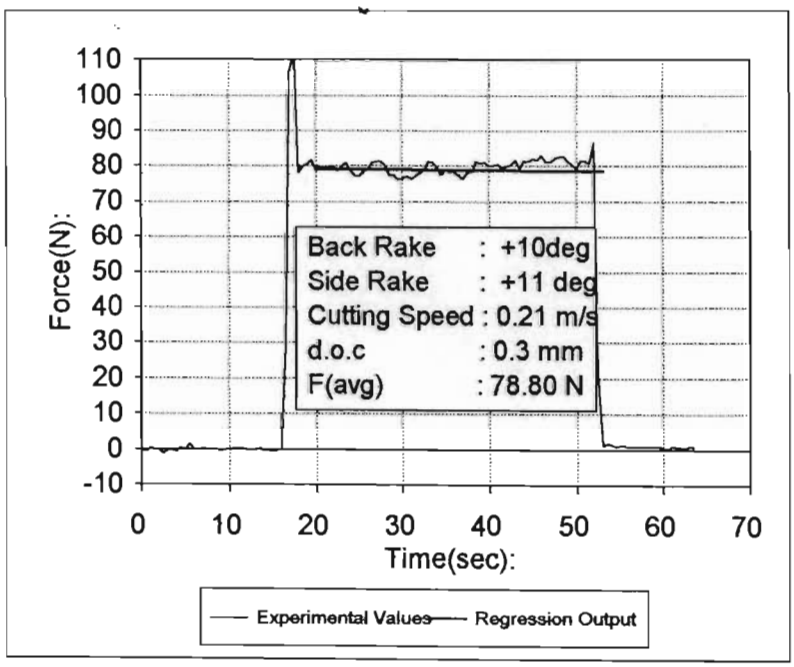

Figure 6.3[e] Comparison of effect of temperature compensation on the force data.

6.4 Evaluation of on-line control capabilities.

During experimental work using the *unidirectional optimization procedure*, minimum force positions are reached for both experiment 1[a] and experiment 1[b].

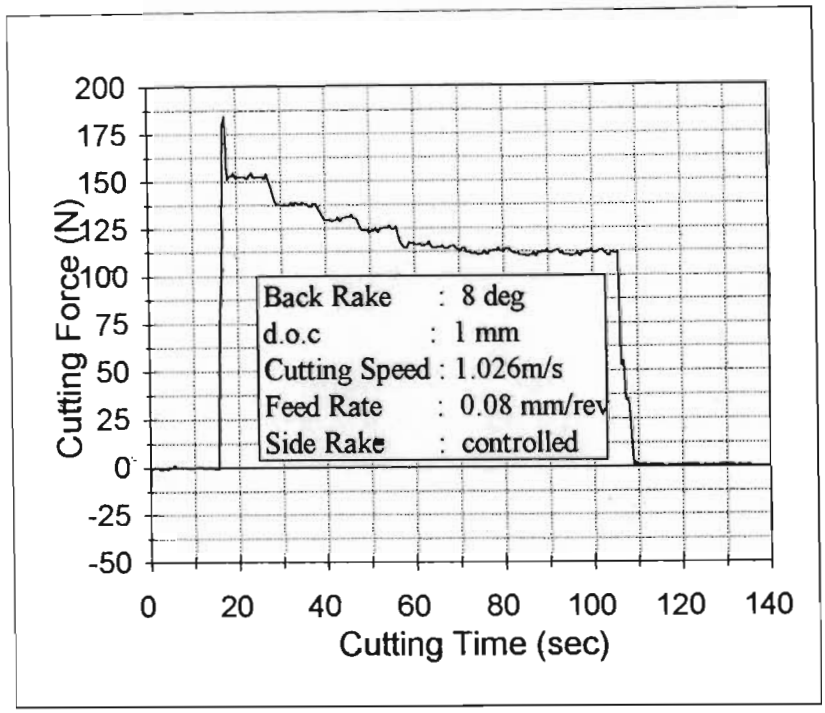

Figure 6.4[a] Evaluation of performance of Unidirectional Optimization procedure for side rake angle optimization.

As demonstrated in figure 6.4[a], the cutting force decrease for the first forty second of machining and then settles down to a relative stable value. Many steps are evident in the force vs time curve during the initial forty seconds of machining. These steps are due to the controller's optimization procedure increasing the side rake angle with three degrees at a time. Since this action results in substantial lower forces, a jump in the force curve is evident with each adjustment. When the side rake is increased up to six degrees, the controlling procedure jumps one degree at a time

resulting in small variations in the force value. Eventually at eight degrees side rake the force stabilize at a minimum value. Once this minimum force value is reached, the orientator will test continuously to see if the current force value is not more negative than the previous one. If a smaller value is found, angular position will be adjusted to a more positive value. The time taken to reach this optimal cutting condition varies depending on the initial tool geometry. With the initial side rake angle at -6 degrees, it took the controller about forty seconds to adjust the side rake angle to an angle of eight degrees.

As demonstrated in figure 6.4[b], the cutting forces also decrease for an initial forty second of machining and then settles down to a relative stable value.

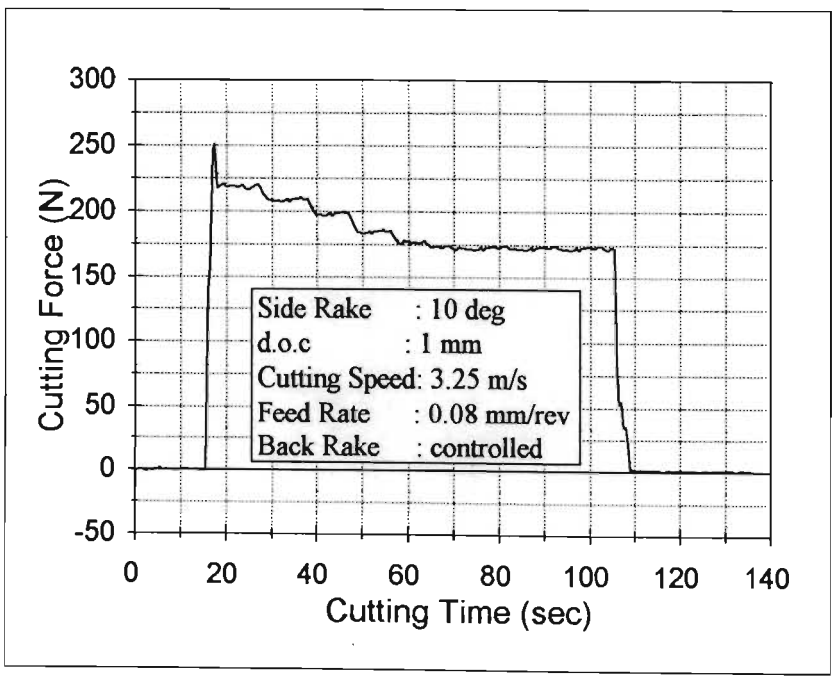

Figure 6.4[b] Evaluation of performance of Unidirectional Optimization procedure for Back rake angle optimization.

Many steps are again evident during this forty seconds of machining. These steps are due to the controller's optimization procedure decreasing the back rake angle with three degrees at a time. Since this action results in substantial lower forces, a jump in the force curve is evident with each adjustment.
When the back rake angle is decreased to minus one degrees, the controller starts changing the angle with only one degree at a time resulting in much lower steps in the output curve. The back rake angle settles at minus two degrees back rake with a minimum force value of about 172 Newtons, where the initial force at the start of machining was around 218 Newtons. At this back rake angle setting, the controller still monitors the cutting forces continually.

When *the continuous evaluative optimization procedure* is used, the system continuously changes the cutting angles to check for better cutting conditions.
The orientator change the angle to the new position where the force value is lower, but will change it back if cutting conditions change at a later stage. This algorithm never stops trying to obtain the optimum cutting conditions.

The system can adapt to new cutting conditions such as changes in the depth of cut. Changing the feed rate will automatically also change the cutting force as measured. The controller continually tries to improve the cutting forces, and when there is a big jump in cutting forces as will happen with a change in cutting depth, the controller will try to improve this new cutting force. In figure 6.4[c] it can be seen that the cutting forces vary continually as the controller increase and decrease the side rake angle to look for

lower cutting forces.

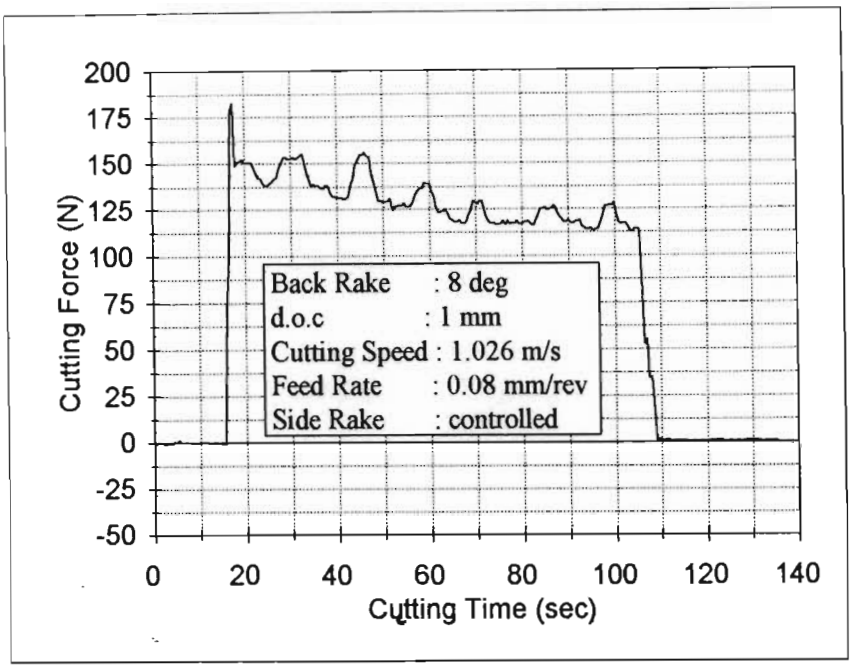

Figure 6.4[c] Evaluation of performance of Continuous Evaluative Optimization procedure for side rake angle optimization.

The force values decreased gradually down to 118 Newtons and then the reduction in cutting forces continues at a reduced rate. This is due to the controller initially searching a six-degree range for lower cutting forces, and then switches to only search a two-degree range.

In figure 6.4[d] it can be seen that the cutting forces vary as the controller increase and decrease the back rake angle to look for lower cutting forces. The mean force value decreased gradually down to about 172 Newtons and then the reductions in cutting forces continue at a reduced rate. This is due to the controller initially searching a six-degree range for lower cutting forces, and then switch to only search a

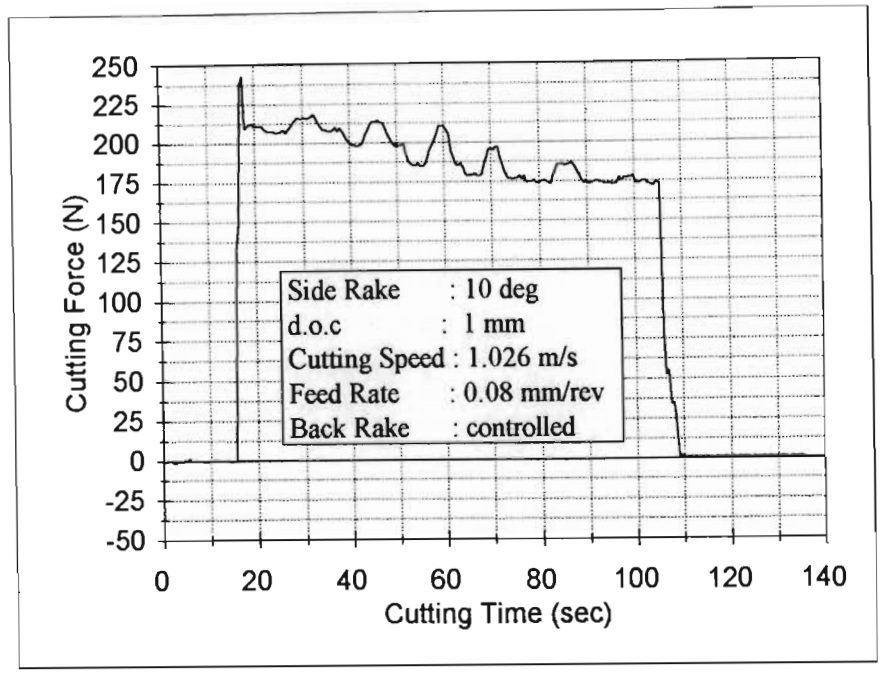

Figure 6.4[d] Evaluation of performance of Continuous Evaluative Optimization procedure for back rake angle optimization.

two degree range. The back rake angle reach minus two degrees after eighty seconds of machining.

The initial evaluative controller with Expert system, functions similar to the second algorithm in that it will continually tries to improve the cutting forces. The advantage of knowing at what cutting angles the optimal forces will be found, helps this algorithm to achieve the correct rake angle setting quicker. Due to the information on optimal cutting conditions for the specific part to be machined, the stepper can vary the tool geometry in bigger steps when the ideal cutting angle is far away from the current one. For this experiment the controller was set to change immediately to the anticipated correct rake angle.

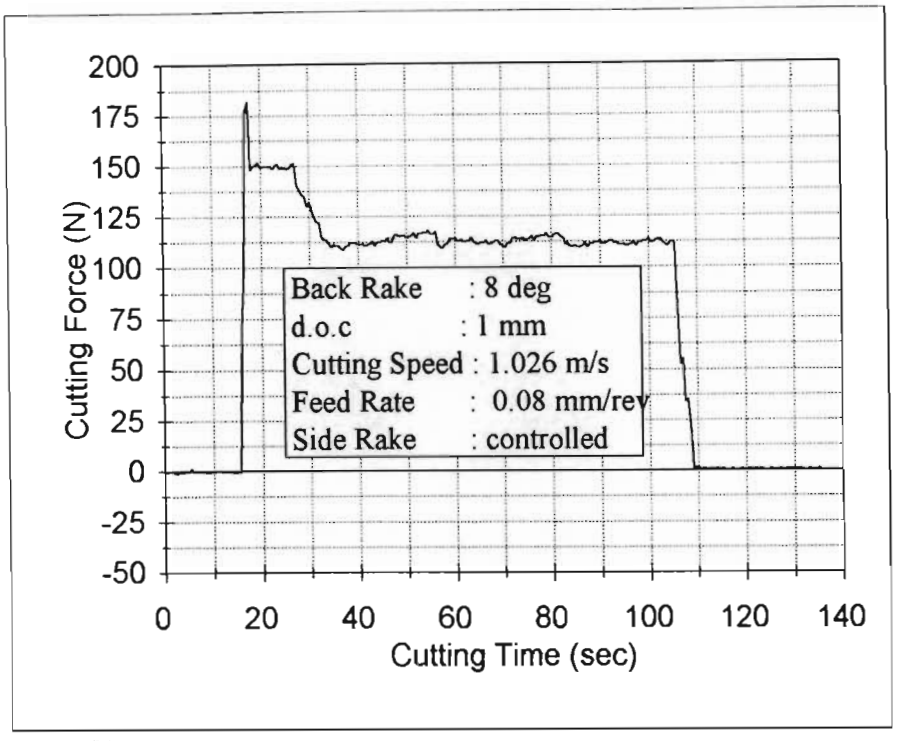

Figure 6.4[e] Evaluation of performance of Initial Evaluative Optimization procedure with Expert system for side rake angle optimization.

Figure 6.4[e] shows an initial reduction in cutting forces from about 145 Newtons to around 113 Newtons. The cutting forces still vary after this initial reduction, but since lower force values are searched for close to the optimal force, variations are low. If the depth of cut should increase during this latter period, the controller will try to optimize the new cutting condition.

Figure 6.4[f] shows an initial reduction in cutting forces from about 218 Newtons to around 172 Newtons. The cutting forces still vary after this initial reduction, but since lower force values are searched for close to the optimal force, variations are low.

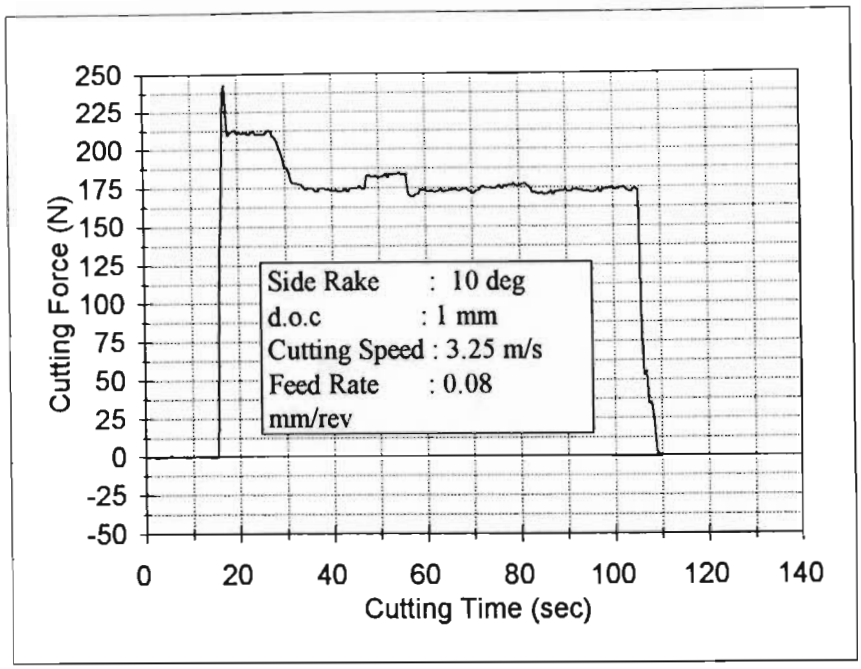

Figure 6.4[f] Evaluation of performance of Initial Evaluative Optimization procedure with Expert system for back rake angle optimization.

6.5 Tool orientator

To vary the tool geometry on-line, a system is required that will always keep the tip of the cutter in the same position. The system must ensure that the only influence of changing the position of the tool orientator on the tool, is a change in either the side rake or back rake angle. No change in depth of cut, metal removal rate, cutting speed or feed rate must occur.

The system developed for this project, had a few shortfalls that can be improved.

- The tool tip has to be set up perfectly with respect to the different circles designed for rotation of the tool orientator around the tool tip. This is the only way to ensure that all the other cutting parameters stay constant. This

setting procedure is difficult to achieve and a margin of error will always occur. A better system can be designed with less slack in the joints.

- The tool tip can be placed on telescopic legs that results in a system with unlimited degrees of freedom. Under computer control all the telescopic legs can align to change the tool geometry while keeping the tool tip at a fixed point in space. This system is better because adjustments for all variations in cutter positions can be made.

6.6 Experimental setup

Different cutting parameters can be monitored like cutting forces, the power consumption during cutting, the stresses in the tool or workpiece, the temperature profile in the tool and the acoustic characteristics of the cut. For the purposes of this project, the cutting force was used for performance evaluation purposes, but an accurate system incorporates all other techniques as well. Much work has been done on using acoustics to evaluate the performance of the cutter. Tool breakage detection and also the wear characteristics of the tool can be detected better than with just a force measurement system. (The acoustic footprint of the cutter change as the tool is wearing.) Temperature measurement of the cutter is difficult but can be done to obtain more information about the cutting process. Forces can be measured more accurately and more stable with the use of pressure transducers and other systems using strain gauges. Pressure transducers are more stable since temperature does not play such a big role in influencing the readings.
The controller program can be improved by making the

system foolproof. The system can check for changes in the cutter performance more often, and then align the system to match.

An ultimate system will detect which metal is being cut, which tool tip is in use and the adapt the cutter geometry to suit the tool tip conditions.

The knowledge base can be improved by importing more data on different machining conditions and metals to be machined. This information could then be used better for optimization purposes.

This system should be included in a CNC machine where feed rate, cutting speed, d.o.c and tool geometry can be all varied together for optimal cutting performance.

CHAPTER 7

7 CONCLUSION

7.1 General.

The on-line control of tool geometry can effectively optimize cutting conditions, when cutting forces are monitored to determine the effect of changes in geometry. Rake angles were identified as having the biggest impact on cutting conditions.

Due to the limitations of the experimental apparatus, the evaluation process was limited to relative low metal removal rates. More expensive equipment will be required to evaluate the process at higher metal removal rates. In the range of cutting conditions tested, the effect of changes in the tool geometry became progressively more visible as the metal removal rate increased. The effect of changes in the tool geometry should be more visible at even higher cutting speeds, but the influence of other cutting parameters like the tool/workpiece interface temperature, power consumption of the lathe, vibration of the tool and noise generated, could be evaluated in another project to obtain the precise effect of each parameter.

Cutting forces vary with variations in the Rake angles, but are also dependant on many other variables namely:

- Feed rate
- Side rake angle
- Cutting Speed
- Depth of cut

Tool type
Tool condition
Vibrations in the tool
Type of material being cut
Work material variability
Stability of the machine tool

The experimentally determined variations in cutting forces with rake angles compare well with the theoretical model in chapter two and previous research results as discussed in chapter two. The comparison is good especially when the huge number of possible combinations between these variables is considered. The use of the force values as obtained from the strain amplifier to control the tool geometry is justified. The optimal controlling of tool geometry can be improved by monitoring parameters like the tool/workpiece interface temperature, the power consumption of the lathe, vibrations of the tool and noise generated by the tool.

Experimental work conducted, proves that the idea of controlling the tool geometry on-line works effectively. The evaluation process was limited to relative low metal removal rate cutting conditions. The higher cutting forces at the higher metal removal rates should make the effect of changes in the tool geometry more visible, and therefore easier to control.

7.2 The effective control of the tool geometry.

The on-line controlling capabilities of the Turbo Pascal program proofed to be effective.

The *unidirectional optimization procedure* works well

for stable cutting conditions where the minimum force value either at higher or lower rake angle values. The big benefit is a quick change of rake angle values in the right direction, without the time-consuming process of switching the direction of rake angle adjustment to verify if the rake angles are still being adjusted in the right direction.

The *Continuous evaluative procedure* always finds the optimum rake angle though cutting conditions might vary dramatically during the process due to depth of cut variations etc. Due to the constant evaluation of rake angles around the current angle, the time to obtain the optimum tool geometry takes longer.

The *Initial evaluative procedure with Expert System* is the fasted to obtain optimal cutting conditions. An estimated rake angle for optimal cutting conditions is determined at the start of the optimization procedure. The rake angle is then immediately adjusted to this value with the continuous evaluative procedure being used from this point for further optimization.

The controlling program can be improved by combining the different procedures into a controller that automatically switch between different controlling modes as required.

7.3 The performance of the tool orientator.

The tool orientator designed to change the cutting geometry during the machining process works effectively to prove the viability of varying tool angles on-line for optimization of the cutting process. The following aspects of the system can be improved:

1) The system relies on rotation around the tip of the tool to ensure that a change in tool geometry does not influence the other cutting conditions. The tip of the tool must be aligned very precisely relative to the tool orientator to ensure that the tip is at the centre of rotation. This process is prone to error during setups, and will change anyway as the tool is wearing. When using the idea of tool optimization in production, a more accurate mechanism should be developed.

2) The tool orientator is more unstable than a conventional tool mounting post, since it consists of many moving parts. This inherent instability results in vibrations when the metal removal rate is increased. Due to these factors, testing the operation of the system at high feed rates or high cutting speeds was not possible. When this system is adapted for mounting on a production tool, the tool orientator must be stronger.

3) The stepper motors used for adjustment of the tool geometry, worked effectively and smoothly also when accelerating or decelerating. The speed of adjustment process can be improved however, since this will improve the reaction time required to obtain optimal cutting conditions.

4) With more money available, the system can be designed more elegantly to obtain all of the above improvements.

5) The robustness of the system can be improved.

7.4 The accurate measurement of Cutting forces.

The force measurement process can be improved a lot by using load cells to measure the cutting forces. The system used for this project, relies completely on

bending in the tool holder to elongate strain gauges. The elongation in the tool holder can be related to the Cutting force at the tip of the tool. Since the actual bending under the load of the cutting force is small, the sensitivity of the measuring process, and therefore the accuracy will be influenced. This measuring technique also requires elaborate calibrations to verify what values are being measured. Other variables like the tool, workpiece and chip temperature, power consumption of the lathe and acoustic output of the tool during machining, can be evaluated to evaluate the cutting conditions better.

7.5 The Force vs Back Rake angle relationship.

Controlling of back rake angles at very low cutting speeds is risky. The measurement of cutting forces at the low cutting speed of 1.004 m/s was unreliable at high and low feed rates. Improvements in the cutting conditions can still be obtained, but since the force values are imprecise, the back rake angle will sometimes be adjusted in the wrong direction.

Accuracy of the optimization process can be improved by monitoring other values like the tool temperature (using temperature effected paint changing colour), the acoustic noise print of the tool (using microphones) or using pressure transducers to obtain a more reliable cutting force value.

The accuracy of experimental data increases a lot when the cutting speed increase. At cutting speeds of 3.25 m/s and 4.663 m/s the data is reliable enough to be used reliably for tool geometry optimization.

Generally the following can be said about the controlling of back rake angles by measuring cutting forces:

-Cutting forces increase with increase in the back rake angle.

-The cutting force vs back rake angle curve, does not always follow the same trend of increasing cutting forces with an increase in rake angles. At a cutting speed of ±one m/s the cutting forces first decrease and then increase when the back rake angle is steadily increased from -10 degrees.

-The force value variations for different back rake angle values are large at all cutting speeds when the feed rate is as low as 0.08 mm/rev.

-When the feed rate is at 0.2 mm/rev variations in force values for different back rake angles are very small at low cutting speeds.

The program controlling the tool geometry, must consider these limitations in the measurement of cutting forces when determining a more optimal back rake angle. A more advanced controller will use different procedures as the need arises to test for general trends in force vs rake angle relation.

7.6 The Force vs Side Rake angle relationship.

The Controlling of Side rake angles by monitoring the cutting forces is more reliable than with back rake angles.

Generally the following can be said about the

controlling of side rake angles by measuring cutting forces:

-Cutting forces decrease with an increase in side rake angle values when the feed rate is 0.08 mm/rev.

-At higher feed rates, side rake angle with a minimum cutting force value can be obtained. At higher or lower side rake angle values, the cutting forces increase.

-There is a certain cutting speed where changes in the side rake angles give uncertain information regarding the cutting forces. At higher and lower cutting speeds the difference in cutting forces are more pronounced.

The program controlling the tool geometry, must consider these limitations in the measurement of cutting forces when determining a more optimal side rake angle.

REFERENCES

1. T.H. Stoferle, B. Bellmann, (1974), Continuous measuring of flank wear, Lehrstuhl fur Technologie und Werkzeugmaschinen, 573-578. West Germany.
2. Robert Eade, (1989), Cutting Tools: Where the action is, Manufacturing Engineering, Aug, 37-41.
3. R.A.Saletri, D.E. Sisler, (1993), Geometry Lesson: A Tool User's Perspective, Manufacturing Engineering, July 1993, 61.
4. E.J.A Armarego, R.H Brown, (1969), Practical machining operations, Turning operations, The Machining of Metals, chapter 7, 156-175, Eaglewood Cliffs New Jersey: Prentice Hall.
5. A.G. Ulsoy, T.R. Ko, Y. Koren, J. Park, (1989/90), Model-Based Tool wear estimation in metal cutting, Proceedings NSF Design and manufacturing Systems, 237-238.
6. H.V. Ravindra, Y.G. Srinivasa, R. Krishnamurthy, (1993), Modelling of tool wear based on cutting forces in turning, Elsevier Sequoia, 25-32.
7. J. Taylor, (1980), A combined approach to obtaining and using tool life data, 133-139, University of New South Wales, Sydney, Australia.
8. T. Shi, S. Ramalingam, (1991), Slip-Line Solution for Orthogonal Cutting with a Chip breaker and Flank Wear, Int. J. Mech. Sci. Vol. 33, No. 9, 689-704.
9. D.A.Taminiau, J.H. Dautzenberg, (1991), Bluntness of the Tool and Process Forces in High-Precision Cutting, CIRP, Vol. 40, No. 1, 65-68.
10. E.M.Trent, (1991), Metal Cutting, 17-18, 57-86, 87-126, Heinenmann Ltd, Butterworth.
11. E.J.A Armarego, R.H Brown, (1969), Economics of machining, Cost optimization for turning Operations, The Machining of Metals, Chapter 9, 254-287. Eaglewood

Cliffs New Jersey: Prentice Hall.

12. J Bussmann, R Granow, (1981), Economics of CNC Lathes, 1-14. Institute of Manufacturing Technology, University of Hanover, West Germany.
13. Proca Zbiorowa, (1960), Recommended cutting Conditions in turning of Steel and Cast Iron, Collective work Machining Time Standards, Vol I, Turning Part II. CONF MPC, Warszawa,50-122.
14. J Taylor, G.C. Lin, (1972), The Accurate Determination of Cutting Forces, 233-239, University of New South Wales, Sydney, Australia.
15. C.Granger, (1989), Carbides: Beneath the surface, Machining and Production Engineering, 35-42.
16. C.Wick, (Nov. 1988), The Facts about Diamonds, Manufacturing Engineering, 63-68.
17. R.R.Schreiber, (Feb 1992), Cut a Path to Productivity, Manufacturing Engineering, 29-32.
18. R.Tourrett, (1985), Performance of Metal Cutting Tools, 35-169, London: Butterworth Scientific Publications.
19. Doyle, Keyser, Lech, Scharder, Singer, (1969), How metals are cut, Manufacturing Processes and Materials for engineers, 436-468.
20. J.R.Davis, (1989), Metals Handbook 9th edition, Vol 16 Machining, 135-153.
21. B.Worthington, (1975), A Comprehensive literature survey of chip control in the turning process, Machine Tool design and Research Conference, 103-116.
22. G.Boothroyd, (1975), Mechanics of Metal Cutting, Fundamentals of Metal Machining and Machine Tools, 61-89. Washington DC: Mcgraw-Hill.
23. B.E.Klamecki, (1989), Chip Control in Turing, Department of Mechanical Engineering University of Minnesota, Minneapolis.
24. C.L.Kenneth, R.M.Caddell, A.G. Atkins, (1987),

Manufacturing Engineering, 215-270, Prentice Hall, New Jersey.

25. E.J.A Armarego, R.H Brown, (1969), Tool Wear, The Machining of Metals, chapter 6, 121-125, Eaglewood Cliffs New Jersey: Prentice Hall.
26. M Field, J.F.Kapiles, W.P.Koster, Surface finish and surface integrity, Mechanics of Machining, 19-36.
27. Colding, (1991), A Tool temp/Tool life Relationship covering a wide Range of Cutting data, Annals of CIRP, Vol 40/1.
28. Unknown, (Jan 1991), The changing face of Milling, Manufacturing Engineering, 35-38.
29. J.R. Koelsch, (1994), Precision Machining: On The Money, Manufacturing Engineering, March 1994, 67-72.
30. Kuang-Hua Fuh, Chung-Shin Chang, (1994), A force model for single point tools with chamfered main cutting edge, Journal of Materials Processing Technology, Vol 42, 319-340.
31. K.Nakayama, M. Arai, (1992), Comprehensive Chip Form Classification Based on the Cutting Mechanism, Annals of the CIRP, Vol. 41, 71-74.
32. G.T. Smith, M.J. Allsop, (1991), Some aspects in the surface integrity associated with turning of powder metallurgy compacts, Wear, 151 (1991), 289-302.
33. R. Du, B. Zhang, W. Hungerford, T. Pryor, (1993), Tool condition monitoring and compensation in finish turing using optical sensor, DSC-Vol. 50/PED-Vol. 63, Symposium on Mechatronics, 245-253. ASME.
34. N.N. Popok, (19989), Tool Wear in Rotary Tool Turning, Stanki I Instrument, Vol. 60, No. 8, 9-10,. Allerton Press, Insc.
35. S.S. Babu, A,K, Chakraborty, A.B. Chattopadhyay, (1993), Microscopic study on chips formed by sharp and bevelled turning carbide inserts, Journal of Materials Processing Technology, 37, 781-789. Elsevier Science

Publishers B.V.

36. J.S. Strenkowski, K. Moon, (1989/90), A Thermo-Viscoplastic Model of the cutting Process Including Chip Geometry and Temperature Prediction, Proceedings of 1989/90 NSF Design and Manufacturing Systems Conference, 197-205.
37. I.E. Minis, E.B. Magrab, I.O. Pandelidis, (1990), Improved Methods for the Prediction of Chatter in Turning, Part 3: A Generalized Linear Theory, Journal of Engineering for Industry, Feb, Vol. 112, 28.
38. I.N. Tansel, (1993), A Unified Transfer Function Approach for the Modeling and Stability Analysis of Long Slender Bars in 3-D Turning Operations, Journal of Engineering for Industry, May, Vol. 115, 193-204.
39. M.N.Hamdon, A.E.Bayonni, (1989), An Approach to study the effects of tool geometry on the primary chatter Vibration in orthogonal cutting, Journal of Sound and Vibrations, 128(3), 451-469.
40. I.E. Minis, E.B. Magrab, I.O. Pandelidis, (1990), Improved Methods for the Prediction of Chatter in Turning, Part 2: Determination of Cutting Process Parameters, Journal of Engineering for Industry, Feb, Vol. 112, 25.
41. Sandvik Coromant, (July/August 1996), Spotlight on Cutting Tools, MTM Southern Africa, 2-30.
42. C. Sikdar, S. Paul, A.B. Chattopadhyay (1992), Effect of variation in edge geometry on wear and life of coated carbide face milling inserts, Elsevier, 111-126.
43. P.M. Noaker, (1991), Turning Up Iron and Steel Machining, Manufacturing Engineering, Jan, 28-33.
44. J.R. Coleman, (1990), Make Money with Multicoats, Manufacturing Engineering, Jan, 38-42.
45. S. Ehuland, (1981), High Speed steel symposium, p 3.

46. D.A.Lucca, Y.W. Seo, R. Komanduri, R.L. Rhorer, (!991), Energy Dissipation in Ultra-Precision Machining, Proceedings of 1991 NSF Conference, 263-267.
47. E.E. Sprow, (1993), Face Up to Fine Finishing: Time Yet for Cermets?, Manufacturing Engineering, Jan. 1993, 55-58.
48. Machining data handbook, (1980), Vol 2, 3rd edition. Metal cutting Research Associates.
49. Y. Wang, S.M. Wu, (1989/90), The Application of Upper Bound Approach to Oblique Cutting Including Chip Curl and Build-Up Edge, Proceedings of 1989/90 NSF Conference, 207-214.
50. G. Byrne, (1992), A New Approach to the Theoretical Analysis of Surface Generation Mechanisms in Machining, Annals of the CIRP, Vol 41, 1, 67-70.
51. S.G. Chen, A.G. Ulsoy, Y. Koren, (1993), Prediction of the Resultant Contouring Force in Metal Cutting on a Lathe, DSC-Vol. 50/PED-Vol. 63, Symposium on Mechatronics, 113-117. ASME.
52. E.J.A Armarego, R.H Brown, (1969), Deformation of metals during machining, The Machining of Metals, chapter 2, 28-31, Eaglewood Cliffs New Jersey: Prentice Hall.
53. E.J.A Armarego, R.H Brown, (1969), Mechanics of oblique cutting, The Machining of Metals, Chapter 4, 75-93, Eaglewood Cliffs New Jersey: Prentice Hall.
54. E.J.A Armarego, R.H Brown, (1969), Mechanics of orthogonal cutting, The Machining of Metals, Chapter 3, 36-69, Eaglewood Cliffs New Jersey: Prentice Hall.
55. O. Masory, Y. Koren, (1980), Adaptive Control Systems for Turning, Ann CIRP, Vol 29, No. 1, 618-625.
56. M. Weck, K. Schafer, (1977), Direct Digital Control for Turning Operations, RWTH Aachen, 61-66.
57. W. Ehrfeld, F. Gotz, D. Munchmeyer, W. Schelb, D.

Schmidt (1988), Liga Process: Sensor construction techniques via x-ray lithography, Rec. of the IEEE solid-State Sensor and Actuator Workshop, 1-4. Kernforschungszentrum Karlsruhe Gmbh.

58. P. Balakrishnan, E.Kannatey-Asibu, H.Trabelsi, E.Emel, (1989/90), A Sensor Fusion Approach to Cutting Tool Monitoring, Proceedings of 1989/90 NSF Design And Manufacturing Systems, 101-108.

59. R.Teti, D.Dornfeld, (1989), Modelling and Experimental Analysis of Acoustic Emission from Metal Cutting, Journal of Engineering for Industry, Aug. 1989, Vol.111, 229-236.

60. L.E. Stockline, (1991), Tool Condition Monitoring Systems, 411-417. Promess, Inc.

61. K. Yamazaki et al, (1974), A study on adaptive control of a NC milling machine, Annals of the C.I.R.P., Vol. 23, 51.

62. D.L. Polla, R.S. Muller, R.M.White, (1986), Integrated Multi sensor Chip, IEEE Electron Device Lett., Vol. EDL-7, No. 4, April 1986, 254-256.

63. S. Damodarasamy, S. Raman, (1993), An Inexpensive system for classifying tool wear states using pattern recognition, Elsevier Sequoia, 149-160.

64. K. Petersen, C. Kowalski, J.Brown, H. Allen, J. Knutti, (1985), A force Sensing Chip Designed for Robotic Manufacturing Automation Applications, Rec. Of the 3rd Int. Conf. On Solid state Sensors and Actuators, 30-32.

65. BK Fussell, K. Srinivasan, (1991), Adaptive Control of Force in End Milling Operations: An Evaluation of Available Algorithms, Journal of Manufacturing Systems, Vol, 10, No. 1, 8-19.

66. O. Masory, Y. Koren, (1983), Variable Gain Adaptive Control System for Turning, Journal of Manufacturing Systems, Vol. 2, No. 2, 165-173.

67. S.B.Billatos, P.Tseng, (1990), Knowledge-Based Optimization for Intelligent Machining, Journal of Manufacturing Systems, Vol 10, No. 6, 464-475.

68. J.R. Koelsch, (1993), Cutting Edge Repeatability,Manufacturing Engineering, July 1993,53-59.

69. Bruce Eckel, (1987), A programmer's guide to the parallel port, Turbo Technix, Nov/Des, 74-79.

70. P.G.Maropoulos, S. Hinduja (1991), Automatic tool selection for rough turning, Int. J. Prod. Res., Vol. 29, No. 6, 1185-1204. Taylor & Francis Ltd.

71. A.A. Samoilov, V.A. Khrul'kov, B.I. Vorob'ev (1989), Cutting rates for difficult to machine materials in automated lathes, Stanki I Instrument, Vol. 60, No. 8, 17-21. Allerton Press.

APPENDICES

4.3[a] Strain gauge sensitivity.

The strain gauge sensitivity k, is the proportionality factor between the relative change of resistance and the strain to be measured:

$$\frac{\Delta R}{R_0} = k.\varepsilon$$

The strain sensitivity is a figure without dimension and is generally called the gauge factor.

In this case we have four gauges in series for maximum sensitivity.

$$R_{EQ} = R_1 + R_2 + R_3 + R_4$$

Where R_{EQ} is the equivalent resistance for the four gauges in series.
These four gauges are connected in parallel with the temperature compensation gauge R_C. The value for R_0 is therefore:

$$R_0 = \frac{R_{EQ} R_C}{R_{EQ} + R_C}$$

The bigger the value of R_{EQ}, the bigger the relative change in resistance and the more sensitive the strain gauge set-up.

4.4[a] Description of the strain indicator operational principles.

The V/E -20A strain gauge indicator is provided with an isolated variable output DC Power Supply for gauge or bridge excitation. This power supply is extremely stable. This ensures that voltage variations over the strain gauge is due to elongation, or shortening of the gauge. The indicator also provides bridge completion circuits and circuits to achieve initial bridge balance, with appropriate calibration circuits. The voltage measured over the strain gauges is amplified by a build-in fixed gain DC differential amplifier before the voltage is displayed by a LED display.

The principal features of the V/E -20A Digital Strain Indicator is listed below:

-Ultra stable amplifier with near-zero drift.
-Extreme immunity to electrical noise on the input.
-Direct-reading LED display representing micro strain with a resolution of one με.
-Wide range of span control. (Forty to one) approx.
-Built in shunt-calibration circuit to simulate one thousand με at gage factor of two in half or quarter-bridge operation. (any resistance)

4.4[b] The correct wiring techniques

The wiring techniques used when connecting the strain gauges to each other and to the bridge amplifier, can have a pronounced effect on the measurements. As mentioned previously, symmetry in lead wire resistance is highly desirable to reduce the effects of changes

in ambient temperature on these wires. Lead wires should be grouped together in a bundle to reduce temperature differentials between leads. The lead wires must also be as short as possible to obtain good accuracy.

To ensure that the least amount of electrical noise is picked-up from the environment, the following precautions have to be made: (This noise is normally in the fifty or sixty hertz range related to power sources in the area.)

- twisted multi-conductor wire had to be used. Shielded wire works the best.
- Shielding has to be kept well clear of magnetic fields such as transformers, motors, relays and heavy power wiring. (Shields do not protect against them.)
- A half bridge on or near the specimen shows less noise than a true quarter-bridge connection.
- The gauge amplifier had to be calibrated first
- Instrument zero was checked.
- An oscilloscope output voltage socket is provided in the back for further analysis of the dynamic strain gauge values.

4.6[a] Using the Parallel port for I/O.

Figure 4.6.1[a] names each pin and provides its port address, which data bit affects the pin, whether data is inverted between a data bus and the pin, and what the physical inputs and outputs looks like electrically to the outside world.

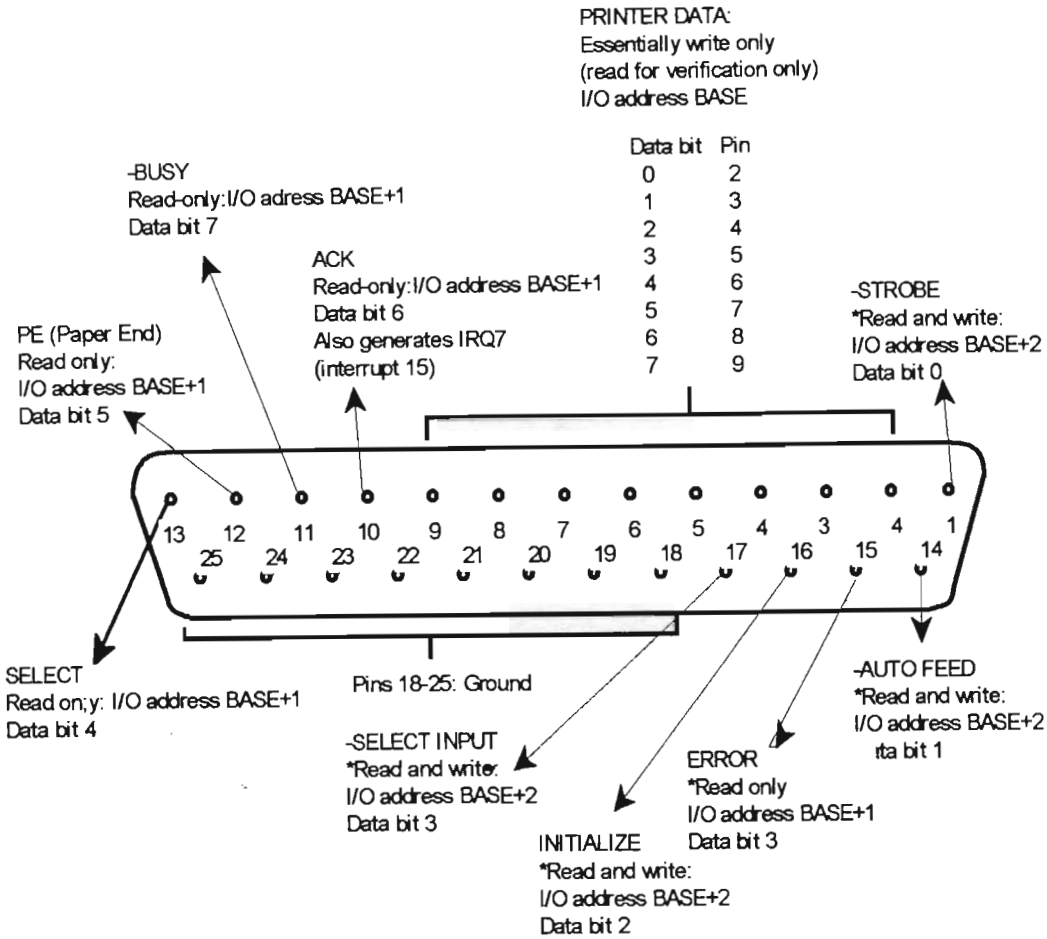

Figure 4.6.1[a] The PC parallel port.

The card is contacted through three consecutive I/O addresses: BASE (the starting address), BASE + 1, and BASE + 2. BASE is set by dip switches or jumpers on the printer board. Standard addresses are 0*378 for LPT1, and 0*278 for LPT2.

On the pins, less than or equal to 0.8 volts indicates a zero, and 2.7 volts or more indicates a 1. These are the voltages coming out of pins 2-9 (the printer data pins), if a voltmeter is connected directly to the pins. Pins 1,14,16 and 17 are pins that work both ways, i.e. data may be read into the computer from external devices, or data may be output to a device external to the computer. The I/O address BASE reads

and writes the eight bits of printer data on pins 2-9. Data can however only be read back if it is presently written to the port. As a result, the Port is good for output but virtually no good for input. For the purposes of this project, values were read out to pins 2-9 to effect movement in the stepper motors.

4.6[b] Computer program.

The computer program (controller) is supplied on a stiffy at the back of the thesis.

5.2[a] Lead screw displacement for change in Back Rake Angle

The lead screw displacement can be calculated for a change in back rake angle. The geometrical displacement of the tool orientator is displayed in figures 5.2[a] and 5.2[b]. With the help of these figures, the angle variation with lead screw rotation is calculated.

Calculate z: z is constant for any value of angle Θ
x = 192.5 mm (when part 1 is horizontal)
y = 48 mm (when part 1 is horizontal)

Thus:

$$z=\sqrt{x^2+y^2}$$

$$\underline{z=198.39mm}$$

Calculate e: e is constant for any value of angle Θ

Thus:

$$e=y+b$$

$$\underline{e=62.5mm}$$

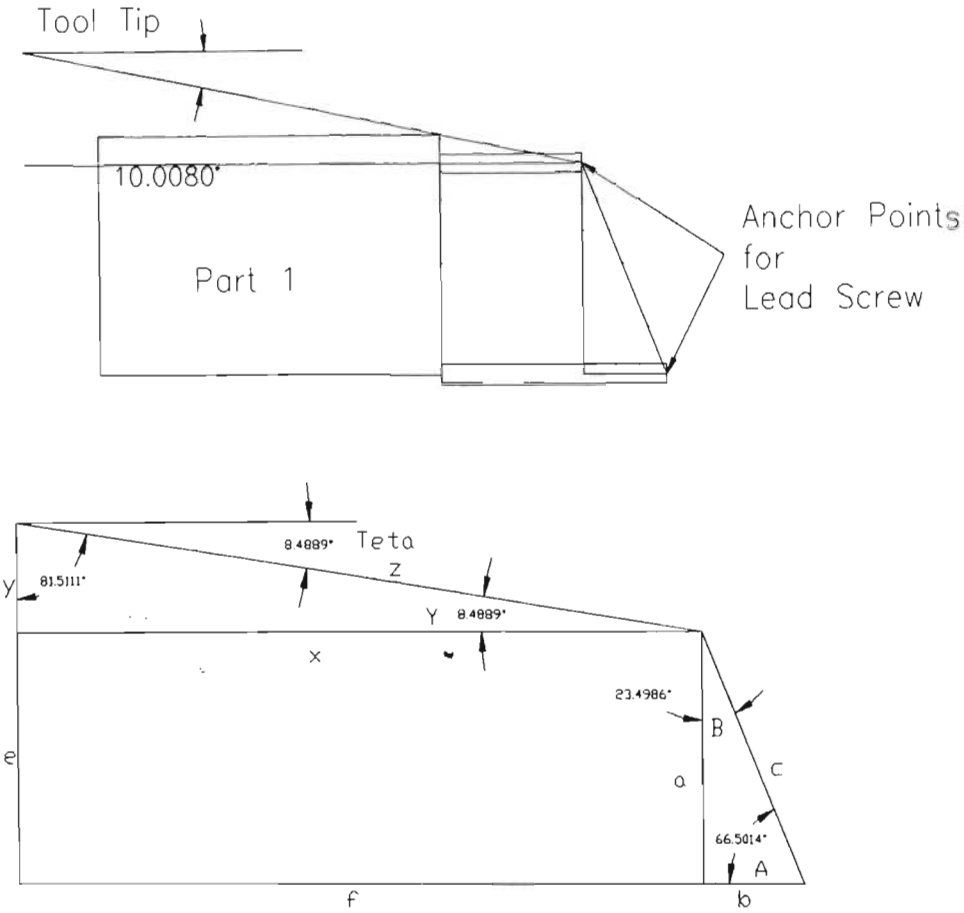

Figure 5.2.1[a]

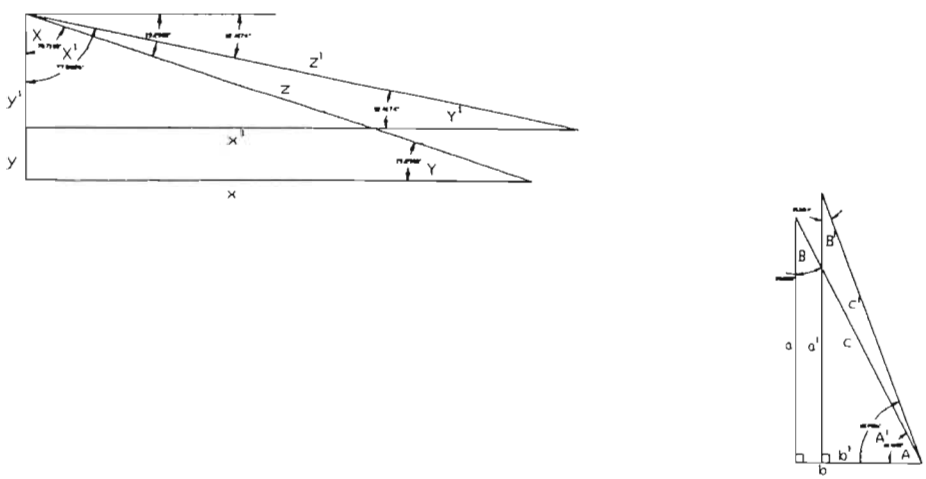

Figure 5.2.1[b]

Calculate f: f is constant for any value of angle Θ

Thus:

$$f=x+b$$

$$\underline{f=207mm}$$

Calculate Θ:

$$\Theta=90°-X$$

$$\frac{y}{z}=\cos X$$

$$X=\arccos\frac{y}{z}$$

$$X=\arccos\frac{48}{198.39}$$

$$\rightarrow\underline{\Theta=14°}$$

$$\underline{X=76°}$$

This is true for the horizontal position of part 1. We now want to know the value of c for different values of Θ. (See figure 5.2[a])

$$X'=90°-\Theta'$$

$$Y'=90°-X'$$

$$x'=z\cos Y'$$

$$y'=z\sin Y'$$

$$a'=e-y'$$

$$b'=f-x'$$

$$A'=\arctan\frac{a'}{b'}$$

$$\frac{b'}{c'}=\cos A'$$

$$\Rightarrow c'=\frac{b'}{\cos A'}$$

Example: If $\Theta=10^\circ$ then find the length of the lead screw.

-One revolution of the lead screw results in a change in length of 0.5 mm.

-One revolution of the lead screw needs 200 steps by the stepper-motor.

X'=90°-10°=80°

Y'=90°-80°=10°

x'=195.38mm

y'=34.45mm

a'=28.05mm

b'=11.62mm

c'=30.36mm

For $\Theta=14°$ the value of $c=20.51mm$

Thus

$$\Delta C=C'-C$$

$$\Delta C=9.85mm$$

This means 19.7 rotations of the lead screw and 3941.56 steps by the stepper-motor is required to change the back rake angle from 14° to 10°. Therefore 4.925 rotations is required to change the back rake angle with one degree.

5.2[b] Lead screw displacement for change in Side Rake Angle

The lead screw displacement can also be calculated for a change in side rake angle. The geometrical displacement of the tool orientator is shown in figure 5.2.2[a], 5.2.2[b], 5.2.2[c], 5.2.2[d] and 5.2.2[e]. Using these figures, the angle variation with lead screw rotation can be calculated.

Calculate d: d is the distance between swivel joints on the lead screw for 0° side rake.
d = 66 mm

Calculate x: Constant for all side rake angles.

$$x=\sqrt{171^2+198^2}$$

$$x=261.62mm$$

Calculate Θ: See figure 5.2.2[b]
Φ=side rake angle adjustment in degrees

$$\frac{z}{\sin\Phi}=\frac{x}{\sin\Theta}$$

$$\Theta = \frac{180-\Phi}{2}$$

$$z = \frac{x \sin\Phi}{\sin\frac{180-\Phi}{2}}$$

Calculate d2: See figure 5.2.2[c] and 5.2.2[d].

$$\alpha = \arccos\frac{171}{261.62} = 49.18°$$

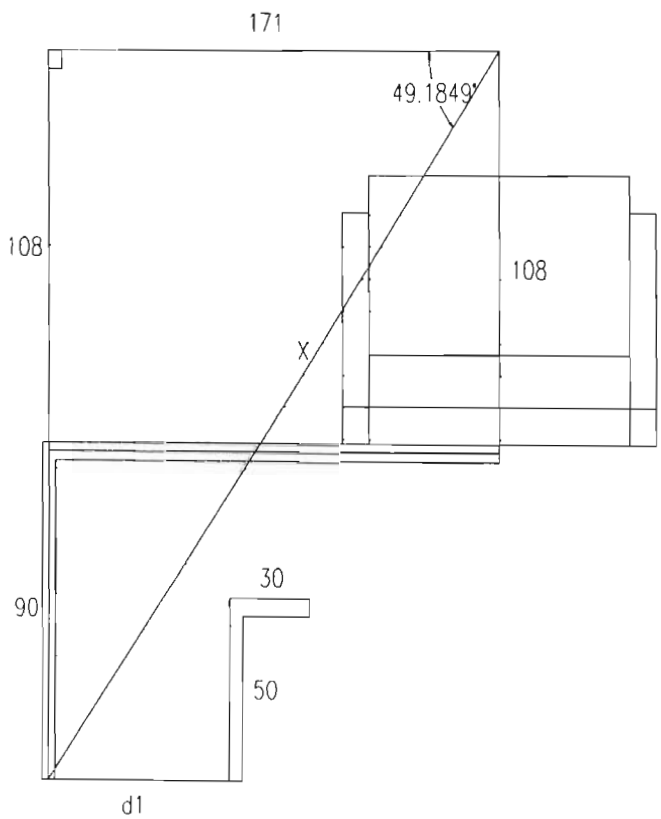

Figure 5.2.2[a]

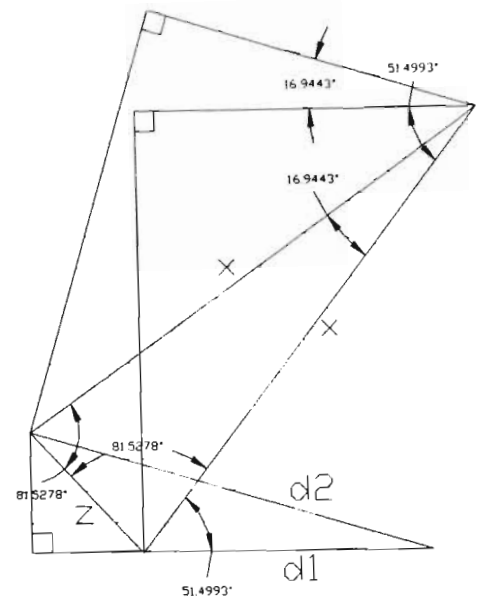

Figure 5.2.2[b]

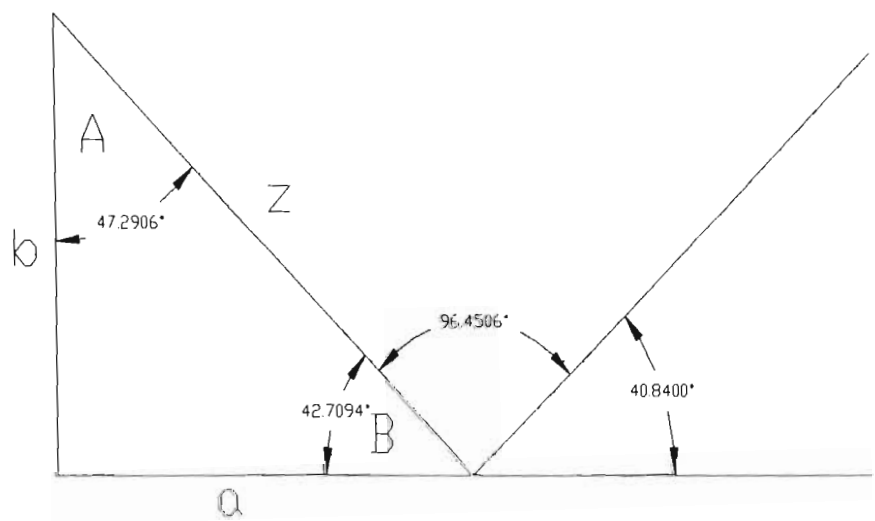

Figure 5.2.2[c]

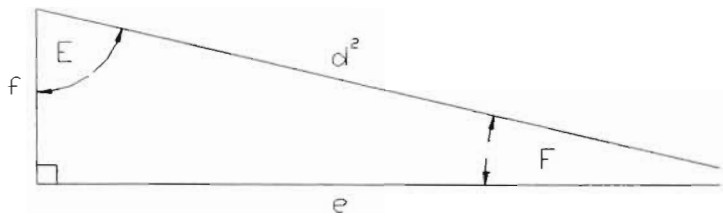

Figure 5.2.2[d]

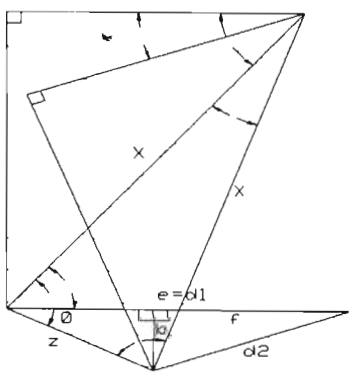

Figure 5.2.2[e]

$$B=180-\Theta-\Phi$$

$$A=90-B$$

$$a=z\cos B$$

$$b=z\sin B$$

Calculate d2 for negative side rake angles.

See figure 5.2.2[e]

z can be found as previously.

Θ is also the same.

a and b can found as before.

$$f=e-a$$

$$\underline{d2=\sqrt{b^2+f^2}}$$

$$e=d+a$$

$$f=b$$

$$\underline{d2=\sqrt{b^2+e^2}}$$

Example: If side rake = 20° find d2.

Θ = 80°

Z = 90 86 mm

B = 50 86°

A = 39.18°

a = 57.4 mm

b = 70.43 mm

d2 = 142.08 mm

⇒ Δd = 142.08 - 66 = 76.08 mm for 20°

⇒ <u>Δd = 3.8 mm/°</u>

This means 7.6 rotations of the lead screw is required to change the side rake angle with one degree.

5.5[a] Experimental procedure for back rake evaluation.

1) Ensure that the back rake angle, cutting speed and feed rate is set correctly. (The three cutting speeds must be researched at both the feed rates. After every fifteen experiments either the cutting speed or the feed rate or both have to be varied. The back rake angle must be varied for every experiment.)

2) Take a pilot cut to ensure that the zero depth is precise. (This would ensure that any effect of the movement of the tool tip would be removed from the results of the test. This pilot cut removes about 0.2 mm from the surface of the workpiece. After this pilot cut the cutting parameters is not varied again.)

3) Set the depth of cut accurately. For the purposes of this project, one millimetre has to be added to the depth of the pilot cut.

4) Take the cut while monitoring the forces. The cutting operation should take about one minute with about thirty seconds before and after the operation to ensure stability of the cutting forces.

5) Change the rake angle and repeat the sequence above until the tests have been conducted for the whole range of rake angles.

6) After the whole range of fifteen rake angles have been researched, the other cutting parameters like cutting speed and feed rates have to be adjusted.

5.6[a] Experimental procedure for side rake evaluation.

For every experiment, a sequence of operations had to be followed to ensure accurate data.

-Ensure that the side rake angle, cutting speed and feed rate is set correctly. (The experiments must be conducted to ensure that all side rake angles are tested with all three cutting speeds at the different feed rates.)

-Take a pilot cut to ensure that the zero depth is precise. (This will ensure that any possible movement of the tool tip does not affect the results of these tests. After the pilot cut the test is conducted without varying the parameters again.)

-The depth of cut must be set accurately at one millimetre.

-Take the cut while the cutting forces are monitored. The length of the tests must be about one minute with another thirty seconds before and after the actual cutting starts. The thirty minute periods ensure that the measurement of cutting forces was stable before and after the cutting process.

-Change the side rake angle, and repeat the sequence above until the tests have been conducted for the whole range of rake angles.

-When all the side rake angles have been researched for the set of cutting parameters, the cutting speed and feed rate have to be adjusted and the tests have to be repeated for the new set of cutting parameters.

5.8[a] Expert system description.

An expert system works by asking the user a series of questions designed to progressively narrow down the answers to a problem. Problems that involve determining one of many possible solutions are very well suited to expert systems. This makes an expert system ideally suited to the problem of identifying the correct machining parameters for given machining conditions. The controlling program incorporates a very simple expert system, that can be developed much further for future research into the optimization of cutting conditions using the tool angles.